Nonlinear Vibration Analysis of Inflatable Dams

by

Maarten James Leeuwrik

Thesis submitted to the Faculty of the

Virginia Polytechnic Institute and State University

in partial fulfillment of the requirements for the degree of

Master of Science

in

Civil Engineering

APPROVED:

Raymond H. Plaut, Chairman

Siegfried M. Holzer

Richard M. Barker

April 1987

Blacksburg, Virginia

Nonlinear Vibration Analysis of Inflatable Dams

by

Maarten James Leeuwrik

Raymond H. Plaut, Chairman

Civil Engineering

(ABSTRACT)

In recent years the use of inflatable dams has become more widespread throughout the world. Various people have done studies on the shape and membrane tension of these structures; however, only a few authors have considered dynamic behavior. Due to the nature of the applications and the material composition of these structures, a study considering the dynamic response of an inflatable dam is warranted.

In this study, the equation of motion for an air-inflated dam is derived, then solved using the Galerkin approximation method. The solution is performed for a one-term approximation and a two-term approximation, where both solutions use a sine function to approximate the deflected shape of the dam. Frequencies and amplitudes are calculated and presented in tables and plots for the first four modes, and three different values of the central angle of the dam. Comparisons to the results of other studies are presented at the conclusion of this study.

Acknowledgements

I would like to express my appreciation to Dr. R. H. Plaut, whose guidance as thesis advisor greatly enhanced the value of this study, and offer special thanks to Dr. Siegfried Holzer and Dr. Richard Barker, for being members of my graduate committee.

Table of Contents

List of Illustrations

List of Tables

Introduction

The use of inflatable dams is becoming increasingly common around the world. The first application was by water resource engineer Norman Imbertson in 1957. He showed that they are an effective, economical, and very versatile alternative to other types of dams. Since then, many organizations have begun using them for a variety of purposes. Some of the most common uses are tidal control and land reclamation, flood control, or addition of height to spillways of existing fixed dams. Additionally, inflatable dams have been used for less obvious purposes such as small boat locks, wildlife and fisheries management, and the creation of recreational or aesthetic reservoirs.

In general an inflatable dam is a cylindrical tube made of a rubberized fabric. Inflatable dams have been made from high strength nylon coated with a synthetic rubber called Neoprene. The dams vary in size, and can be as tall as 17 feet with a length of 350 feet, or as small as 1 1/2 feet high with a length of 16 feet. The dams are usually continuously anchored to a smooth surface, such as a concrete slab. For the larger dams, a downstream as well as an upstream anchoring device is used. The dams can be inflated with air, water, or a combination of both. Figure 1 gives an illustration of the general concept of an inflatable dam.

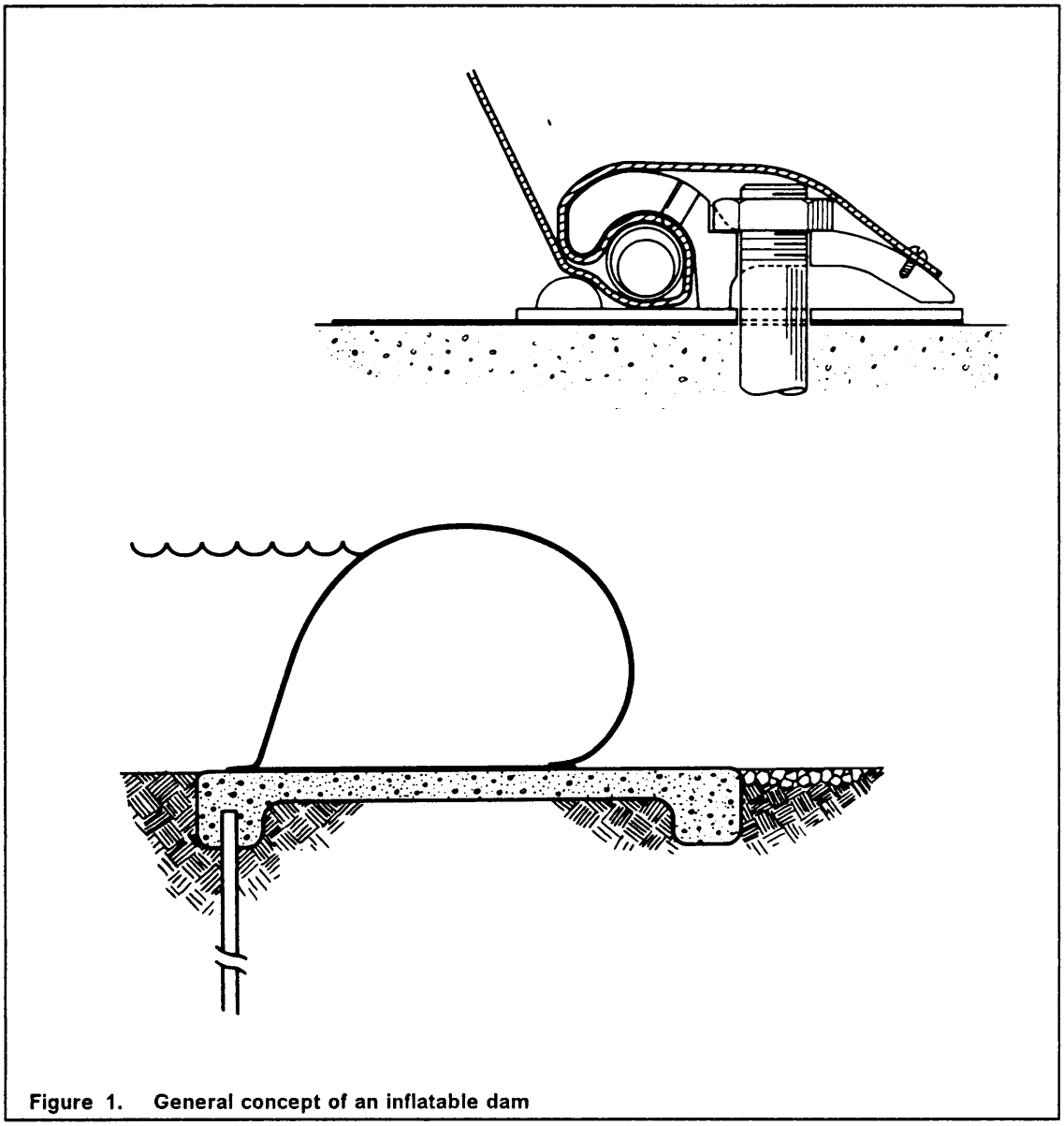

Figure 1. General concept of an inflatable dam

Various papers have been published directly relating to the subject of inflatable dams; however, in comparison to other subjects, there is relatively little literature available on the subject. Papers include methods for determining static and dynamic shapes, methods of stress analysis, technical and economic evaluations of specific applications of inflatable dams, as well as the results of model tests with comparisons to analytical work. Since there have been several inflatable dam failures, investigation reports have also been published. Failures of the Belmore Fabridam in Australia [15] and the Mangla Dam in Pakistan [3] have been studied in great detail, and reports prepared as to the causes of failure.

The methods used to predict dynamic behavior of inflatable dams tend to be based on the observations of previous applications, or scale model tests. Few authors have presented methods to theoretically determine the response of an inflatable dam that is dynamically excited. This thesis will consider an air-inflated dam, assuming its material to be inextensible and its self weight to be negligible. The equations of motion will be presented, and then solved using the Galerkin approximation method. Since there are geometric nonlinearities inherent in the response of an inflatable dam, the equations of motion will include the nonlinear terms up to the third order. Solutions will be found for both a one-term approximation and a two-term approximation, for modes one to four and their combinations, and various parameters. Since the equations are complex, they will be solved using a FORTRAN computer program that calls the International Mathematical and Statistical Library (IMSL) subroutine DVERK [9]. This subroutine is a powerful one that solves complex differential equations using the Runge-Kutta-Verner fifth and sixth order method, and facilitates the rapid solution of the equations for the many different cases. Calculated frequencies and amplitudes will be presented in both tabular and graphical forms, with comparisons to the results of analyses by others.

Literature Review

Compared to other areas of engineering study, relatively few papers have been written on the subject of inflatable dams, and most of them only present static analyses or methods of finding the shape under various static conditions. H. O. Anwar [1] developed some of the first theoretical equations governing the static shape, and others like H. B. Harrison [6], R. D. Parbery [12,13], and G. M Binnie [2,3] refer to his work. Most of these authors also offer improvements to, or alternate methods for, Anwar's methods. V. Firt's [5] work covers a large range of topics pertaining to air-supported structures, and his presentation of the dynamic analysis of cylindrical inflated membranes is closely related to the topic of this thesis. Since he is the only author who deals with the dynamic behavior of these types of structures, the discussion of his work will be more detailed than those of the others.

H. O . Anwar

In his paper, Anwar develops equations that define the shape of an air-inflated dam for hydrostatic and hydrodynamic conditions. He also develops the shape equations of a water-inflated dam for hydrostatic conditions. Anwar then compares the results he obtained to scale model tests he conducted. For each of these cases, Anwar works from the basic assumptions

that the self-weight and elasticity of the dam are negligible, and that the internal pressure is proportional to the upstream head.

For the static case, the internal pressure, p_i, is proportional to the upstream water level, H, which is also assumed to be the height of the dam, and the diameter of the circular portion of the dam.

$$p_i = \alpha \rho g H \,, \qquad [2.1]$$

where α = proportionality ratio, ρ = specific gravity of water, and g = the acceleration due to gravity.

For the hydrostatic case, the shape of the air-inflated dam is defined by two equations, one for the upstream shape and one for the downstream shape. Since the internal pressure is uniform, Anwar implies that the downstream shape is semi-circular. He writes expressions for the vertical and horizontal force components, and combines them into an expression that describes the tangent of the dam at a point P. He differentiates this expression with respect to the x coordinate and introduces non-dimensional coordinates ξ and η. Then, by applying boundary conditions, he solves this resulting expression and arrives at the solution

$$\xi = \sqrt{2\alpha}\left\{2\hat{E}\left(\sqrt{\frac{\alpha}{2}}\right) - \hat{F}\left(\sqrt{\frac{\alpha}{2}}\right) - E\left[\arccos\left(\frac{\eta}{\alpha} - 1\right), \sqrt{\frac{\alpha}{2}}\right] + \frac{1}{2}F\left[\arccos\left(\frac{\eta}{\alpha} - 1\right), \sqrt{\frac{\alpha}{2}}\right]\right\}, \qquad [2.2]$$

where $\xi = x/H$, $\eta = y/H$, and E and F are elliptical integrals of the first and second kind, respectively. The circumflex over the E and F indicates that the integral is complete.

For the hydrostatic case, the shape of the water-inflated dam is also defined by an upstream and a downstream equation. Here Anwar determines that the upstream shape is semi-circular, and using a similar procedure, develops equation 2.3 for the downstream shape:

$$\xi + C_2 = \sqrt{2a_1 + \delta}\ E(k_1\ \varphi) - \frac{\delta}{\sqrt{2a_1 + \delta}}\ F(k_1\ \varphi)\,, \qquad [2.3]$$

where $\delta = (1 + \alpha)^2 + 2a_1C_1$, C_1 and C_2 are integration constants, and $a_1 = (1 + 3\alpha)/6$.

For the hydrodynamic case, Anwar only considers the air-inflated dam. Water flow over the crest of the dam is assumed for simplicity. The initial assumptions are the same as those for the static cases, except that the internal pressure is proportional to the total upstream depth:

$$p_i = \alpha\rho g(h + H)\,, \qquad [2.4]$$

where h = height of the crest overflow.

Again, Anwar implies that the downstream profile is circular, and using a similar procedure he develops the differential equation

$$\begin{aligned} &\left[\frac{\alpha}{2}(h + H)H + Xy - \int_0^X \varphi(X)dX - xy + \int_0^X y dx\right. \\ &\left. -\alpha(h + H)y\right]y'' + \left[X'y + Xy' - \frac{d}{dx}\int_0^X \varphi(X)dX - xy'\right. \\ &\left. -\alpha(h + H)y'\right]y' = [g(x) + y - \alpha(h + H)]\,, \end{aligned} \qquad [2.5]$$

where Figure 2 describes the parameters of the dam for the hydrodynamic case, the origin of coordinate system being at the top of the dam; $g(x)$ and $\varphi(X)$ are unknown functions describing the pressure and the horizontal force distribution, respectively; $X = \xi + 2\gamma - \frac{\gamma}{\beta}\xi^2 + 2$; $\gamma = \frac{h}{a}$; and $\beta = \frac{a}{H}$.

Equation 2.5 cannot be solved as it contains unknown functions $g(x)$ and $\varphi(x)$, but since $\varphi(X)$ can be found given $f(x)$ and $g(x)$, an approximate solution can be found writing $f(x)$, $g(x)$, and $\varphi(X)$ as power series of x:

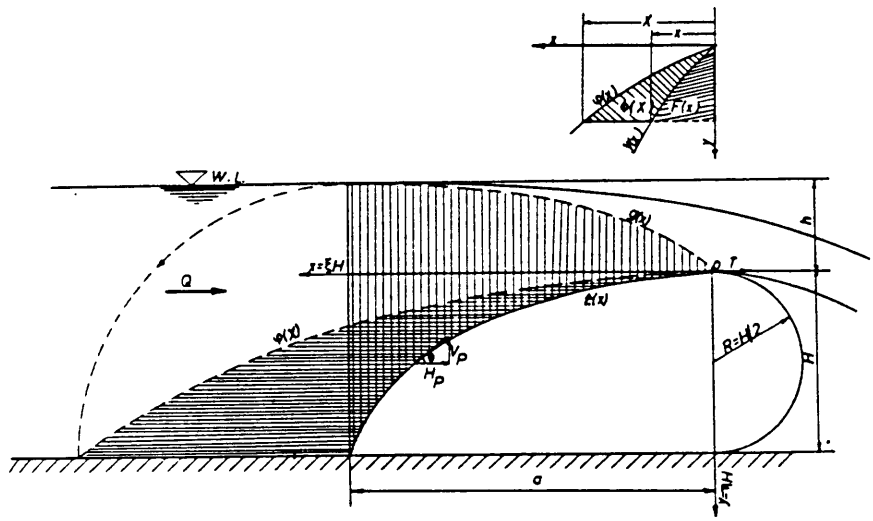

Figure 2. Parameters of inflatable dam for hydrodynamic case [1]

$$
\begin{aligned}
y(x) &= A_1(y)x + A_2(y)x^2 + A_3(y)x^3 + \ldots \\
g(x) &= B_1(y)x + B_2(y)x^2 + B_3(y)x^3 + \ldots \\
\varphi(X) &= C_1(y)X + C_2(y)X^2 + C_3(y)X^3 + \ldots
\end{aligned}
\qquad [2.6]
$$

Anwar is then able to solve equation 2.5 with the aid of a computer. He first tries a solution using only the first term of the series expansion, but the results are unacceptable. The second attempt, substituting in the first two terms of the expansion and boundary conditions

$$
\begin{aligned}
y'(0) = 0 \quad , \quad y(a) = H \ , \\
g'(a) = 0 \quad , \quad g(a) = h \ , \\
\varphi'(0) = 0 \quad , \quad \varphi(a + h + H) = H \ ,
\end{aligned}
\qquad [2.7]
$$

into equation 2.5 yields the non-dimensionalized differential equation

$$
\begin{aligned}
&\left[X'\eta + X\eta' - \frac{X'X^2}{(1+\sigma+\beta)^2} - \xi\eta' - \alpha(\sigma+1)\eta'\right]\eta' + \left[\frac{\alpha}{2}(\sigma+1)X\eta\right. \\
&\left. - \frac{X^3}{3(1+\sigma+\beta)^2} - \xi\eta + \frac{1}{3}\left(\frac{1}{\beta}\right)^2\xi^3 - \alpha(\sigma+1)\eta\right]\eta'' \\
&+ \left[\eta\gamma\xi - \frac{\gamma}{\beta}\xi^2 + \eta - \alpha(\sigma+1)\right] = 0 \ ,
\end{aligned}
\qquad [2.8]
$$

where $(\,)' = \frac{d}{d\xi}$ and $\sigma = \frac{h}{H}$. Results of the numerical solution of equation 2.8 are shown in Figure 3.

Model tests designed to verify the theoretical results were conducted in a glass wall flume 24 inches wide by 20 inches high. The dam was constructed out of commercial polythene and was 12 inches high for the hydrostatic tests. The height was reduced to 9 inches for the hydrodynamic tests.

The measured profiles of the hydrostatic tests were in good agreement with those calculated. Comparisons of these results are shown in Figure 4 and Figure 5.

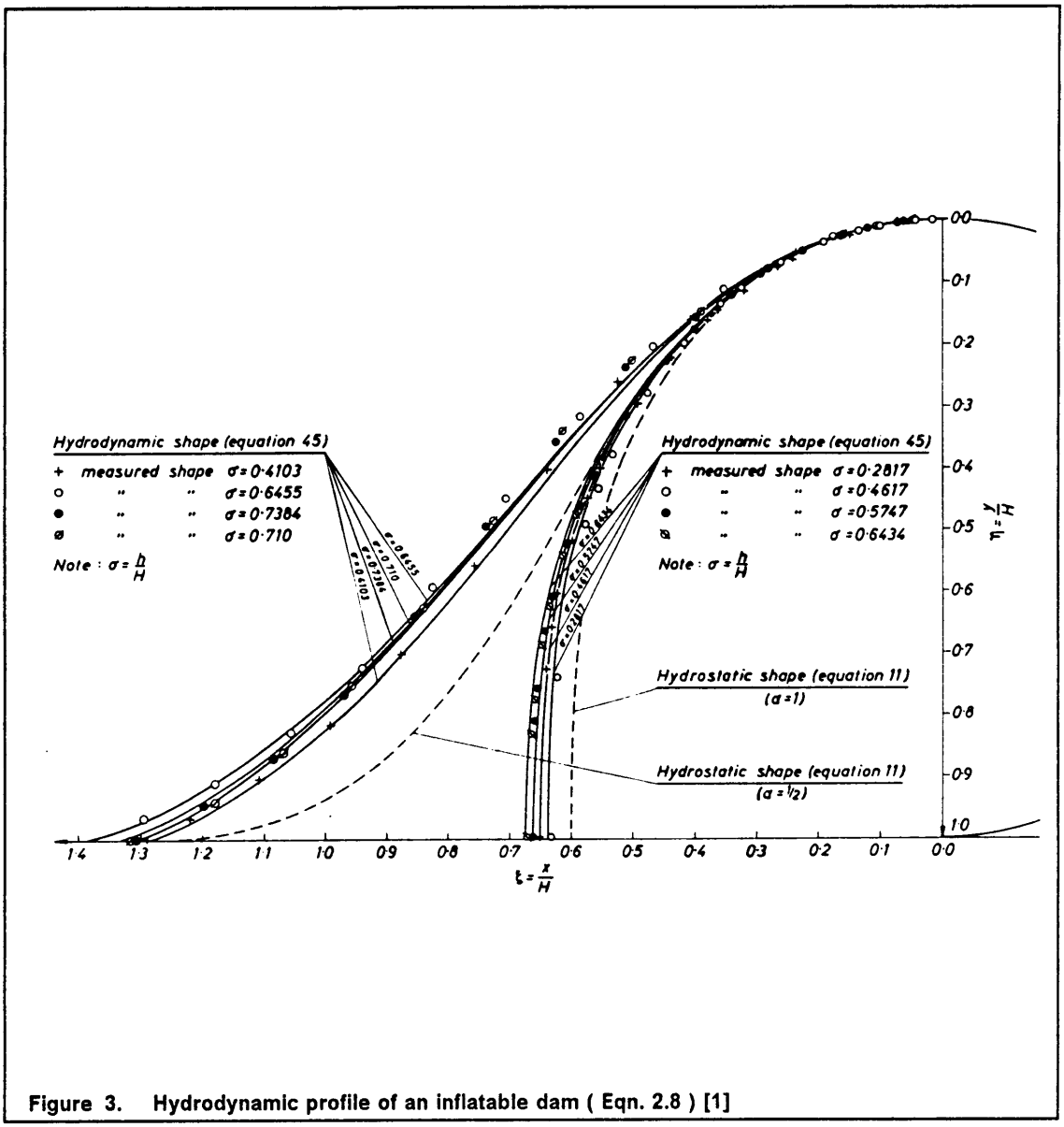

Figure 3. Hydrodynamic profile of an inflatable dam (Eqn. 2.8) [1]

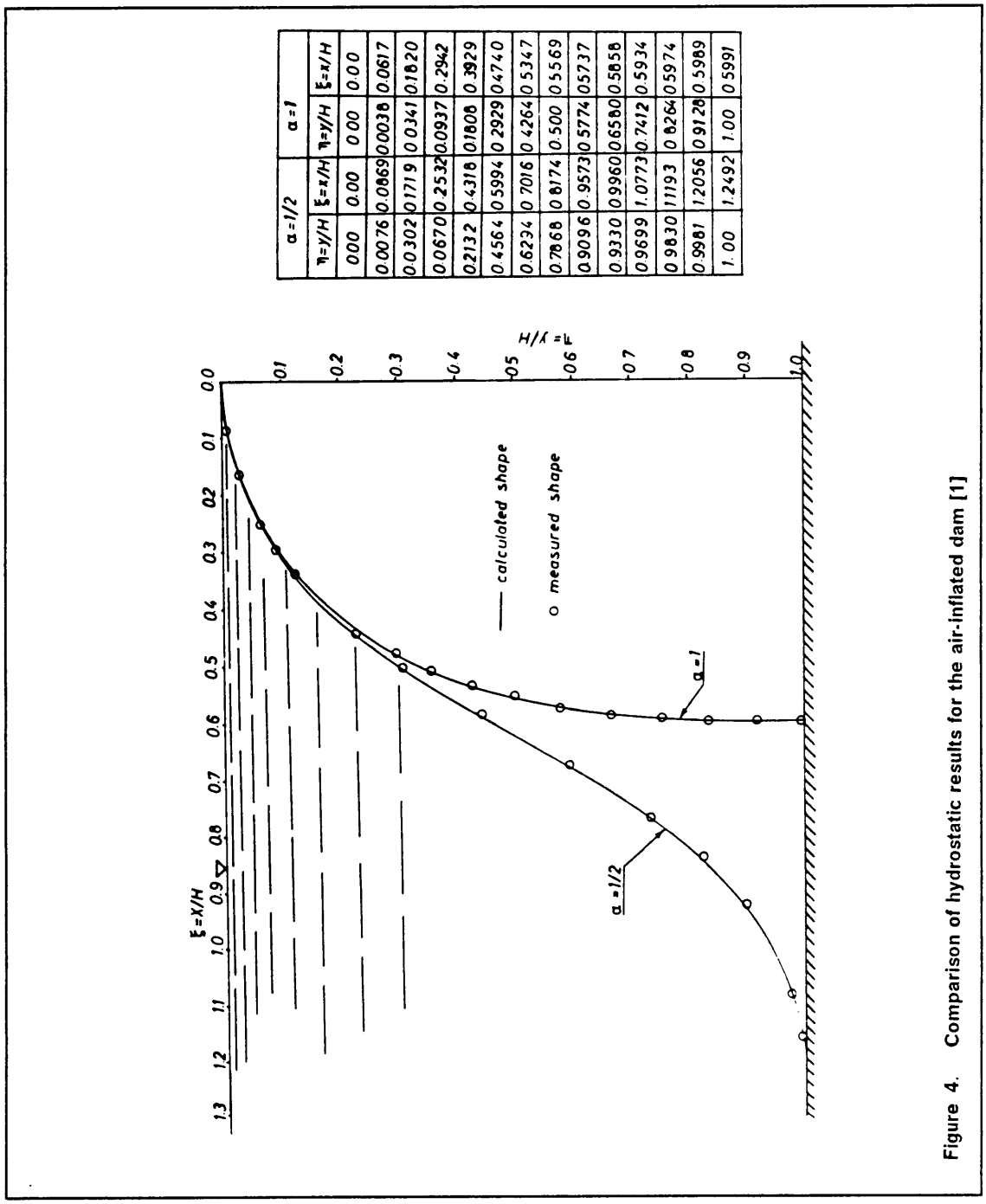

Figure 4. Comparison of hydrostatic results for the air-inflated dam [1]

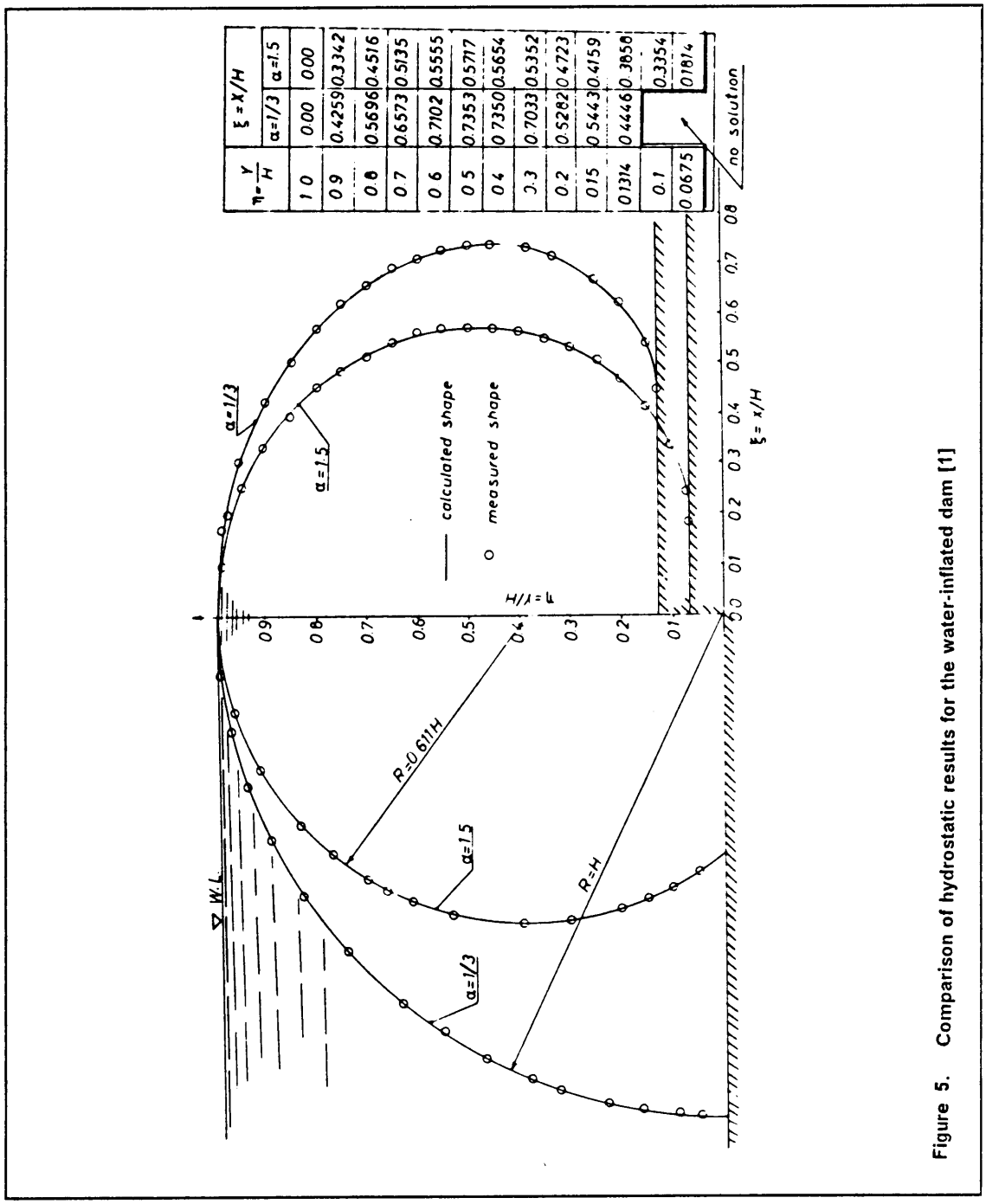

Figure 5. Comparison of hydrostatic results for the water-inflated dam [1]

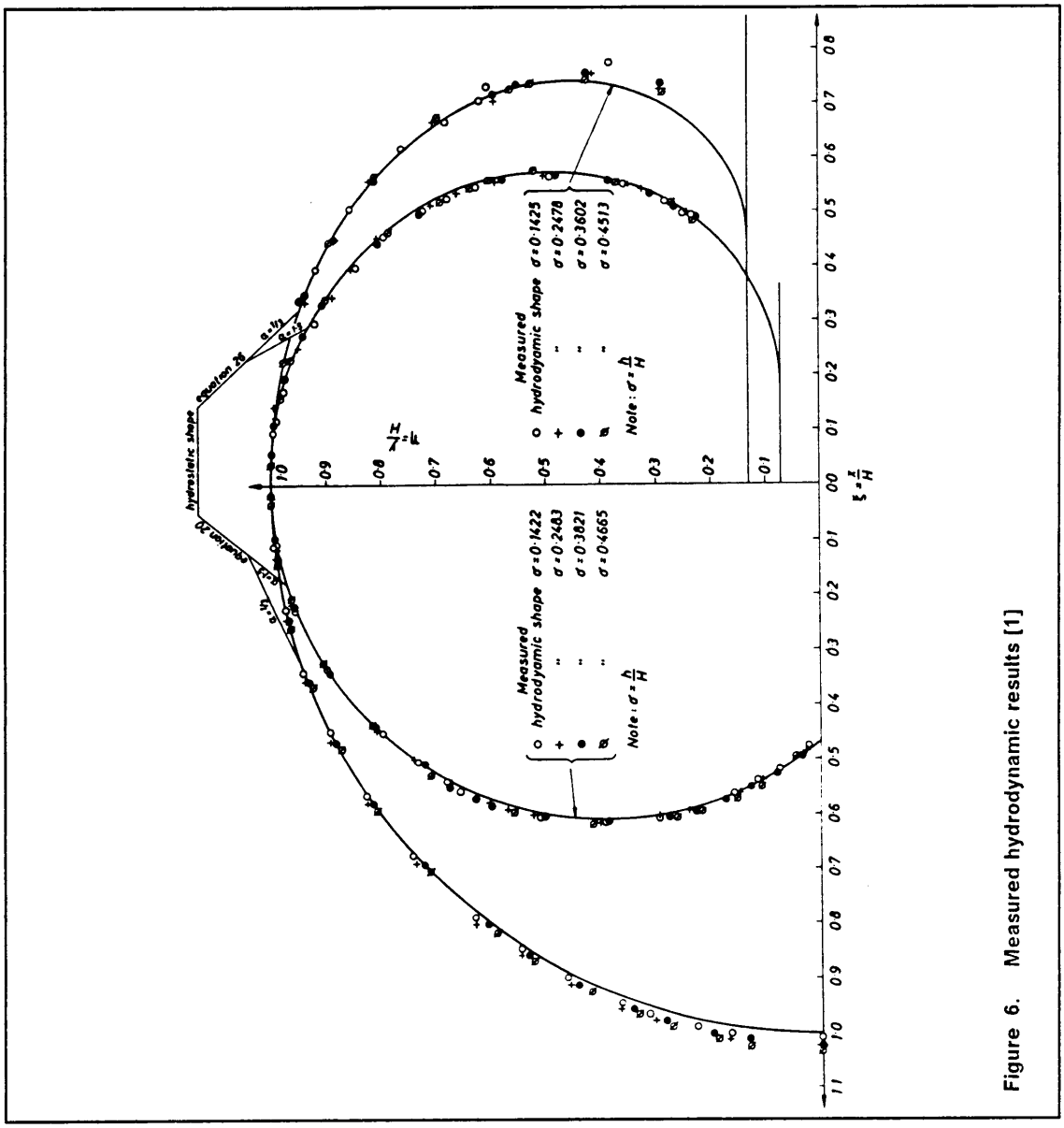

Figure 6. Measured hydrodynamic results [1]

The measured profiles of the hydrodynamic tests are shown in Figure 6. The results show that the hydrodynamic shape of the dam differs from the hydrostatic shape for both the air-, and water-inflated cases. The difference for the water-inflated case occurs when the α factor is less than or equal to 1/3. This shows that the air-inflated dam may not be suitable for a wide range of overflows, and that neither may be suitable for large crest overflows.

In conclusion, Anwar states that the shape of the inflatable dam can be described by the equations he presents in the text of his paper, which are either circular or involve elliptical integrals, depending on the case being considered. Anwar also concludes that, in view of the results of the hydrodynamic tests, use of the water-inflated dam is recommended, as it is less susceptible to vibration, and that inflatable dams are not suitable for applications where a large overflow height is anticipated.

H. B. Harrison

Harrison [6] recognizes that the shape of the inflatable dam is controlled by the external and internal applied loads. This means that the assumption that deformations are small is not valid, thereby making standard methods of analysis not applicable. He presents a numerical method for performing a static stress analysis, that considers the geometric non-linearities of the structure. Harrison uses a finite element model, and considers both an air-inflated dam and a water-inflated dam.

Harrison makes two basic assumptions, first that the behavior of a three-dimensional dam can be adequately represented by a two-dimensional cross section, and second that the perimeter of the cross section can be modelled by an assembly of finite elements, each treated as a straight element with applied forces broken into concentrated loads acting at its ends.

Harrison uses an iterative algorithm to perform his analysis. He first selects trial values for the elemental tension and the upstream incidence angle. Then he resolves the applied forces into concentrated nodal forces and solves the equilibrium equations around the profile of the dam. At the final node he calculates the values of misclosure, the discrepancy between the calculated position of the final node and the toe of the downstream profile, and, using them, he calculates improved initial values. The process is repeated until the calculated coordinates of the last node adequately match those of the toe of the downstream profile of the dam. For convenience, Harrison uses a computer program to implement the solution algorithm.

Harrison conducts his analysis of both the air- and water-inflated dams on the numerical example shown in Figure 7.

The first step in each of the cases is to find what internal pressure is necessary for the dam to be stable. For the water-inflated case Harrison uses the program to determine the relationship between internal head and the dam height. He determines that a minimum of 33 ft. of internal head is required for dam stability. For the air-inflated case he determines that at least 4 lbs./ sq. in. is necessary for the dam height to exceed the upstream water level of 19 ft. He finds that lower values of internal pressure allow the program to converge when a lower upstream water level is considered.

Harrison then considers the response of the dam to a rising upstream head, and plots the variation of the dam shapes. The plots for each case are shown in Figure 8. Harrison finds in each case that the dam appears to resist rising upstream water head by an overall decrease in membrane tension, the air-inflated case even more so than the water-inflated case.

In conclusion, Harrison restates his findings that in order for his alogrithm to converge to a valid solution, the internal pressure must be greater than 33 ft. of head for the water-inflated case and 4 psi. for the air-inflated case. He adds that in both cases the dam appears to resist rising upstream head by decreasing membrane tension. Harrison observes that if the mem-

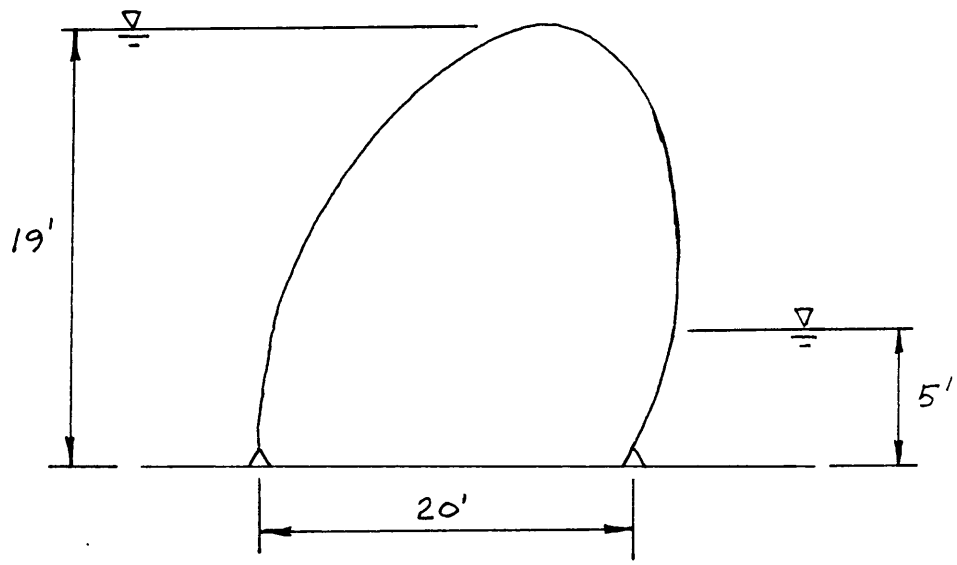

Perimeter Length = 60 feet

Base Length = 20 feet

Upstream Head = 19 feet

Downstream Head = 5 feet

Figure 7. Numerical example used in Harrison's study [6]

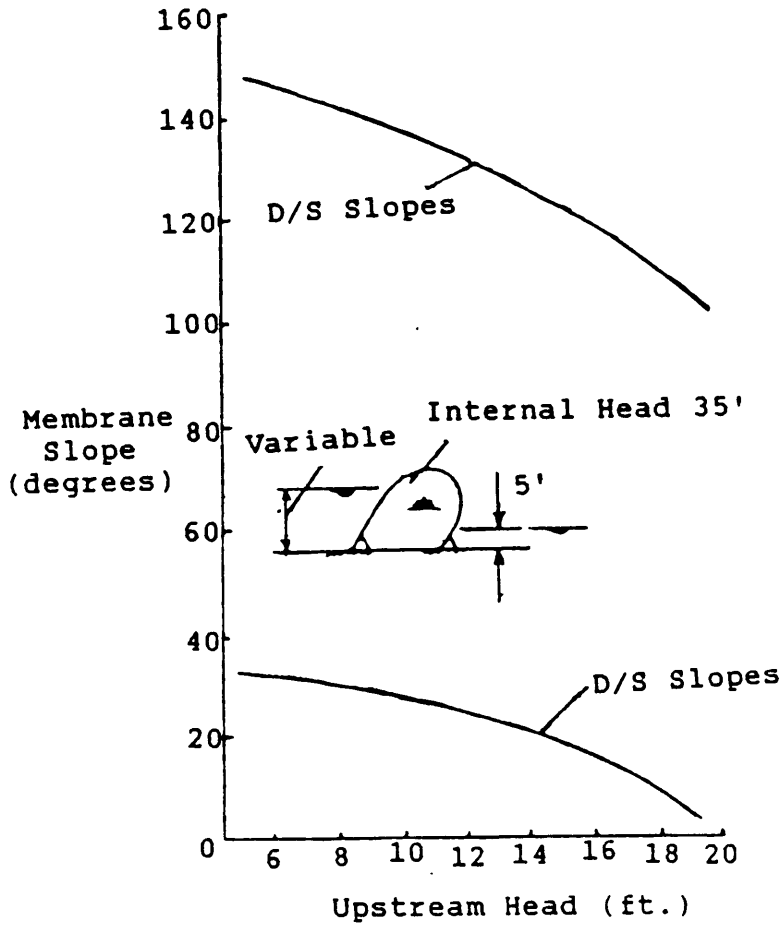

Figure 8. Variation of dam shape due to rising upstream water level [6]

brane is damaged, the risk of explosive failure is greater for the air-inflated case, and suggests that using water inflation would reduce such a risk.

R. D. Parbery

In his first paper, Parbery [12] presents a continuous method for the solution of the equilibrium equation of an inflatable dam under hydrostatic conditions. He conducts his analysis on two numerical examples and compares his results with those of Harrison's analysis.

In order to determine the profile shape and membrane tension, Parbery begins with two assumptions, first, that the dam material has some self-weight, and second, that the dam material has elastic properties, or that there is a strain that is a function of stress.

Beginning with an elemental strip with applied internal and external unit forces, Parbery sums radial and tangential forces. Then, substituting and differentiating, he arrives at an equation that describes the equilibrium shape:

$$\frac{d\varphi}{dS} = -\left[\frac{f\sigma}{(T_o + wy)}\right](p - w\cos\varphi)\,, \qquad [2.9]$$

where φ is the angle between the membrane and the horizontal axis at any point on the dam, S is the distance along the perimeter, f is a length ratio, t is the material thickness, T is the tension in the membrane, w is the membrane weight, and $\sigma = \frac{T}{t}$.

Parbery imposes the following boundary conditions:

$$\begin{aligned} x(0) &= 0 \quad , \quad x(L) = B \,, \\ y(0) &= 0 \quad , \quad y(L) = 0 \,, \end{aligned} \qquad [2.10]$$

where x and y are coordinates which are functions of s, which is the distance along the perimeter of the dam, B is the base length of the dam, and L is the length of the unstretched membrane in the s direction.

Since the equation is nonlinear, an iterative procedure is required for solution. Parbery selects a method that is equivalent to Harrison's method, but states that it may not be suitable when the dam is nearly full, as there may be more than one solution and the membrane may be laid flat at the downstream anchor point. Parbery eliminates these problems by prescribing the angle at the upstream anchor point, solving for upstream head and tension, and writing H as a function of T. The results of Parbery's numerical solution are shown in Figure 9. Parbery's results are in good agreement with Harrison's finite element method results.

In his second paper, Parbery [13] assesses the effect of perimeter length, membrane weight, and elasticity on an air-inflated dam. He derives a closed-form solution to the equilibrium equation that will define the upstream profile of an inflatable dam for varied upstream head.

Parbery states that, for a given base length, the variables that most significantly affect the shape are the method of inflation, the internal pressure, the head of the impounded volume of water, and the dam perimeter. He adds that increasing upstream head results in deformation of the profile, displacement of the profile, and reduction in membrane tension.
The most significant contribution, in terms of interest to this thesis, is Parbery's reassessment of the effects of material weight and elasticity. Parbery calculates a collection of profiles for varied weights and values of elasticity, and finds that the differences between the profiles are negligible. Comparisons of results are shown in Figure 10. Parbery then redevelops his theoretical solution for the upstream profile in a manner very similar to Anwar's, resulting in an equation involving elliptical integrals. This equation is shown as equation 2.11:

Upstream Head (ft)	Internal Head (ft)	Air Pressure (lb/sq.in.)	Tension, lb/ft, by	
			Finite Elements	Continuous Method
5	35	0	16,120	16,117
19	35	0	15,055	15,042
5	5	4	7,612	7,578
19*	5	4	5,924	5,749

Figure 9. Results of numerical solution to equation 2.9 [12]

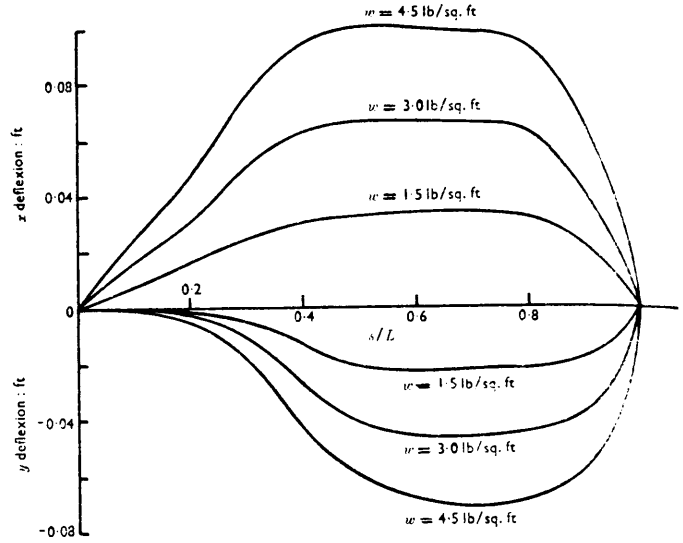

Figure 10. Comparison of profiles for varied weight and elasticity [13]

$$x = \frac{2}{ak}\left\{2\left[E(k,\frac{\varphi_o}{2}) - E(k,\frac{\varphi}{2})\right] + (k^2 - 2)\left[F(k,\frac{\varphi_o}{2}) - F(k,\frac{\varphi}{2})\right]\right\} \qquad [2.11]$$

Parbery states that the downstream profile is circular.

In conclusion, Parbery supports the work of Anwar and Harrison, stating that rising upstream head will change the shape of the dam and cause reduction of membrane tension. He confirms the use of elliptical integrals and circular functions to define the shape of an inflatable dam, and most important to this thesis, he shows that elasticty and self-weight of the membrane can be neglected without significantly affecting the results of the analysis.

G. M. Binnie

Binnie [2] is the author of a paper on static shape finding of inflatable dams, and is also a co-author of a paper discussing the events of the Mangla Dam failure in Pakistan. In the first paper, he discusses Anwar's theories, with which he has some differences. He mentions that Anwar failed to consider the effects of base length and the curved length of the perimeter. Binnie develops equations for a water-inflated dam. His downstream equation includes elliptical integrals and his upstream profile is circular, much the same as Anwar's. Binnie shows his results in tabular form.

In the second paper, Binnie [3], in conjunction with his colleagues Thomas and Gwyther, discusses the events leading up to and after the failure of the Mangla Dam. Much of the paper is of no relation to the topic of this thesis; however, it is interesting to note that the sequence of events includes various dynamic phenomena. Prior to the failure of the dam, longitudinal surges were observed, and attributed to out of phase lateral vibrations along the length of the bag. It was also noted that as the discharge levels increased, the vibrations became more intense, and the dam became unstable. It was concluded after the scale model tests prior to

construction of the dam, that vibrations could be damped out by fluctuating the inflation levels; however, it was discovered during the failure that this was only a temporary remedy for the uncontrolled vibrations.

Binnie and colleagues conclude that, although the concept of inflatable dams should not be discarded because of this failure, care should be exercised in their design and extra strength should be provided to account for unforeseen modes of vibration.

V. Firt

Firt's [5] text on air-supported structures is one of the more comprehensive discussions of the subject available. He covers all the areas pertaining to these types of stuctures. The first half of the book deals with statics and formfinding of air-supported structures. Firt presents the fundamental geometric relationships of the theory of surfaces, and goes on to develop the equilibrium equations for various types of surfaces. The portion dealing with cylindrical surfaces relates more closely to this thesis. Firt discusses equilibrium equations, snow loads, wind loads, necessary internal overpressure, and deformation for the cylindrical inflated membrane. Then he discusses shape finding of the same types of structures.

Of closer relation to the topic of this thesis is the second part of the book, dynamic analysis of air-supported membranes, and particularly the section dealing with cylindrical membranes. Firt presents the derivation of differential equations describing the free vibration of a cylindrical membrane. The solution of this equation is of particular interest as it is similar to the efforts of the author of this thesis, and Firt's results will be used for comparison. The following paragraphs will present a more detailed description of Firt's dynamic analysis of the air-inflated cylindrical membrane.

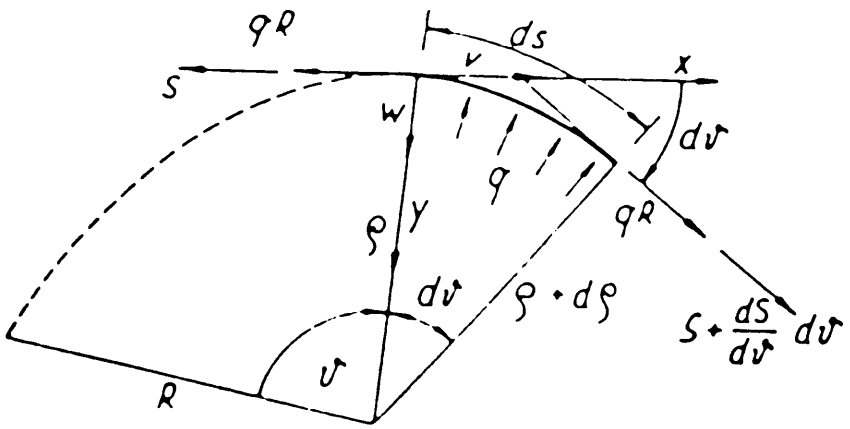

Figure 11. Elemental model for derivation of equation 2.20 [5]

Firt's derivation of the differential equation defining the free vibration of the cylindrical membrane is based on the model shown in Figure 11. The cylindrical membrane is comprised of an assembly of circular arcs, and the circular element, ds, in the figure represents a membrane strip of unit width. Summing forces in both the x and y directions yields two dynamic equilibrium equations:

$$-\bar{S} - qR + (\bar{S} + \frac{\partial \bar{S}}{\partial \theta} d\theta + qR)\cos d\theta - \mu ds \frac{\partial^2 \bar{v}}{\partial t^2} = 0 \qquad [2.12]$$

$$(\bar{S} + qR)\cos(\frac{\pi}{2} - d\theta) - qds - \mu ds \frac{\partial^2 \bar{w}}{\partial t^2} = 0 \qquad [2.13]$$

where qR is the static force and $\mu ds \partial^2 \bar{v}/\partial t^2$ and $\mu ds \partial^2 \bar{w}/\partial t^2$ are the inertial forces in the x and y directions, respectively. The bar indicates that the quantity is a function of both the angle, θ, and time.

Making the approximation that dynamic deflections are small, Firt reduces the equilibrium equations to

$$\frac{\partial \bar{S}}{\bar{\rho} \partial \theta} - \mu \frac{\partial^2 \bar{v}}{\partial t^2} = 0 \ , \qquad [2.14]$$

$$\frac{1}{\bar{\rho}} \bar{S} + q(\frac{R}{\bar{\rho}} - 1) - \mu \frac{\partial^2 \bar{w}}{\partial t^2} = 0 \ . \qquad [2.15]$$

Neglecting elongation during vibrations, the following geometric relations are true for a circular arc:

$$\frac{1}{\rho} = (1 + \frac{\partial \bar{\varphi}}{\partial \theta})\frac{1}{R} \quad , \quad \bar{w} = \frac{\partial \bar{v}}{\partial \theta} \ , \qquad [2.16]$$
$$\bar{\varphi} = \frac{1}{R}(\frac{\partial \bar{w}}{\partial \theta} + \int \bar{w} d\theta) \ ,$$

and therefore,

$$\frac{1}{\bar{\rho}} = \frac{1}{R}\left(1 + \frac{1}{R}\frac{\partial^2 \bar{w}}{\partial \theta^2} + \frac{1}{R}\bar{w}\right) . \qquad [2.17]$$

Substitution of equation 2.16 into equations 2.14 and 2.15 yields

$$\frac{1}{R}\frac{\partial^2 \bar{S}}{\partial \theta^2} - \mu\frac{\partial^2 \bar{w}}{\partial t^2} = 0 , \qquad [2.18]$$

$$\frac{1}{R}\bar{S} + \frac{q}{R}\left(\frac{\partial^2 \bar{w}}{\partial \theta^2} + \bar{w}\right) - \mu\frac{\partial^2 \bar{w}}{\partial t^2} = 0 . \qquad [2.19]$$

After elimination of $\bar{S}$, Firt obtains the differential equation for the radial deflection of a freely vibrating cylindrical membrane:

$$\frac{\partial^4 \bar{w}}{\partial \theta^4} + \frac{\partial^2}{\partial \theta^2}\left(\bar{w} - \frac{\mu R}{q}\frac{\partial^2 \bar{w}}{\partial t^2}\right) + \frac{\mu R}{q}\frac{\partial^2 \bar{w}}{\partial t^2} = 0 \qquad [2.20]$$

This equation is satisfied by the solution $\bar{w} = w\sin\omega t$, where w is the amplitude of the radial deflection and ω is the angular frequency. Substituting this solution into equation 2.20, Firt obtains the fourth order ordinary differential equation for the radial deflection,

$$\frac{d^4 w}{d\theta^4} + (1 + \lambda)\frac{d^2 w}{d\theta^2} - \lambda w = 0 , \qquad [2.21]$$

where $\lambda = \mu\omega^2 R/q$.

Next Firt presents the general solution to equation 2.21. He writes the characteristic equation of equation 2.21 as

$$\beta^4 + (1 + \lambda)\beta^2 - \lambda = 0 . \qquad [2.22]$$

This equation has the roots

$$\beta_{1,2} = \pm \frac{i}{\sqrt{2}} \sqrt{1 + \lambda + \sqrt{1 + 6\lambda + \lambda^2}} \ ,$$
$$\beta_{3,4} = \pm \frac{i}{\sqrt{2}} \sqrt{-1 - \lambda + \sqrt{1 + 6\lambda + \lambda^2}} \ , \qquad [2.23]$$

where $i = \sqrt{-1}$. Firt writes the general form of the solution for w as

$$w = C_1 \sin a\frac{\theta}{\alpha} + C_2 \cos a\frac{\theta}{\alpha} + C_3 \sinh b\frac{\theta}{\alpha} + C_4 \cosh b\frac{\theta}{\alpha} \ , \qquad [2.24]$$

where α is the central angle of the circular arc under consideration. To obtain an expression for v, Firt integrates equation 2.24 since $\overline{w} = \partial\overline{v}/\partial\theta$ is known from equation 2.16. This yields

$$v = -C_1\frac{\alpha}{a} \cos a\frac{\theta}{\alpha} + C_2\frac{\alpha}{a} \sin a\frac{\theta}{\alpha} + C_3\frac{\alpha}{b} \cosh b\frac{\theta}{\alpha} + C_4\frac{\alpha}{b} \sinh b\frac{\theta}{\alpha} + C_5 \ . \qquad [2.25]$$

Firt states that $C_5 = 0$ as it represents the displacement of the arc due to rotation around its center, and due to the nature of the anchoring of the structure, this type of rotation cannot occur.

Substituting equations 2.24 and 2.25 with $\theta = 0$ and $\theta = \alpha$ into the boundary conditions,

$$w(0) = 0 \ , \ w(\alpha) = 0 \ ,$$
$$v(0) = 0 \ , \ v(\alpha) = 0 \ , \qquad [2.26]$$

Firt obtains the homogeneous algebraic system from which he can determine the characteristic numbers for the differential equation:

$$\begin{bmatrix} 0 & 1 & 0 & 1 \\ \sin a & \cos a & \sinh b & \cosh b \\ -1/a & 0 & 1/b & 0 \\ -\dfrac{\cos a}{a} & \dfrac{\sin a}{a} & \dfrac{\cosh b}{b} & \dfrac{\sinh b}{b} \end{bmatrix} \begin{bmatrix} C_1 \\ C_2 \\ C_3 \\ C_4 \end{bmatrix} = 0 \ . \qquad [2.27]$$

Firt obtains the characteristic equation for this system by successive elimination of the integration constants from the equations. He obtains

$$2(1 - \cos a \cosh b) + \frac{b^2 - a^2}{ab} \sin a \sinh b = 0 \ . \qquad [2.28]$$

From this equation, Firt determines the first four characteristic values for the cylindrical membrane with a central angle $\alpha = \pi$:

$$\lambda_1 = 1.71 \quad \lambda_2 = 5.97 \quad \lambda_3 = 13.07 \quad \lambda_4 = 21.86 \qquad [2.29]$$

The equation for λ, in terms of ω, and the relationship between ω and f, the frequency, are known: $\lambda = \mu\omega^2 R/q$, and $f = \frac{\omega}{2\pi}$, Firt calculates angular frequencies and natural frequencies for modes one through four and $q = 150N/m^2$, $R = 10m$, and $\mu = 1kg/m^2$:

$$\begin{aligned} \omega_1 &= 5.06 \frac{1}{\text{sec}} & f_1 &= 0.81 \frac{1}{\text{sec}} \\ \omega_2 &= 9.46 \frac{1}{\text{sec}} & f_2 &= 1.51 \frac{1}{\text{sec}} \\ \omega_3 &= 13.99 \frac{1}{\text{sec}} & f_3 &= 2.22 \frac{1}{\text{sec}} \\ \omega_4 &= 18.12 \frac{1}{\text{sec}} & f_4 &= 2.89 \frac{1}{\text{sec}} \end{aligned} \qquad [2.30]$$

Firt presents an alternative method of determining the natural frequencies for a cylindrical membrane, which he calls the semi-deformation method. First, he derives the fundamental semi-deformation equations; then, he applies them to a numerical example.

Four unknowns are introduced, w_i, v_i, w_j, and v_j. These are the displacements at the ends of a circular arc, and they are shown in Figure 12 in their positive senses. The constants, C_1, C_2, C_3, and C_4, are eliminated from the derivation by writing them in terms of w and v and substituting them into equations 2.24 and 2.25. This results in expressions for the four constants in terms of w_i, w_j, v_i, v_j, α, a, and b. Substituting equations 2.24 and 2.25 into the third expression of equation 2.16, then substituting the expressions for the constants into the result, Firt obtains the first two semi-deformation equations:

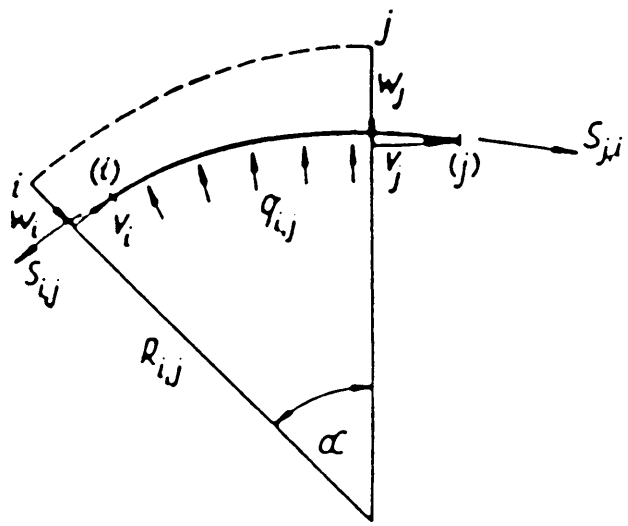

Figure 12. Elemental model for semi-deformation equations [5]

$$\varphi_{i,j} = \frac{1}{R_{i,j}}\left[- Aw_i - Bw_j - Cv_i + Dv_j\right],$$
$$\varphi_{j,i} = \frac{1}{R_{i,j}}\left[Bw_i + Aw_j + Dv_i - Cv_j\right], \qquad [2.31]$$

where i and j indicate the start and end of the element under study, and A, B, C, and D are complex algebraic expressions that are functions of the non-dimensional parameters α and λ. Since Firt has previously assumed harmonic motion, substituting $\overline{w} = w \sin \omega t$ and $\overline{S} = S \sin \omega t$ into equation 2.19, he obtains

$$S = - q\left[\frac{d^2w}{d\theta^2} + (1 + \lambda)w\right] . \qquad [2.32]$$

Substituting the expressions derived for the constants, C_1 through C_4, with $\theta = 0$ and $\theta = \alpha$, into the equations 2.24 and 2.25, and then substituting the result into equation 2.32, he obtains the second two semi-deformation equations:

$$S_{i,j} = q_{i,j}\left[- Ew_i - Fw_j - Gv_i + Hv_j\right]$$
$$S_{i,j} = q_{i,j}\left[- Fw_i - Ew_j - Hv_i + Gv_j\right] \qquad [2.33]$$

where E, F, G, and H are also complex algebraic expressions that are functions of the non-dimensional parameters α and λ.

The structure that Firt analyzes in the numerical example is shown in Figure 13. The following input parameters are used:

$$v_o = 15\, m/\sec\,,\ q_o = 200\, N/m,\ \mu = 1\, kg/m^2\,,$$
$$R = 10\, m,\ \alpha = \pi\,.$$

Firt calculates the radial wind loads:

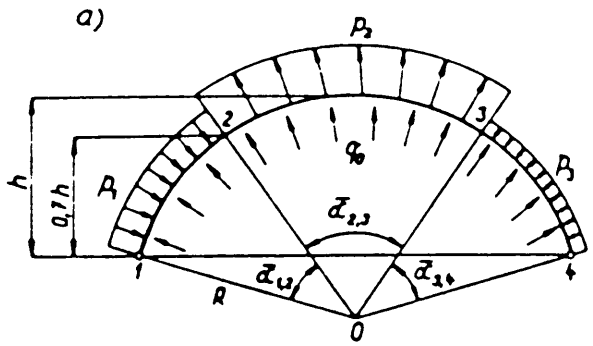

Figure 13. Numerical example for semi-deformation method [5]

$$p_1 = -98.4\, N/m^2,$$
$$p_2 = 168.75\, N/m^2,$$
$$p_3 = 56.25\, N/m^2.$$

From these initial values, Firt proceeds through the steps of the calculation that are required to specialize the semi-deformation equations to his specific numerical example. He calculates all the quantities for the three segments of the membrane, and using $\lambda = \mu\omega^2 R/q$ and $f = \omega/2\pi$, he computes the frequencies:

$$\begin{aligned} \omega_1 &= 8.46\ \text{sec}^{-1} & f_1 &= 1.35\ \text{sec}^{-1} \\ \omega_2 &= 16.187\ \text{sec}^{-1} & f_2 &= 2.58\ \text{sec}^{-1} \\ \omega_3 &= 22.47\ \text{sec}^{-1} & f_3 &= 3.58\ \text{sec}^{-1}. \end{aligned} \qquad [2.34]$$

Others

Other work on the dynamic behavior of inflatable dams has been done by Fagan [4] and Hsieh [8] at the Virginia Polytechnic Institute and State University. This work has either recently been done or is still in progress. Fagan has recently shown that the effects of the self-weight are negligble, and Hsieh, in the process of his work, has calculated the following natural frequencies:

$$
\begin{array}{cc}
\underline{\alpha = \pi/2} & \\
\lambda_1 = 12.6182 & \omega_1 = 3.5522 \\
\lambda_2 = 30.1920 & \omega_2 = 5.4947 \\
\lambda_3 = 60.3991 & \omega_3 = 7.7717 \\
\lambda_4 = 94.1245 & \omega_4 = 9.7018 \\
\underline{\alpha = \pi} & \\
\lambda_1 = 1.7040 & \omega_1 = 1.3054 \\
\lambda_2 = 5.9622 & \omega_2 = 2.4418 \\
\lambda_3 = 13.0526 & \omega_3 = 3.6128 \\
\lambda_4 = 21.7363 & \omega_4 = 4.8114 \\
\underline{\alpha = 3\pi/2} & \\
\lambda_1 = 0.2872 & \omega_1 = 0.5359 \\
\lambda_2 = 1.8037 & \omega_2 = 1.3430 \\
\lambda_3 = 4.6862 & \omega_3 = 2.1648 \\
\lambda_4 = 8.5026 & \omega_4 = 2.9159
\end{array}
\qquad [2.35]
$$

where λ and ω are non-dimensionalized and $\lambda = \omega^2$.

Method of Analysis

Introduction

To perform the analysis, the initial parameters of the inflatable dam must first be defined. The structure considered in this chapter is a cylindrical membrane of radius R and mass μ per unit length. The initial circular shape of the membrane is supported by a constant internal air pressure, q, with no external loads applied. This represents the static equilibrium state of the inflatable dam. An illustration of the analysis model is shown in Figure 14.

Three basic assumptions are made to define the mathematical model. First, it is assumed that the material weight is negligible. The mass of the membrane is considered when writing the dynamic equations; however, the work by Parbery [13] and Fagan [4] shows that the weight has little effect on the response of the inflatable dam. Second, it is assumed that the material is inextensible. Parbery's work also supports this assumption. And third, it is assumed that the dam is sufficiently long so that a strip of unit width can be used to represent the three-dimensional structure. Three-dimensional effects will not be considered in this thesis.

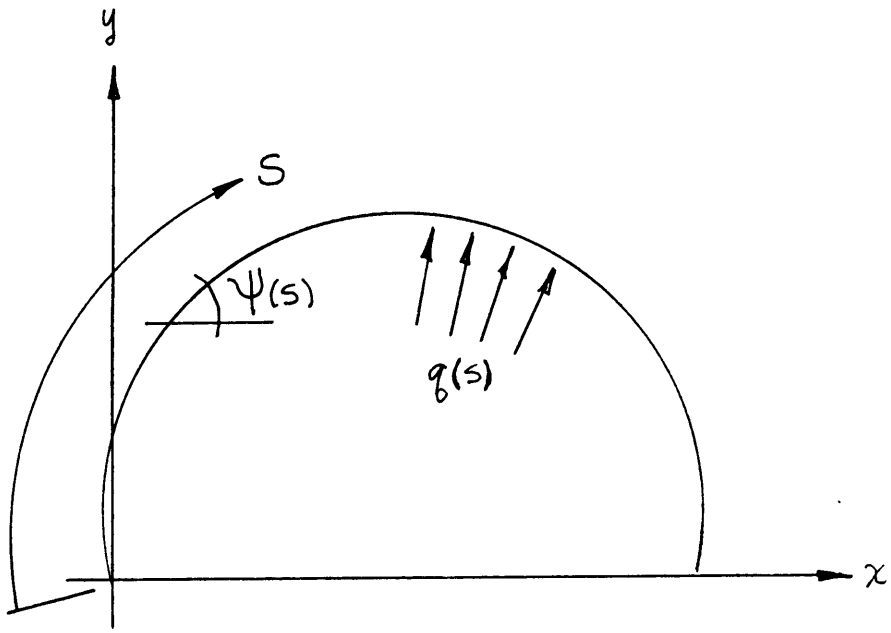

Figure 14. Model of the inflatable dam for analysis

Derivation of Equation of Motion

Statics - The model for the general static case is shown in Figure 15. $\Psi_o(S)$ is the angle defining the shape of the dam, S is the distance along the perimeter, and T_o is the tension in the membrane. The subscript indicates that the parameter pertains to the static case.

Summing tangential forces shows that T_o must be constant. Summing forces in the radial direction yields

$$T_o = qR\,. \qquad [3.1]$$

Geometrically, the following are true for the static model:

$$\frac{d\Psi_o}{dS} = -\frac{1}{R}\,,\ \frac{dx}{dS} = \cos\Psi_o\,,\ \frac{dy}{dS} = \sin\Psi_o\,. \qquad [3.2]$$

Substituting equation 3.1 into equation 3.2, the static equations become

$$\frac{d\Psi_o(S)}{dS} = -\frac{q(S)}{T_o}\,,\ \frac{dx}{dS} = \cos\Psi_o\,,\ \frac{dy}{dS} = \sin\Psi_o\,. \qquad [3.3]$$

Henceforth, the coordinates x and y for the static case will be written x_o and y_o.

Dynamics - The model for the dynamic case is shown in Figure 16, where N is the undeformed length, M is the deformed length, w is the radial displacement, and v is the tangential displacement. The strain in the tangential direction can be derived as follows:

$$\varepsilon = \frac{M-N}{N},\quad N = Rd\Psi,\quad M = (R-w)d\Psi + (v+dv)\frac{(R-w)}{R} - \frac{(R-w)}{R}v.$$

Substituting the expressions for M and N into the expression for ε yields

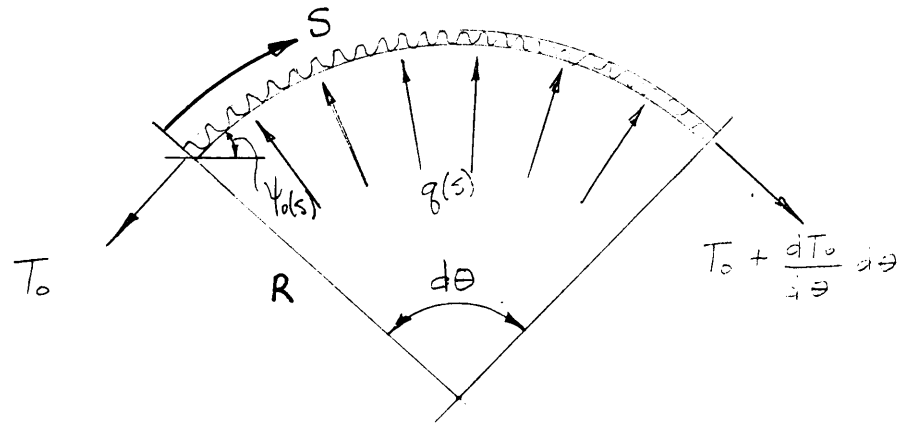

Figure 15. Static model of the inflatable dam for analysis

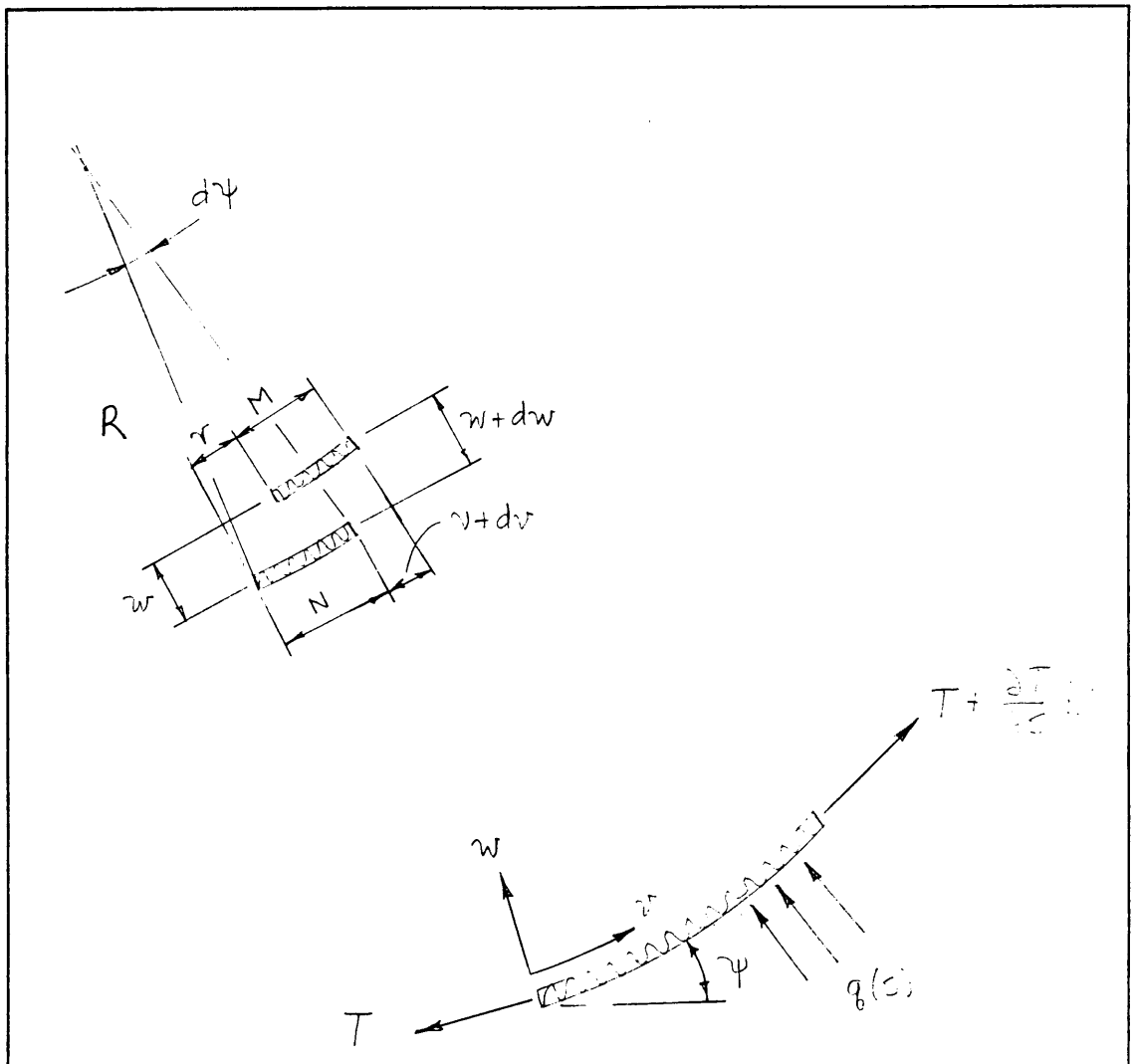

Figure 16. Dynamic model of the inflatable dam for analysis

$$\varepsilon = \frac{1}{R}\left[- w + \frac{dv}{d\Psi}\left(1 - \frac{w}{R}\right)\right], \qquad [3.4]$$

where $\frac{w}{R}$ is small and is therefore neglected. As the assumption that the membrane is inextensible has been made, $\varepsilon = 0$, and equation 3.4 leads to

$$w = \frac{dv}{d\Psi}. \qquad [3.5]$$

Summing inertial and static forces in the tangential direction yields

$$\mu dS\frac{\partial^2 v}{\partial t^2} = (T + \frac{\partial T}{\partial S}dS + qR)\cos d\Psi - T - qR. \qquad [3.6]$$

Assuming that $d\Psi$ is small one can let $\cos d\Psi = 1$. Equation 3.6 reduces to

$$\mu\frac{\partial^2 v}{\partial t^2} = \frac{\partial T}{\partial S}. \qquad [3.7]$$

Summing inertial and static forces in the radial direction yields

$$\mu dS\frac{\partial^2 w}{\partial t^2} = qdS + (T + \frac{\partial T}{\partial S}dS)\frac{d\Psi}{2} + T\frac{d\Psi}{2}, \qquad [3.8]$$

which reduces to

$$\mu\frac{\partial^2 w}{\partial t^2} = q + T\frac{\partial \Psi}{\partial S}. \qquad [3.9]$$

Differentiating equation 3.7 with respect to Ψ and substituting in equation 3.5 into the resulting expression yields

$$\mu\frac{\partial^2 w}{\partial t^2} = \frac{\partial}{\partial \Psi}\left[\frac{\partial T}{\partial S}\right]. \qquad [3.10]$$

Solving equation 3.9 for T yields

$$T = \left(\frac{\partial \Psi}{\partial S}\right)^{-1}\left[\mu\frac{\partial^2 w}{\partial t^2} - q\right]. \qquad [3.11]$$

Differentiating equation 3.11 with respect to S yields

$$\frac{\partial T}{\partial S} = -\left(\frac{\partial \Psi}{\partial S}\right)^{-2}\frac{\partial^2 \Psi}{\partial S^2}\left[\mu\frac{\partial^2 w}{\partial t^2} - q\right] + \left(\frac{\partial \Psi}{\partial S}\right)^{-1}\left[\mu\frac{\partial^3 w}{\partial S \partial t^2} - \frac{\partial q}{\partial S}\right]. \qquad [3.12]$$

Substituting equation 3.12 into equation 3.10 yields

$$\mu\frac{\partial^2 w}{\partial t^2} = \left[2\left(\frac{\partial \Psi}{\partial S}\right)^{-4}\left(\frac{\partial^2 \Psi}{\partial S^2}\right)^2 - \left(\frac{\partial \Psi}{\partial S}\right)^{-3}\frac{\partial^3 \Psi}{\partial S^3}\right]\left[\mu\frac{\partial^2 w}{\partial t^2} - q\right] - 2\left(\frac{\partial \Psi}{\partial S}\right)^{-3}\frac{\partial^2 \Psi}{\partial S^2}\left[\mu\frac{\partial^3 w}{\partial S \partial t^2} - \frac{\partial q}{\partial S}\right] + \left(\frac{\partial \Psi}{\partial S}\right)^{-2}\left[\mu\frac{\partial^4 w}{\partial S^2 \partial t^2} - \frac{\partial^2 q}{\partial S^2}\right]. \qquad [3.13]$$

Now, to relate Ψ to Ψ_o, w, and v, an expression is taken from Henrych's book on the dynamics of frames and arches [7]. Henrych writes, in his own notation,

$$\frac{\partial \Phi}{\partial S} = \frac{\partial \Phi_o}{\partial S} + \frac{1}{K}\left[\frac{\partial^2 v}{\partial S^2} + \frac{1}{R^2}v + \frac{d}{dS}\left(\frac{1}{R}\right)u\right], \qquad [3.14]$$

where, in the notation of this thesis, $K = 1 + \frac{\partial v}{\partial S} - \frac{\partial \Psi_o}{\partial S}w$, $\frac{1}{R} = -\frac{d\Psi_o}{dS}$, $v = -w$, $u = v$, $\frac{\partial \Phi}{\partial S} = -\frac{\partial \Psi}{\partial S}$, and $\frac{d\Phi_o}{dS} = -\frac{d\Psi_o}{dS}$. Using the expressions above and equation 3.5, equation 3.14 is rewritten as

$$\frac{\partial \Psi}{\partial S} = \frac{d\Psi_o}{dS} + \frac{\partial^2 w}{\partial S^2} + \left(\frac{d\Psi_o}{dS}\right)^2 w + \frac{d^2\Psi_o}{dS^2}v. \qquad [3.15]$$

For the sake of simplicity, the notation is changed to subscript notation, where $(\ )_{st} = \frac{\partial^2}{\partial s \partial t}(\ )$. Also, the following substitutions are made:

$$A = \frac{d\Psi_o}{dS},\ B = \frac{d^2\Psi_o}{dS^2},\ C = \frac{d^3\Psi_o}{dS^3},\ D = \frac{d^4\Psi_o}{dS^4}. \qquad [3.16]$$

Substituting equation 3.15 into equation 3.13, neglecting non-linear terms, and making use of equation 3.5 yields the equation for the static shape, Ψ_o:

$$-(2A^{-4}B^2 - A^{-3}C)q + 2A^{-3}Bq_s - A^{-2}q_{ss} = 0. \qquad [3.17]$$

If q, the internal pressure, is constant, then the term A is constant and the shape is circular.

To obtain the dynamic equation, equation 3.15 is rewritten as

$$\Psi_s = A + w_{ss} + A^2 w, \qquad [3.18]$$

since q is constant and therefore it is known that B, C, and D are zero. Then multiplying equation 3.13 by Ψ_s^4 yields

$$\begin{aligned}\Psi_s^4 \mu w_{tt} = &\left[2\Psi_{ss}^2 - \Psi_s\Psi_{ssss}\right](\mu w_{tt} - q) \\ &- 2\Psi_s\Psi_{ss}\,\mu w_{stt} + \Psi_s^2\,\mu w_{sstt}.\end{aligned} \qquad [3.19]$$

Substituting equation 3.18 into equation 3.19 yields

$$\begin{aligned}0 = &(A^4 + 4A^3 w_{ss} + 4A^5 w + 6A^2 w_{ss}^2 + 6A^6 w^2 + 12A^4 w w_{ss})\mu w_{tt} \\ &+ (A w_{ssss} + A^3 w_{ss} + A^2 w_{ss}^2 + A^4 w w_{ss} + A^2 w w_{ssss} + w_{ss} w_{ssss} \\ &- 2w_{sss}^2 - 4A^2 w_s w_{sss} - 2A^4 w_s^2)(\mu w_{tt} - q) \\ &+ 2(A w_{sss} + A^3 w_s + w_{ss} w_{sss} + A^2 w_s w_{ss} + A^2 w w_{sss} + A^4 w w_s)\mu w_{stt} \\ &- (A^2 + 2A w_{ss} + 2A^3 w + w_{ss}^2 + A^4 w^2 + 2A^2 w w_{ss})\mu w_{sstt},\end{aligned} \qquad [3.20]$$

where terms in w of third order and higher are neglected. Using the expressions $S = R\theta$, $A = -\frac{1}{R}$, $w = RW$, and $t = \sqrt{\mu R/q}\,T$, and knowing that R is constant, equation 3.20 is non-dimensionalized. This yields the equation of motion that is to be solved using the Galerkin approximation method:

$$
\begin{aligned}
0 = {} & (1 - 4W_{\theta\theta} - 4W + 6W_{\theta\theta}^2 + 6W^2 + 12WW_{\theta\theta})W_{TT} \\
& + (- W_{\theta\theta\theta\theta} - W_{\theta\theta} + W_{\theta\theta}^2 + WW_{\theta\theta} + WW_{\theta\theta\theta\theta} + W_{\theta\theta}W_{\theta\theta\theta\theta} \\
& - 2W_{\theta\theta\theta}^2 - 4W_{\theta}W_{\theta\theta\theta} - 2W_{\theta}^2)(W_{TT} - 1) \\
& + 2(- W_{\theta\theta\theta} - W_{\theta} + W_{\theta\theta}W_{\theta\theta\theta} + W_{\theta}W_{\theta\theta} + WW_{\theta\theta\theta} \\
& + WW_{\theta})W_{\theta TT} \\
& - (1 - 2W_{\theta\theta} - 2W + W_{\theta\theta}^2 + W^2 + 2WW_{\theta\theta})W_{\theta\theta TT} .
\end{aligned}
\qquad [3.21]
$$

The non-dimensional terms are illustrated in Figure 17.

Solution of Equation of Motion

One-term solution - The one-term Galerkin approximation for the solution to equation 3.21 is assumed to be

$$W_a = u(T)F(\theta) , \qquad [3.22]$$

where u is a non-dimensional displacement that is a function of time, and F is a chosen function of θ that satisfies the essential and natural boundary conditions of the cylindrical membrane.

A sine function is selected for the function F, and is written

$$F(\theta) = \sin\left(\frac{n\pi\theta}{\alpha}\right) , \qquad [3.23]$$

where α is the central angle of the cylindrical membrane and n varies from 2 to 5. The assumed deflected shapes for $\alpha = \pi$ are shown in Figure 18. The general form of the equation for the Galerkin approximation method is

$$0 = \int_0^{\alpha} F(\theta)\ R(W_a(\theta,T))\ d\theta , \qquad [3.24]$$

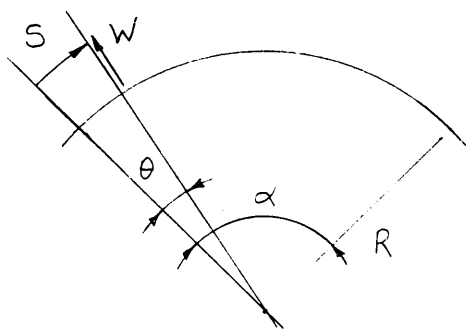

Figure 17. Illustration of non-dimensional terms in equation 3.21

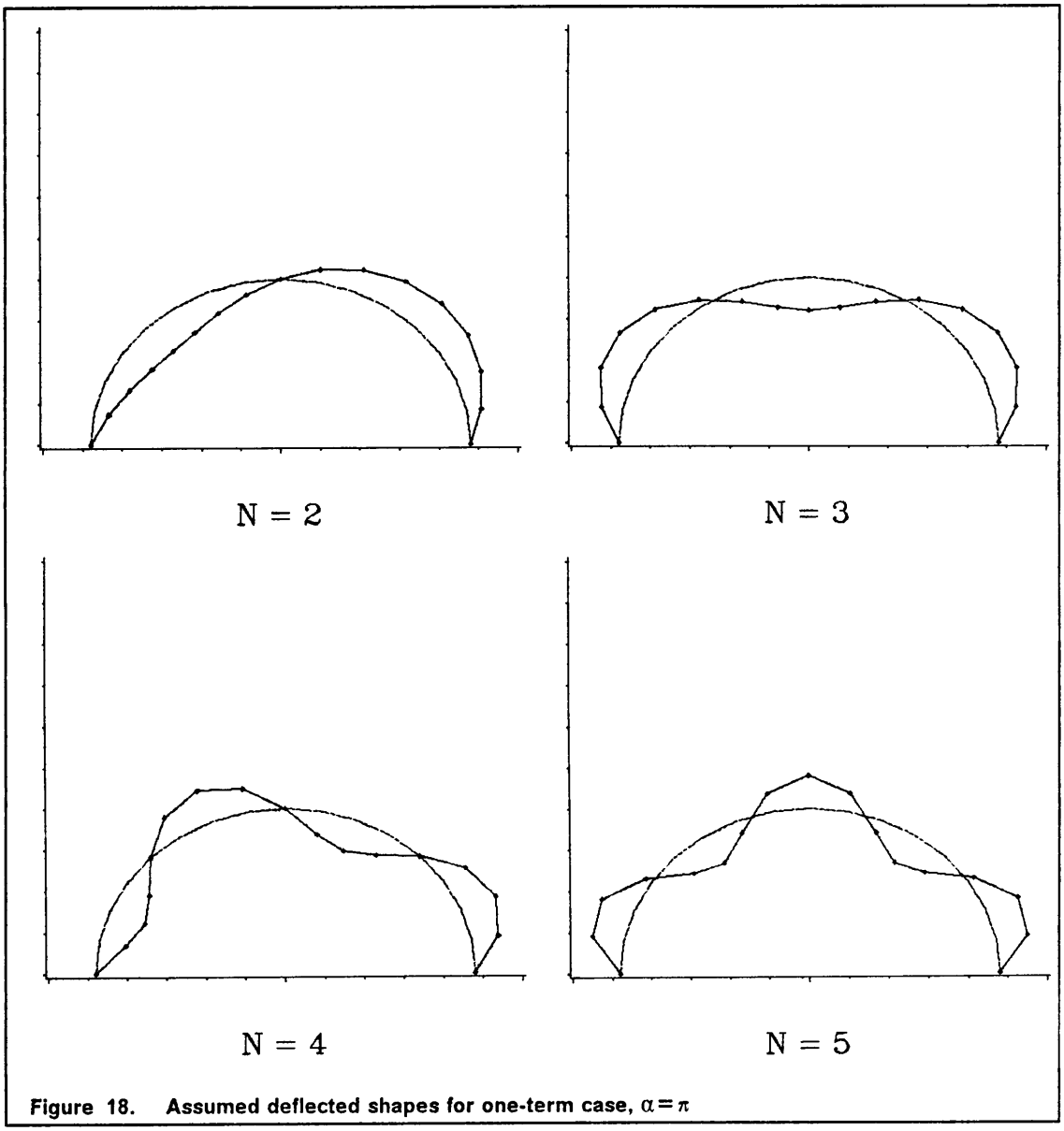

Figure 18. Assumed deflected shapes for one-term case, $\alpha = \pi$

where R is the residual, which is equal to equation 3.21 evaluated with the approximate solution, W_a.

After the integration and algebraic reduction, the resulting expression is written in the form

$$c_1\ddot{u} + c_2 u\ddot{u} + c_3 u^2\ddot{u} + c_4 u + c_5 u^2 = 0\,, \qquad [3.25]$$

where

$$\begin{aligned} c_1 &= (1 + \nu^2)\frac{\alpha}{2}\,, \\ c_2 &= (\nu^2 - 1)(\nu^2 + 2)\frac{4}{3\nu}\left[1 - (-1)^n\right], \\ c_3 &= \frac{9\alpha}{4}(\nu^2 - 1)^2\,, \\ c_4 &= \nu^2(\nu^2 - 1)\frac{\alpha}{2}\,, \\ c_5 &= (\nu^2 - 1)^2\frac{4\nu}{3}\left[1 - (-1)^n\right], \\ \text{and } \nu &= \frac{n\pi}{\alpha}\,. \end{aligned} \qquad [3.26]$$

Now, equation 3.25 is written in first-order form. The variables y_1 and y_2 are introduced, where $y_1 = u$ and $y_2 = \dot{u}$. These variables can be expressed in the first-order form

$$\dot{y}_1 = y_2\,,\ \dot{y}_2 = \frac{(-c_4 y_1 - c_5 y_1^2)}{(c_1 + c_2 y_1 + c_3 y_1^2)}\,. \qquad [3.27]$$

The equations for the constants shown in equation 3.26 and equation 3.27 are incorporated into a FORTRAN program, SOLVE1, that calls the IMSL subroutine DVERK. SOLVE1 is listed in appendix A.

Two-term solution - The two-term Galerkin approximation to equation 3.21 is assumed to be

$$W_a = u_1(T)F_1(\theta) + u_2(T)F_2(\theta)\,, \qquad [3.28]$$

where u_1 and u_2 are non-dimensional displacements that are functions of time, and F_1 and F_2 are chosen functions of θ that satisfy the essential and natural boundary conditions of the cylindrical membrane.

The functions are chosen to be sine functions as in equation 3.23 and are written

$$F_1 = \sin\left(\frac{n_1\pi\theta}{\alpha}\right) \qquad F_2 = \sin\left(\frac{n_2\pi\theta}{\alpha}\right). \qquad [3.29]$$

The assumed deflected shapes for $\alpha = \pi$ are illustrated in Figure 19 and Figure 20. Substituting equation 3.29 into the general form, equation 3.24, where the term F is now F_i, $i = 1,2$, and performing the integration and algebraic reduction yields two equations:

$$\begin{aligned}
0 = {} & \overline{f_1^{\,2}}\left[c_1u_1 + c_2\ddot{u}_1\right] \\
& + \overline{f_1^{\,3}}\left[c_5u_1^2 + c_6u_1\ddot{u}_1\right] \\
& + \overline{f_1^{\,2}f_2}\left[c_7u_1u_2 + c_8u_1\ddot{u}_2 + c_9u_2\ddot{u}_1\right] \\
& + \overline{f_1f_2^{\,2}}\left[c_{10}u_2^2 + c_{11}u_2\ddot{u}_2\right] \\
& + \overline{f_1g_1^2}\left[c_{12}u_1^2 + c_{13}u_1\ddot{u}_1\right] \\
& + \overline{f_1g_1g_2}\left[c_{14}u_1u_2 + c_{15}u_1\ddot{u}_2 + c_{16}u_2\ddot{u}_1\right] \\
& + \overline{f_1g_2^2}\left[c_{17}u_2^2 + c_{18}u_2\ddot{u}_2\right] \\
& + \overline{f_1^{\,4}}\left[c_{19}u_1^2\ddot{u}_1\right] \\
& + \overline{f_1^{\,2}f_2^{\,2}}\left[c_{22}u_2^2\ddot{u}_1 + c_{23}u_1u_2\ddot{u}_2\right] \\
& + \overline{f_1^{\,2}g_1^2}\left[c_{25}u_1^2\ddot{u}_1\right] \\
& + \overline{f_1f_2g_1^2}\left[c_{26}u_1^2\ddot{u}_2 + c_{27}u_1u_2\ddot{u}_1\right] \\
& + \overline{f_1^{\,2}g_1g_2}\left[c_{28}u_1^2\ddot{u}_2 + c_{29}u_1u_2\ddot{u}_1\right] \\
& + \overline{f_1^{\,2}g_2^2}\left[c_{32}u_2^2\ddot{u}_1 + c_{33}u_1u_2\ddot{u}_2\right] \\
& + \overline{f_1f_2g_2^2}\left[c_{34}u_2^2\ddot{u}_2\right],
\end{aligned}$$

$$\begin{aligned}
0 = {} & \overline{f_2^{\,2}}\left[c_3u_2 + c_4\ddot{u}_2\right] \\
& + \overline{f_1^{\,2}f_2}\left[c_5u_1^2 + c_6u_1\ddot{u}_1\right] \\
& + \overline{f_1f_2^{\,2}}\left[c_7u_1u_2 + c_8u_1\ddot{u}_2 + c_9u_2\ddot{u}_1\right] \\
& + \overline{f_2^{\,3}}\left[c_{10}u_2^2 + c_{11}u_2\ddot{u}_2\right] \\
& + \overline{f_2g_1^2}\left[c_{12}u_1^2 + c_{13}u_1\ddot{u}_1\right] \\
& + \overline{f_2g_1g_2}\left[c_{14}u_1u_2 + c_{15}u_1\ddot{u}_2 + c_{16}u_2\ddot{u}_1\right] \\
& + \overline{f_2g_2^2}\left[c_{17}u_2^2 + c_{18}u_2\ddot{u}_2\right] \\
& + \overline{f_1^{\,2}f_2^{\,2}}\left[c_{20}u_1^2\ddot{u}_2 + c_{21}u_1u_2\ddot{u}_1\right] \\
& + \overline{f_2^{\,4}}\left[c_{24}u_2^2\ddot{u}_2\right] \\
& + \overline{f_1f_2g_1^2}\left[c_{25}u_1^2\ddot{u}_2\right] \\
& + \overline{f_2^{\,2}g_1^2}\left[c_{26}u_1^2\ddot{u}_2 + c_{27}u_1u_2\ddot{u}_1\right] \\
& + \overline{f_2^{\,2}g_1g_2}\left[c_{30}u_2^2\ddot{u}_1 + c_{31}u_1u_2\ddot{u}_2\right] \\
& + \overline{f_1f_2g_2^2}\left[c_{32}u_2^2\ddot{u}_1 + c_{33}u_1u_2\ddot{u}_2\right] \\
& + \overline{f_2^{\,2}g_2^2}\left[c_{34}u_2^2\ddot{u}_2\right].
\end{aligned} \qquad [3.30]$$

where $f_i = \sin\ \nu_i\theta$, $g_i = \cos\ \nu_i\theta$, $\overline{(\ )} = \int_0^\alpha (\ )\,d\theta$, and $\nu_i = \left(\frac{n_i\pi}{\alpha}\right)$. The constants are evaluated as follows:

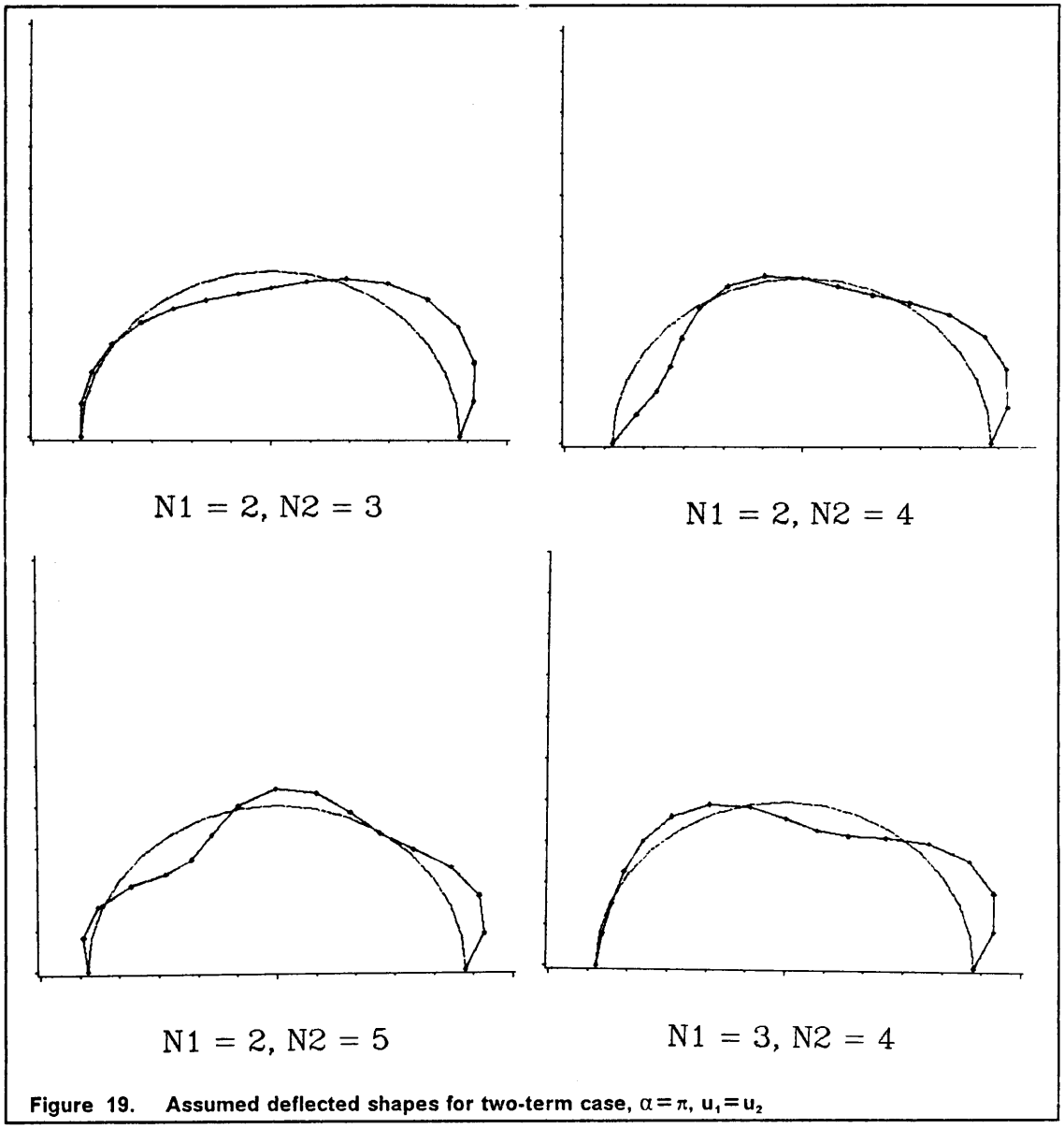

Figure 19. Assumed deflected shapes for two-term case, $\alpha = \pi$, $u_1 = u_2$

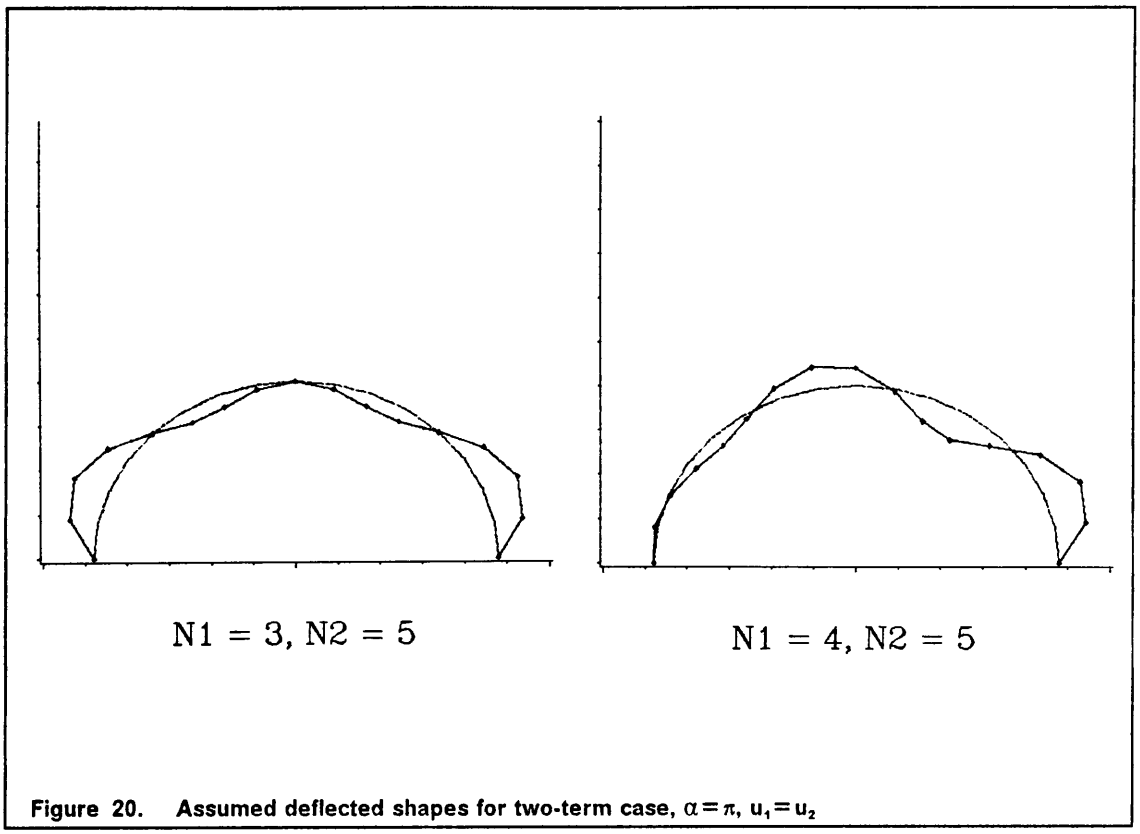

Figure 20. Assumed deflected shapes for two-term case, $\alpha = \pi$, $u_1 = u_2$

$$c_1 = \nu_1^4 - \nu_1^2; \quad c_2 = 1 + \nu_1^2; \quad c_3 = \nu_2^4 - \nu_2^2; \quad c_4 = 1 + \nu_2^2;$$

$$c_5 = \nu_1^2 - 2\nu_1^4 + \nu_1^6; \quad c_6 = -4 + 3\nu_1^2 + \nu_1^4;$$

$$c_7 = -2\nu_1^2\nu_2^2 + \nu_1^2 + \nu_2^2 - \nu_1^4 - \nu_2^4 + \nu_1^2\nu_2^4 + \nu_1^4\nu_2^2;$$

$$c_8 = 5\nu_1^2 - 4 - \nu_1^4 + 2\nu_1^2\nu_2^2 - 2\nu_2^2; \quad c_9 = 5\nu_2^2 - 4 - \nu_2^4 + 2\nu_1^2\nu_2^2 - 2\nu_1^2;$$

$$c_{10} = -2\nu_2^4 + \nu_2^2 + \nu_2^6; \quad c_{11} = -4 + 3\nu_2^2 + \nu_2^4;$$

$$c_{12} = 2\nu_1^6 - 4\nu_1^4 + 2\nu_1^2; \quad c_{13} = 2\nu_1^4 - 2\nu_1^2;$$

$$c_{14} = 4\nu_1^3\nu_2^3 - 4\nu_1\nu_2^3 - 4\nu_1^3\nu_2 + 4\nu_1\nu_2; \quad c_{15} = 2\nu_1^3\nu_2 - 2\nu_1\nu_2;$$

$$c_{16} = 2\nu_1\nu_2^3 - 2\nu_1\nu_2; \quad c_{17} = 2\nu_2^6 - 4\nu_2^4 + 2\nu_2^2;$$

$$c_{18} = 2\nu_2^4 - 2\nu_2^2; \quad c_{19} = 6 - 12\nu_1^2 + 6\nu_1^4;$$

$$c_{20} = 6 - 13\nu_1^2 - \nu_1^6 + \nu_1^4\nu_2^2 + \nu_2^2 - 2\nu_1^2\nu_2^2 + 8\nu_1^4; \qquad [3.31]$$

$$c_{21} = 12 - 13\nu_2^2 + \nu_2^4 - \nu_1^2\nu_2^4 + 12\nu_1^2\nu_2^2 - \nu_1^4 + \nu_1^4\nu_2^2 - 11\nu_1^2;$$

$$c_{22} = 6 - 13\nu_2^2 - \nu_2^6 + \nu_1^2 - 2\nu_1^2\nu_2^2 + 8\nu_2^4 + \nu_1^2\nu_2^4;$$

$$c_{23} = 12 - 13\nu_1^2 + \nu_1^4 - \nu_1^4\nu_2^2 + 12\nu_1^2\nu_2^2 - \nu_2^4 + \nu_1^2\nu_2^4 - 11\nu_2^2;$$

$$c_{24} = 6 - 12\nu_2^2 + 6\nu_2^4; \quad c_{25} = 0;$$

$$c_{26} = -2\nu_1^6 + 4\nu_1^4 - 2\nu_1^2; \quad c_{27} = 2\nu_1^4\nu_2^2 - 2\nu_1^2\nu_2^2 + 2\nu_1^4 + 2\nu_1^2;$$

$$c_{28} = 2\nu_1^5\nu_2 + 2\nu_1\nu_2; \quad c_{29} = -2\nu_1^3\nu_2^3 + 6\nu_1\nu_2^3 + 2\nu_1^3\nu_2 - 2\nu_1\nu_2;$$

$$c_{30} = 2\nu_1\nu_2^5 + 2\nu_1\nu_2; \quad c_{31} = -2\nu_1^3\nu_2^3 + 6\nu_1^3\nu_2 + 2\nu_1\nu_2^3 - 2\nu_1\nu_2;$$

$$c_{32} = -2\nu_2^6 + 4\nu_2^4 - 2\nu_2^2; \quad c_{33} = 2\nu_1^2\nu_2^4 - 2\nu_1^2\nu_2^2 + 2\nu_2^4 + 2\nu_2^2; \quad c_{34} = 0.$$

The integrals are evaluated as follows:

$$
\begin{aligned}
\overline{f_2^{\,2}} &= \overline{f_1^{\,2}} = \frac{\alpha}{2} \\
\overline{f_1^{\,3}} &= \frac{2}{3\nu_1}\left[1-(-1)^{n_1}\right] \\
\overline{f_2^{\,3}} &= \frac{2}{3\nu_2}\left[1-(-1)^{n_2}\right] \\
\overline{f_1^{\,4}} &= \overline{f_2^{\,4}} = \frac{3\alpha}{8} \\
\overline{f_1^{\,2}g_1^2} &= \overline{f_2^{\,2}g_2^2} = \frac{\alpha}{8} \\
\overline{f_1^{\,2}f_2} &= \frac{-2\nu_1^2\left[1-(-1)^{n_2}\right]}{\nu_2(\nu_2^2-4\nu_1^2)} \quad \text{if } \nu_2 \neq 2\nu_1 \quad \text{or} \quad 0 \quad \text{if } \nu_2 = 2\nu_1 \\
\overline{f_1 f_2^{\,2}} &= \frac{-2\nu_2^2\left[1-(-1)^{n_1}\right]}{\nu_1(\nu_1^2-4\nu_2^2)} \quad \text{if } \nu_1 \neq 2\nu_2 \quad \text{or} \quad 0 \quad \text{if } \nu_1 = 2\nu_2 \\
\overline{f_1 g_1^{\,2}} &= \frac{1}{3\nu_1}\left[1-(-1)^{n_1}\right] \\
\overline{f_1^{\,2}f_2^{\,2}} &= \overline{f_1^{\,2}g_2^2} = \overline{f_2^{\,2}g_1^2} = \frac{\alpha}{4} \\
\overline{f_1 f_2 g_1^2} &= -\overline{f_1^{\,2}g_1 g_2} = \begin{cases} 0 & \text{if } 3\nu_1 \neq \nu_2 \\ \frac{\alpha}{8} & \text{if } 3\nu_1 = \nu_2 \end{cases} \\
\overline{f_2 g_1^2} &= \frac{(\nu_2^2-2\nu_1^2)\left[1-(-1)^{n_2}\right]}{\nu_2(\nu_2^2-4\nu_1^2)} \quad \text{if } \nu_2 \neq 2\nu_1 \quad \text{or} \quad 0 \quad \text{if } \nu_2 = 2\nu_1 \\
\overline{f_1 f_2 g_2^2} &= -\overline{f_2^{\,2}g_1 g_2} = \begin{cases} 0 & \text{if } 3\nu_2 \neq \nu_1 \\ \frac{\alpha}{8} & \text{if } 3\nu_2 = \nu_1 \end{cases} \\
\overline{f_1 g_1 g_2} &= \frac{\nu_1\left[1-(-1)^{n_2}\right]}{4\nu_1^2-\nu_2^2} \quad \text{if } \nu_2 \neq 2\nu_1 \quad \text{or} \quad 0 \quad \text{if } \nu_2 = 2\nu_1 \\
\overline{f_2 g_1 g_2} &= \frac{\nu_2\left[1-(-1)^{n_1}\right]}{4\nu_2^2-\nu_1^2} \quad \text{if } \nu_1 \neq 2\nu_2 \quad \text{or} \quad 0 \quad \text{if } \nu_1 = 2\nu_2 \\
\overline{f_1 g_2^2} &= \frac{(\nu_1^2-2\nu_2^2)\left[1-(-1)^{n_1}\right]}{\nu_1(\nu_1^2-4\nu_2^2)} \quad \text{if } \nu_1 \neq 2\nu_2 \quad \text{or} \quad 0 \quad \text{if } \nu_1 = 2\nu_2 \\
\overline{f_2 g_2^2} &= \frac{1}{3\nu_2}\left[1-(-1)^{n_2}\right]
\end{aligned}
\qquad [3.32]
$$

The equations from 3.30 can be written in the form

$$
\begin{aligned}
a\ddot{u}_1 + b\ddot{u}_2 &= c, \\
d\ddot{u}_1 + e\ddot{u}_2 &= f,
\end{aligned}
\qquad [3.33]
$$

where

$$
\begin{aligned}
a &= c_2\overline{f_1^{\,2}} + c_6u_1\overline{f_1^{\,3}} + c_9u_2\overline{f_1^{\,2}f_2} + c_{13}u_1\overline{f_1g_1^2} + c_{16}u_2\overline{f_1g_1g_2} + c_{19}u_1^2\overline{f_1^{\,4}} \\
&\quad + c_{22}u_2^2\overline{f_1^{\,2}f_2^{\,2}} + c_{25}u_1^2\overline{f_1^{\,2}g_1^2} + c_{27}u_1u_2\overline{f_1f_2g_1^2} - c_{29}u_1u_2\overline{f_1^{\,2}g_1g_2} + c_{32}u_2^2\overline{f_1^{\,2}g_2^2} \\
b &= c_8u_1\overline{f_1^{\,2}f_2} + c_{11}u_2\overline{f_1f_2^{\,2}} + c_{15}u_1\overline{f_1g_1g_2} + c_{18}u_2\overline{f_1g_2^2} + c_{23}u_1u_2\overline{f_1^{\,2}f_2^{\,2}} + c_{26}u_1^2\overline{f_1f_2g_1^2} \\
&\quad - c_{28}u_1^2\overline{f_1^{\,2}g_1g_2} + c_{33}u_1u_2\overline{f_1^{\,2}g_2^2} + c_{34}u_2^2\overline{f_1f_2g_2^2} \\
c &= -c_1u_1\overline{f_1^{\,2}} - c_5u_1^2\overline{f_1^{\,3}} - c_7u_1u_2\overline{f_1^{\,2}f_2} - c_{10}u_2^2\overline{f_1f_2^{\,2}} - c_{12}u_1^2\overline{f_1g_1^2} - c_{14}u_1u_2\overline{f_1g_1g_2} \\
&\quad - c_{17}u_2^2\overline{f_1g_2^2} \\
d &= c_6u_1\overline{f_1^{\,2}f_2} + c_9u_2\overline{f_1f_2^{\,2}} + c_{13}u_1\overline{f_2g_1^2} + c_{16}u_2\overline{f_2g_1g_2} + c_{21}u_1u_2\overline{f_1^{\,2}f_2^{\,2}} + c_{25}u_1^2\overline{f_1f_2g_1^2} \\
&\quad + c_{27}u_1u_2\overline{f_2^{\,2}g_1^2} - c_{30}u_2^2\overline{f_2^{\,2}g_1g_2} + c_{32}u_2^2\overline{f_1f_2g_2^2} \\
e &= c_4\overline{f_2^{\,2}} + c_8u_1\overline{f_1f_2^{\,2}} + c_{11}u_2\overline{f_2^{\,3}} + c_{15}u_1\overline{f_2g_1g_2} + c_{18}u_2\overline{f_2g_2^2} + c_{20}u_1^2\overline{f_1^{\,2}f_2^{\,2}} \\
&\quad + c_{24}u_2^2\overline{f_2^{\,4}} + c_{26}u_1^2\overline{f_2^{\,2}g_1^2} - c_{31}u_1u_2\overline{f_2^{\,2}g_1g_2} + c_{33}u_1u_2\overline{f_1f_2g_2^2} + c_{34}u_2^2\overline{f_2^{\,2}g_2^2} \\
f &= -c_3u_2\overline{f_2^{\,2}} - c_5u_1^2\overline{f_1^{\,2}f_2} - c_7u_1u_2\overline{f_1f_2^{\,2}} - c_{10}u_2^2\overline{f_2^{\,3}} - c_{12}u_1^2\overline{f_2g_1^2} - c_{14}u_1u_2\overline{f_2g_1g_2} \\
&\quad - c_{17}u_2^2\overline{f_2g_2^2}
\end{aligned}
\qquad [3.34]
$$

To write equation 3.38 in first order form, the variables y_1, y_2, y_3, and y_4 are introduced, where

$$y_1 = u_1,\ y_2 = \dot{u}_1,\ y_3 = u_2,\ y_4 = \dot{u}_2.$$

Thus, the first order form is written

$$
\begin{aligned}
\dot{y}_1 &= y_2\,, \\
\dot{y}_2 &= \frac{(ce - bf)}{(ae - bd)}\,, \\
\dot{y}_3 &= y_4\,, \\
\dot{y}_4 &= \frac{(af - cd)}{(ae - bd)}\,.
\end{aligned}
\qquad [3.35]
$$

The expressions for the integrals and constants, equations 3.31 and 3.32, and equations 3.34 and 3.35 are incorporated into a FORTRAN program called SOLVE2 that calls the IMSL subroutine DVERK. This program is listed in appendix B.

Computer Analysis

Programs SOLVE1 and SOLVE2 are used to solve the differential equations derived in this chapter. The output of the programs SOLVE1 and SOLVE2 is in the form of data files. These files contain the non-dimensional time, T, with the corresponding non-dimensional displacement, u, u_1, or u_2. Solutions are generated for various initial displacements, values of n, n_1, and n_2, and values of α . Results are shown in the next chapter in tabular and graphical form.

The FORTRAN programs FRQAMP1 and FRQAMP2 are used to read the data files that result from the programs SOLVE1 and SOLVE2 , and to calculate the period, frequency, and amplitude of the response. Programs FRQAMP1 and FRQAMP2 are listed in appendix C.

Results of Analysis

Introduction

This chapter presents the results of the one- and two-term solutions of the equations of motion developed in the previous chapter. Equation 3.25 is solved using SOLVE1, and then the output files are analyzed using FRQAMP1. These results are shown in the following section titled "Results of the one-term solution". Equation 3.30 is solved using SOLVE2, and then the output files are analyzed using FRQAMP2. These results are shown in the following section titled "Results of the two-term solution".

In general, program SOLVE1 was run for the cases of $\alpha = \pi$, $\alpha = \pi/2$, $\alpha = 3\pi/2$, and initial displacement varying from 0.00001 to 0.10, where α is the central angle of the inflatable dam, and the initial displacement is the non-dimensional radial displacement which is a function of radius R. Program SOLVE2 was run for the cases of $\alpha = \pi$, $\alpha = \pi/2$, $\alpha = 3\pi/2$, and initial displacements varying from 0.00001 to 0.05.

For the one-term case, most of the plots of displacement versus time were similar in shape, the only difference being the amplitude. For this reason, only plots for an initial displacement of 0.01 are shown in the body of this chapter.

For the two-term case, most of the plots were also similar in shape, with the only difference being the amplitudes. For the same reason, only plots of representative cases are included in this chapter. Plots for an initial displacement of 0.005 are shown for $\alpha = \pi/2$, and plots for an initial displacement of 0.01 are shown for $\alpha = \pi$ and $3\pi/2$.

In the course of the analysis it was found that the subroutine DVERK could not always find an appropriate solution. In the cases where $\alpha = \pi$, $n=5$, and the initial displacement is greater than 0.02, the results from DVERK represent an alternate mathematical solution that has no physical meaning to this analysis. Similar problems occur when $\alpha = \pi/2$ and $n=3$ or 5. In the cases where no valid solution can be found, those results have been excluded from the plots and tables, and only results that are consistent with the other cases and work done by others are included.

All the plots and tables are shown without units indicated on the axes, since the units have been removed from the analysis by non-dimensionalizing the terms in the equations.

Results of the One-Term Solution

Figure 21 through Figure 25 show plots of u versus time for $\alpha = \pi/2, \pi, 3\pi/2$, and $u_o = 0.01$, where u is the non-dimensional displacement term from equation 3.22, and u_o indicates the initial displacement.

Frequencies and amplitudes for the one-term solution are shown in Table 1 and Table 2, respectively. There is a general trend for the frequency to decrease as the initial displacement

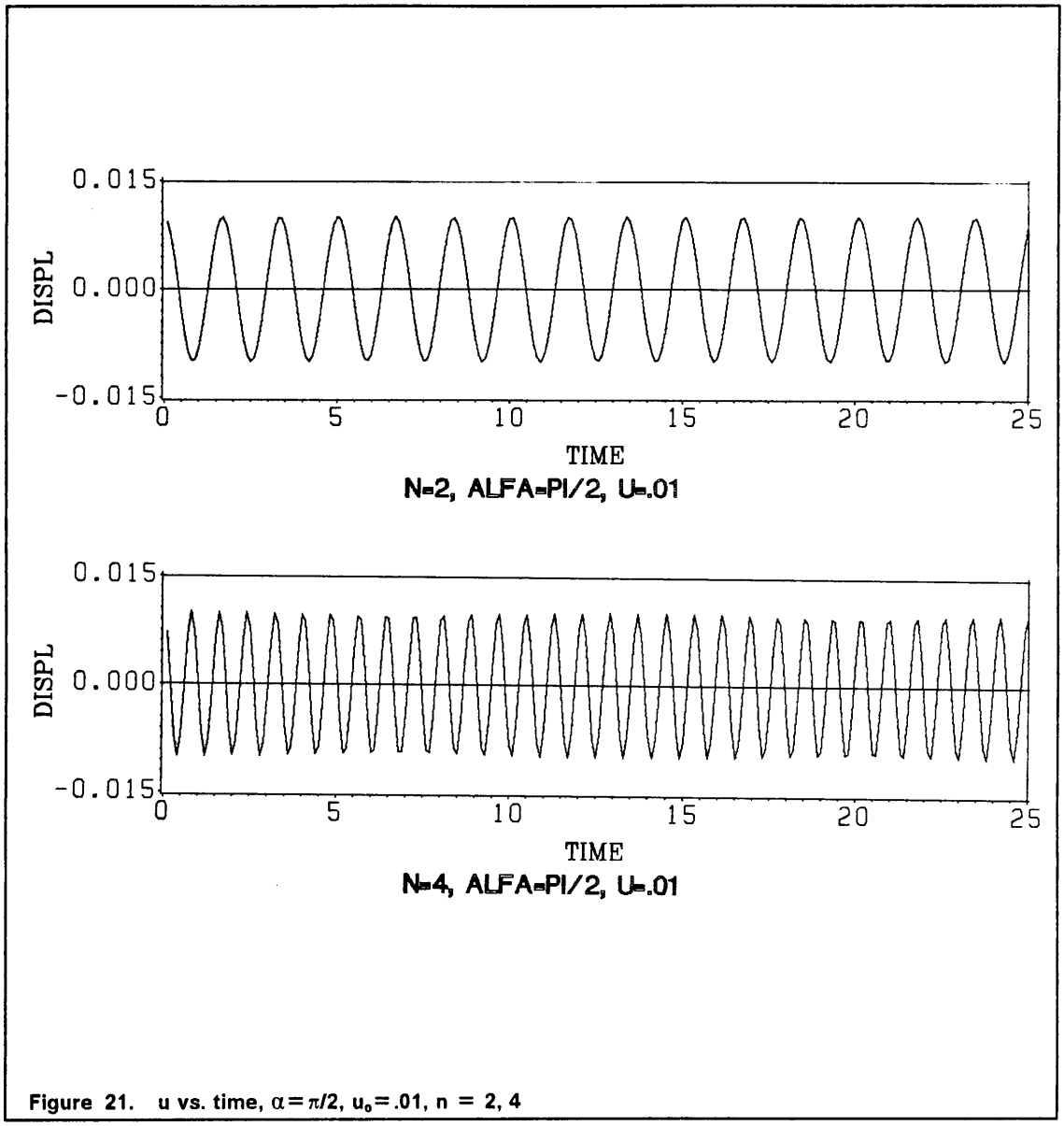

Figure 21. u vs. time, $\alpha = \pi/2$, $u_o = .01$, n = 2, 4

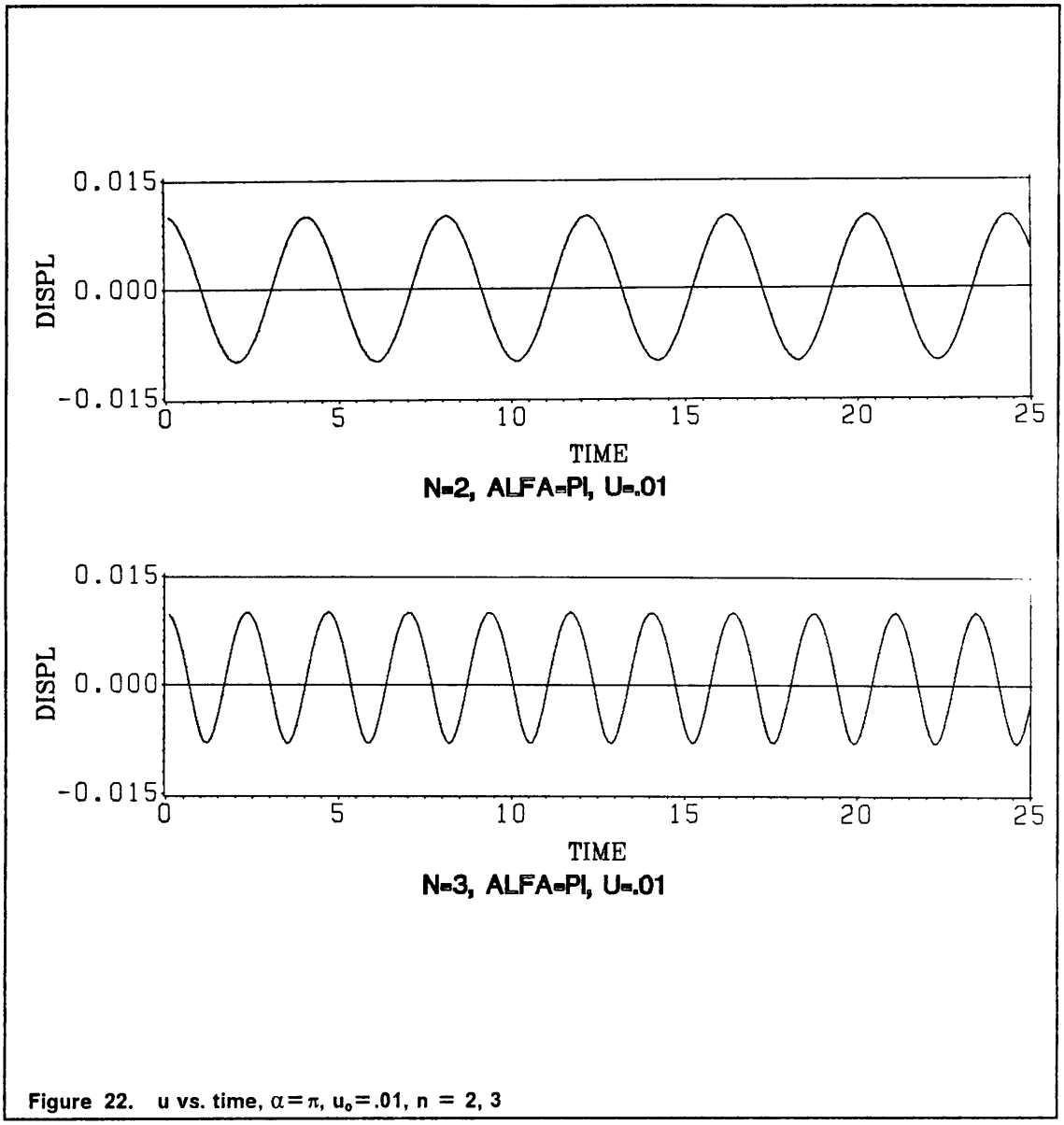

Figure 22. u vs. time, $\alpha = \pi$, $u_o = .01$, n = 2, 3

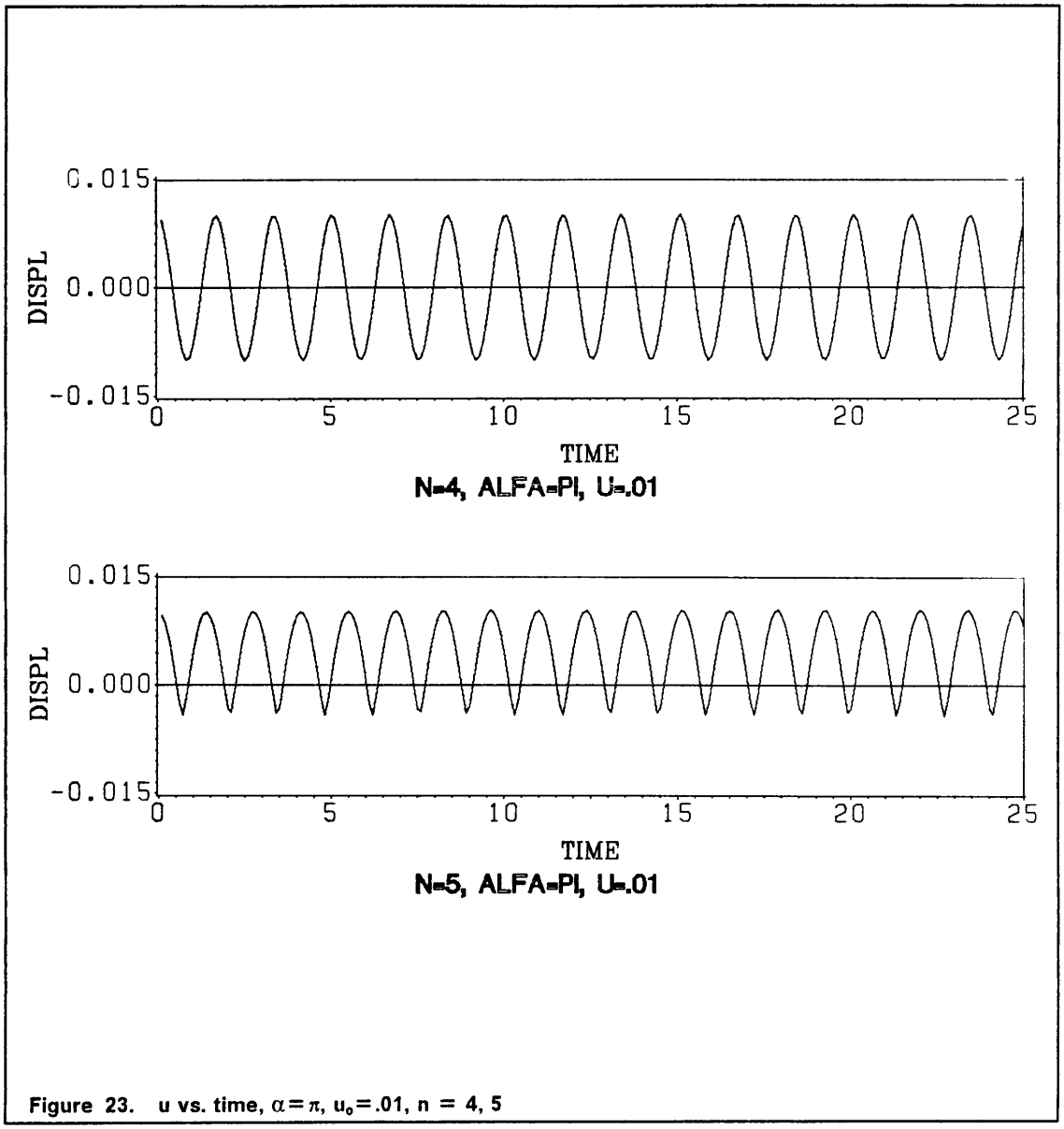

Figure 23. u vs. time, $\alpha = \pi$, $u_o = .01$, n = 4, 5

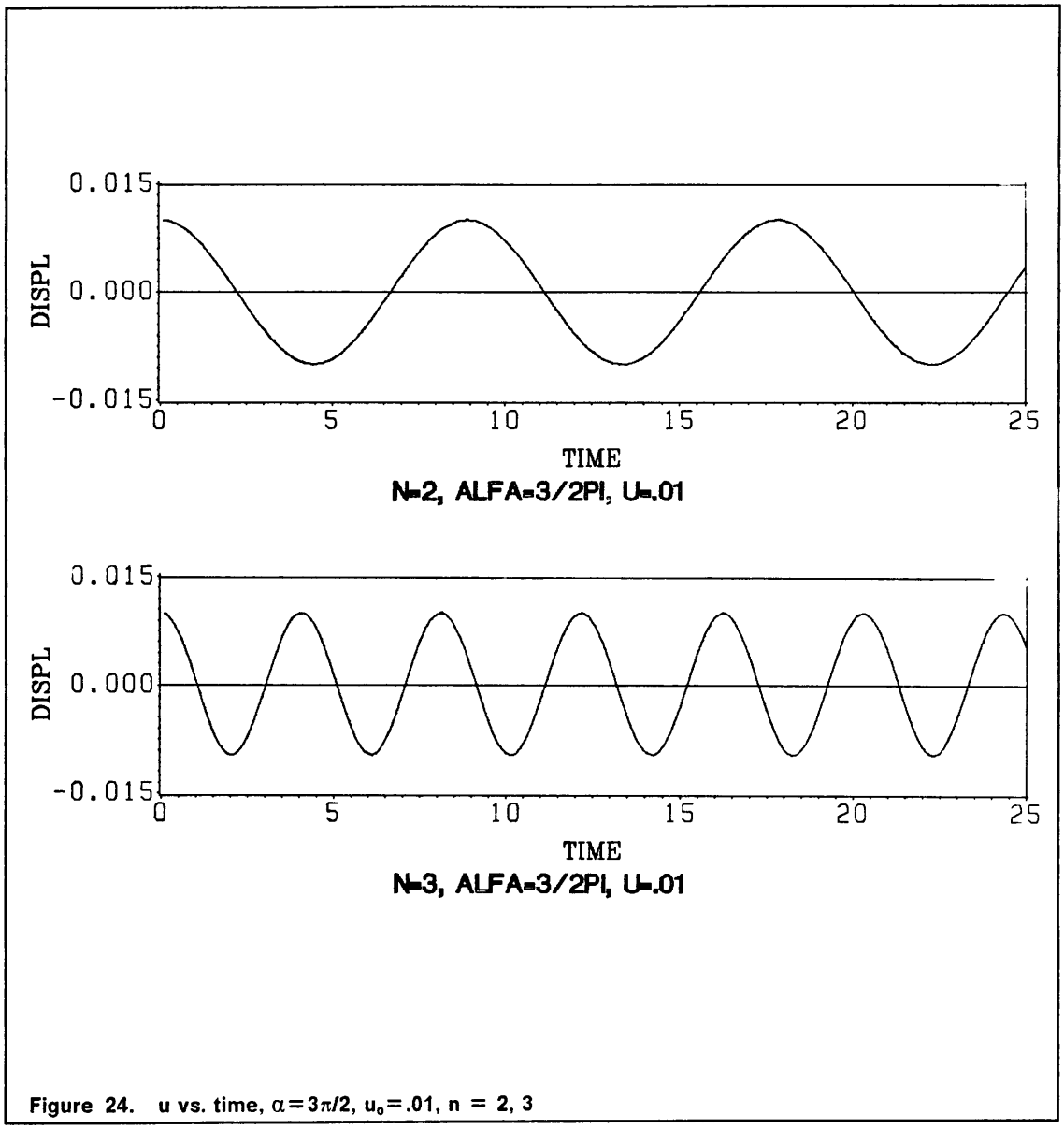

Figure 24. u vs. time, $\alpha = 3\pi/2$, $u_0 = .01$, n = 2, 3

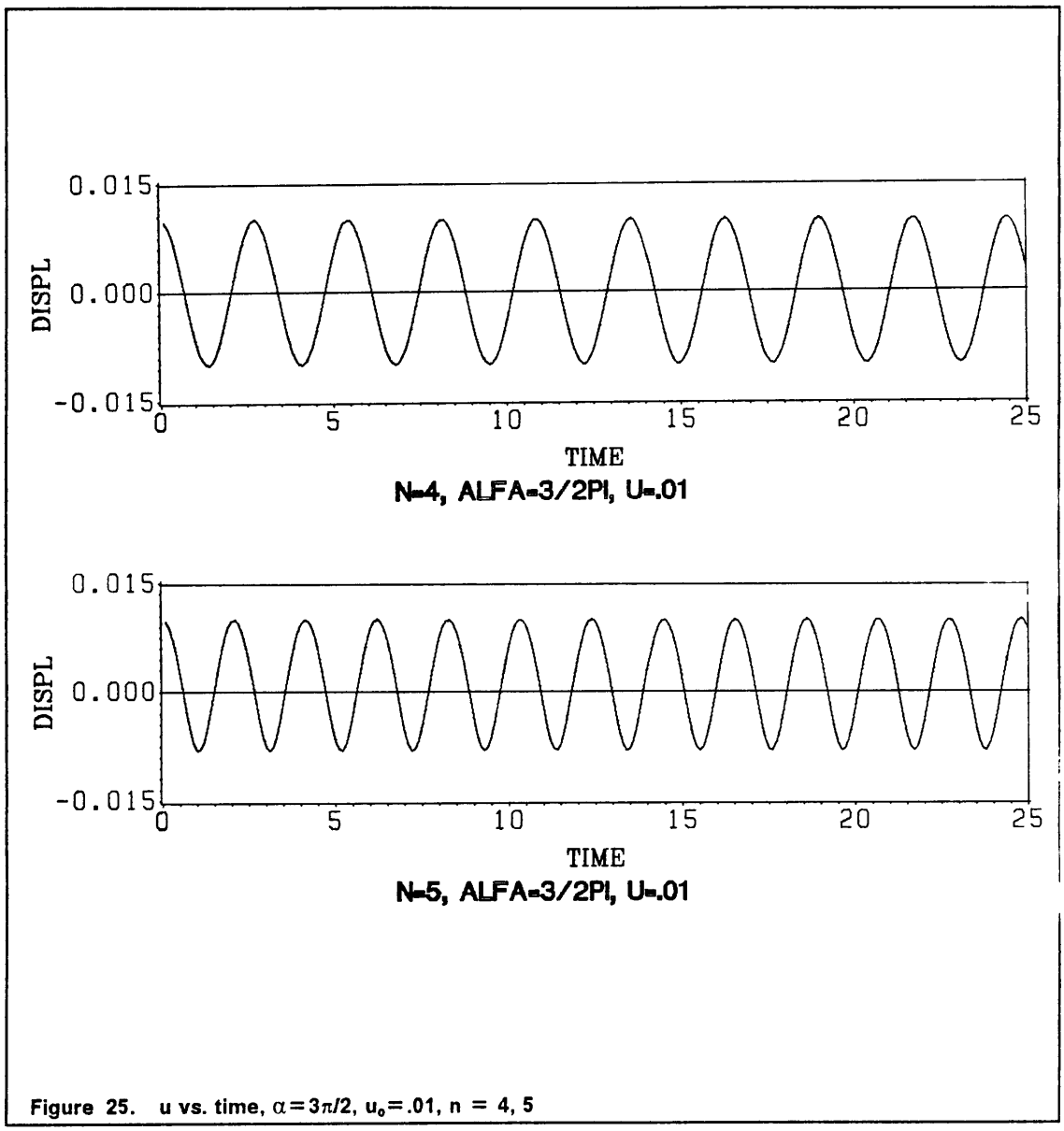

Figure 25. u vs. time, $\alpha = 3\pi/2$, $u_o = .01$, n = 4, 5

Table 1. Table of frequencies for the one-term Galerkin solution

u_o	α	$n = 2$	$n = 3$	$n = 4$	$n = 5$
0.00	π/2	3.7552	5.8358	7.8701	9.8938
	π	1.5497	2.6823	3.7552	4.8082
	3π/2	0.7060	1.5497	2.3145	3.0456
0.01	π/2	3.7472	---	7.7891	---
	π	1.5479	2.6823	3.7472	4.5625
	3π/2	0.7060	1.5497	2.3145	3.0392
0.02	π/2	3.7234	---	7.5655	---
	π	1.5479	2.6794	3.7234	4.2019
	3π/2	0.7060	1.5479	2.3070	3.0265
0.03	π/2	3.6844	---	7.2250	---
	π	1.5445	2.6737	3.6844	---
	3π/2	0.7060	1.5479	2.2996	3.0083
0.04	π/2	3.6288	---	6.8170	---
	π	1.5410	2.6652	3.6288	---
	3π/2	0.7050	1.5479	2.2848	2.9888
0.05	π/2	3.5640	---	6.3875	---
	π	1.5376	2.6511	3.5640	---
	3π/2	0.7050	1.5462	2.2726	2.9631
0.06	π/2	3.4907	---	5.9470	---
	π	1.5325	2.6353	3.4907	---
	3π/2	0.7050	1.5445	2.2541	2.9317
0.07	π/2	3.4034	---	5.5478	---
	π	1.5274	2.6123	3.4034	---
	3π/2	0.7050	1.5445	2.2291	2.9040
0.08	π/2	3.3174	---	5.1713	---
	π	1.5207	2.5896	3.3174	---
	3π/2	0.7040	1.5427	2.2046	2.8684
0.09	π/2	3.2256	---	4.8332	---
	π	1.5140	2.4939	3.2256	---
	3π/2	0.7030	1.5410	2.1831	2.8315
0.10	π/2	3.1348	---	4.5212	---
	π	1.5050	2.5346	3.1348	---
	3π/2	0.7030	1.5376	2.1550	2.7896

Table 2. Table of amplitudes for the one-term Galerkin solution

u_o	α	$n = 2$	$n = 3$	$n = 4$	$n = 5$
0.00	π/2	0.000009	0.000009	0.000009	0.000009
	π	0.000009	0.000009	0.000009	0.000009
	3π/2	0.000010	0.000009	0.000009	0.000009
0.01	π/2	0.009942	---	0.009752	---
	π	0.009999	0.008993	0.009942	0.007148
	3π/2	0.009998	0.009826	0.009978	0.009022
0.02	π/2	0.019884	---	0.019672	---
	π	0.019980	0.016626	0.019885	0.012139
	3π/2	0.019996	0.019344	0.019955	0.016718
0.03	π/2	0.029827	---	0.029772	---
	π	0.029974	0.023433	0.129828	---
	3π/2	0.029993	0.028583	0.029941	0.023597
0.04	π/2	0.039785	---	0.040031	---
	π	0.039961	0.029836	0.039784	---
	3π/2	0.039991	0.037567	0.039912	0.030093
0.05	π/2	0.049738	---	0.050317	---
	π	0.049949	0.035310	0.049738	---
	3π/2	0.049989	0.046314	0.049889	0.035653
0.06	π/2	0.059986	---	0.060667	---
	π	0.059916	0.040876	0.059986	---
	3π/2	0.059988	0.054855	0.059866	0.041600
0.07	π/2	0.069683	---	0.071029	---
	π	0.069934	0.046353	0.069683	---
	3π/2	0.069985	0.063183	0.069847	0.046708
0.08	π/2	0.079669	---	0.081618	---
	π	0.079932	0.052366	0.079669	---
	3π/2	0.079982	0.071331	0.079835	0.051958
0.09	π/2	0.089654	---	0.091646	---
	π	0.089911	0.068977	0.089645	---
	3π/2	0.089982	0.079314	0.089822	.057090
0.010	π/2	0.099629	---	0.010197	---
	π	0.099900	0.061309	0.099629	---
	3π/2	0.099979	0.087133	0.099812	0.062371

increases. The amplitudes for the $n=2$ and $n=4$ cases tend to be slightly less than the initial displacements and don't vary much, while the amplitudes for the $n=3$ and $n=5$ cases tend to be significantly less than the initial diplacements. Looking at the plots of initial displacement versus time, Figure 21 through Figure 25, it can be seen that the $n=3$ and $n=5$ cases show a positive shift, meaning that the dam is not vibrating about the equilibrium state, but some positive value of displacement. It can be seen that as the initial displacement is increased the magnitude of this shift is also increased. The shift phenomenon is seen slightly in the $\alpha = \pi/2$ case for $n=4$, but is much more evident in the $\alpha = \pi$ and $3\pi/2$ cases where $n=3$ and 5.

Figure 26 through Figure 31 show plots of initial displacement versus frequency and amplitude versus frequency, for $\alpha = \pi/2$, π, and $3\pi/2$. The shift phenomenon can be seen in the plots of amplitude versus frequency. The curves for the $n=3$ case where $\alpha = \pi$ and the $n=3$ and 5 cases where $\alpha = 3\pi/2$ do not extend as far upward in the positive direction of the amplitude axis as the curves for the other mode cases.

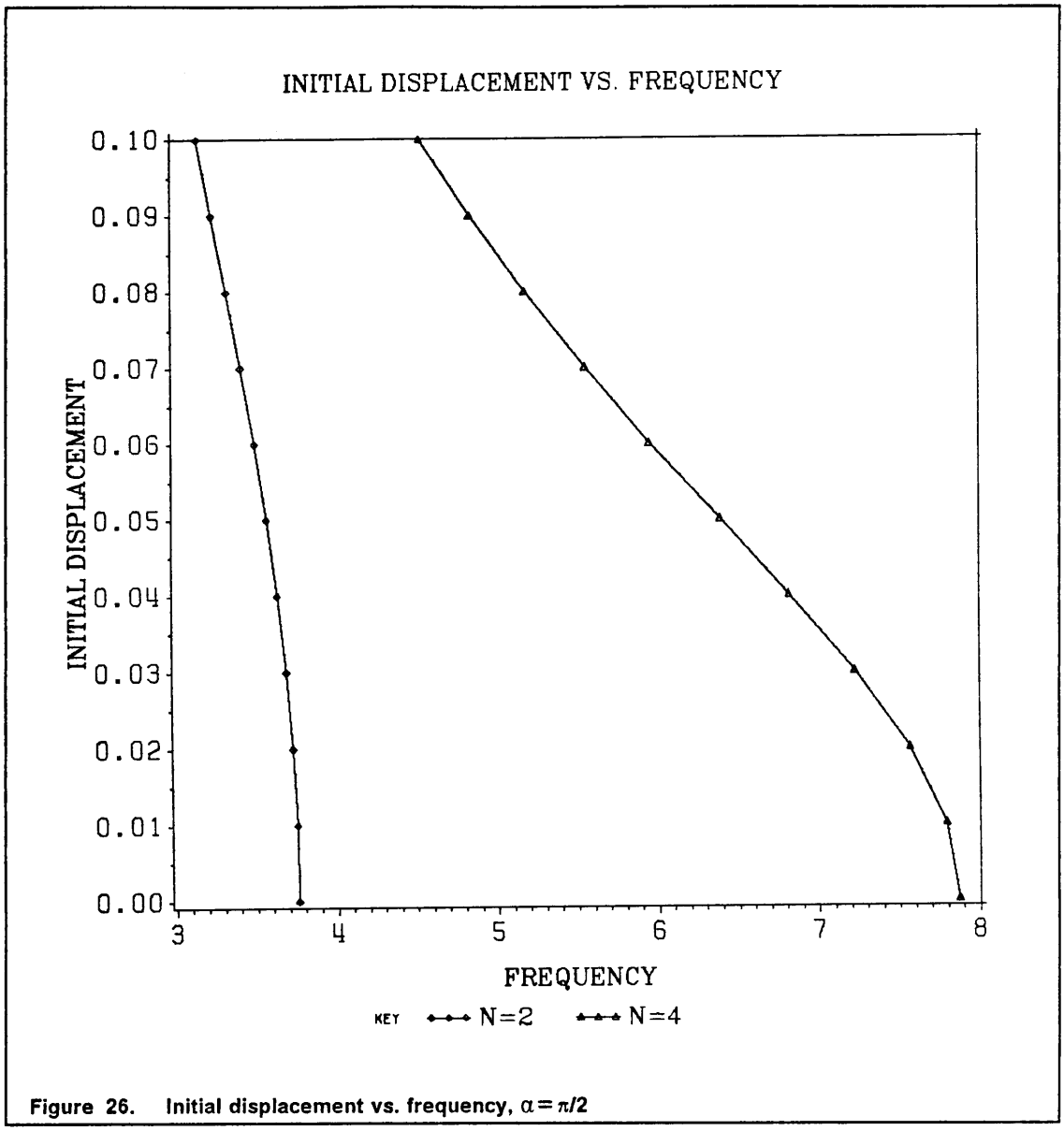

Figure 26. Initial displacement vs. frequency, $\alpha = \pi/2$

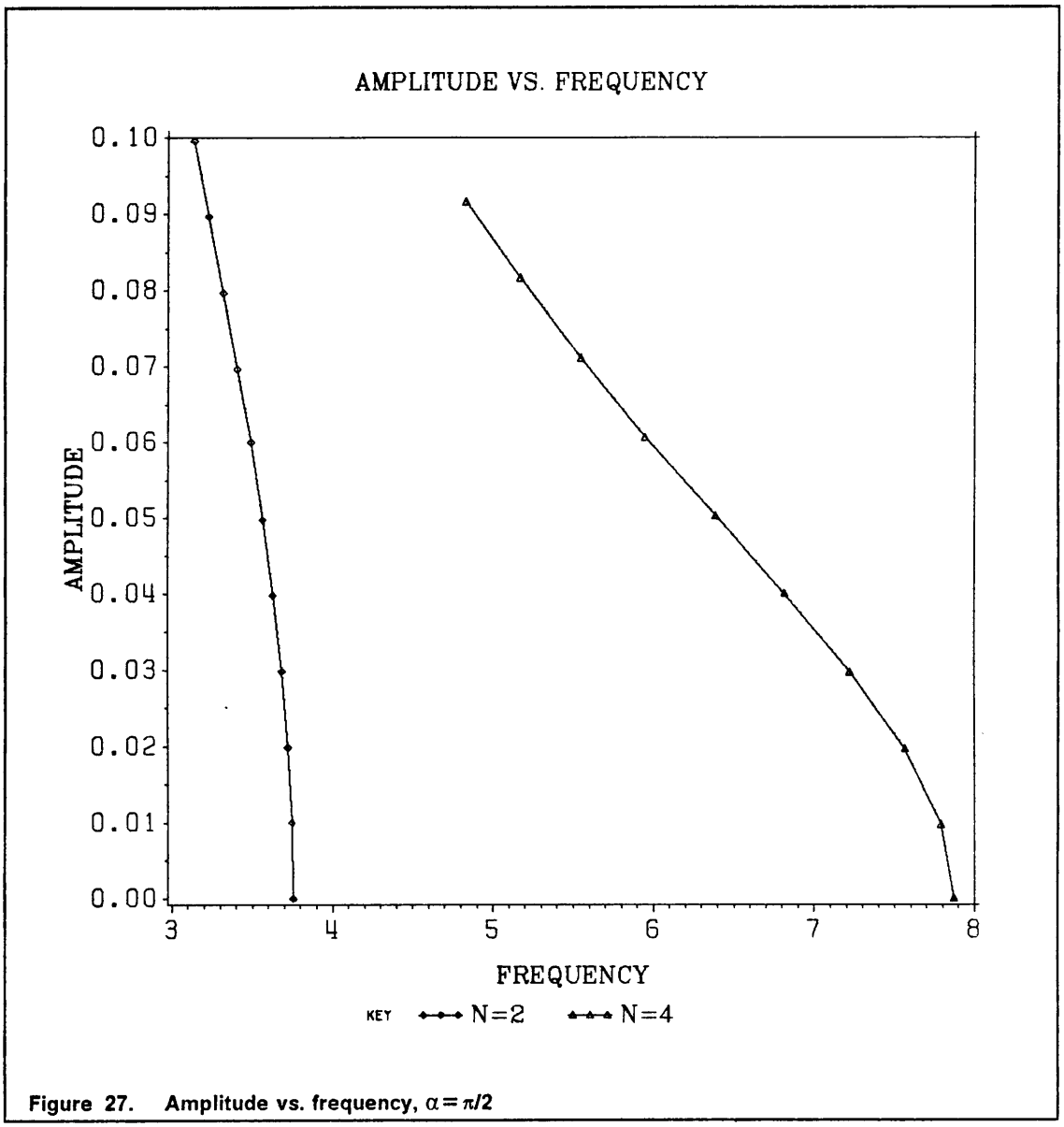

Figure 27. Amplitude vs. frequency, $\alpha = \pi/2$

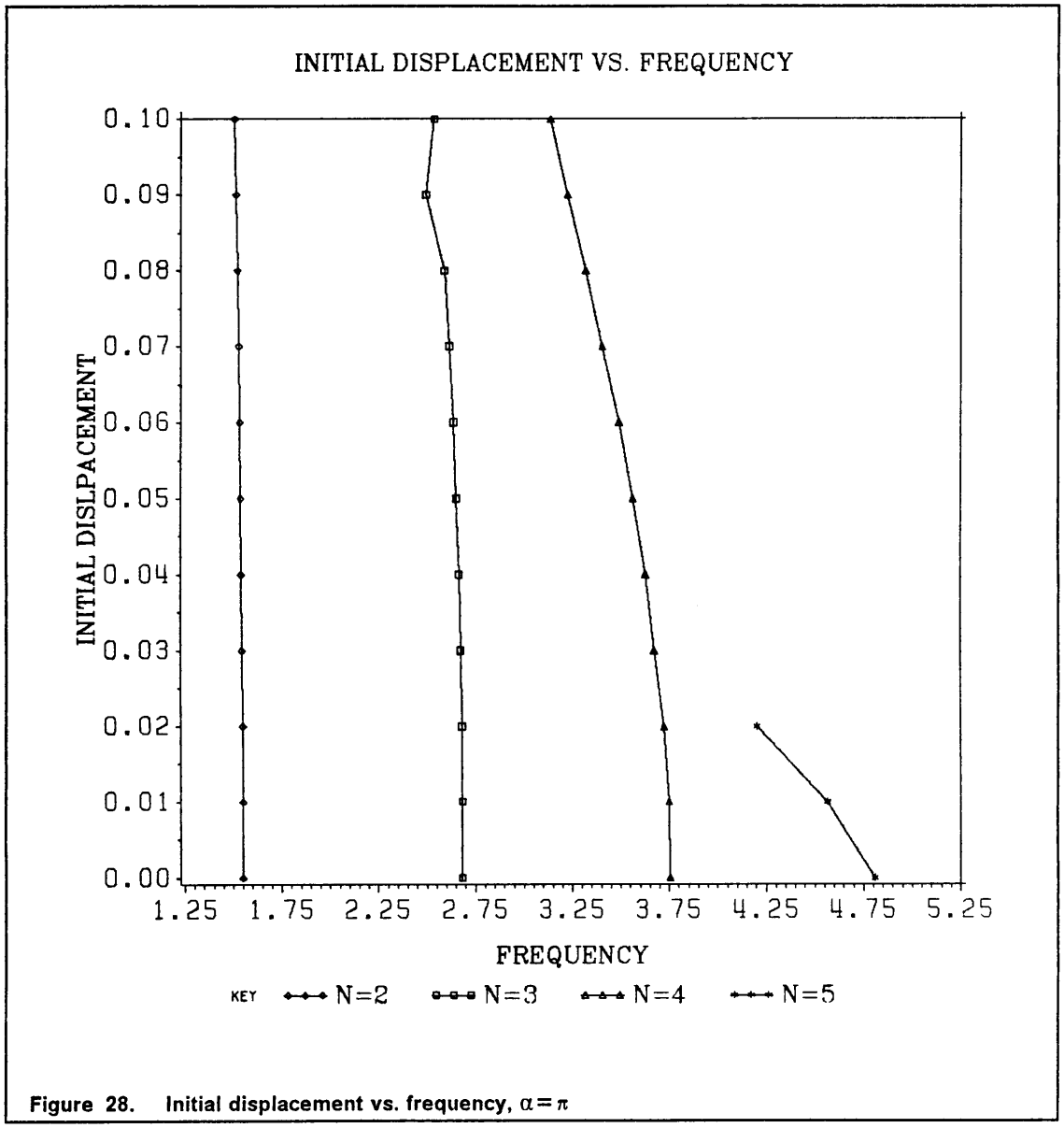

Figure 28. Initial displacement vs. frequency, $\alpha = \pi$

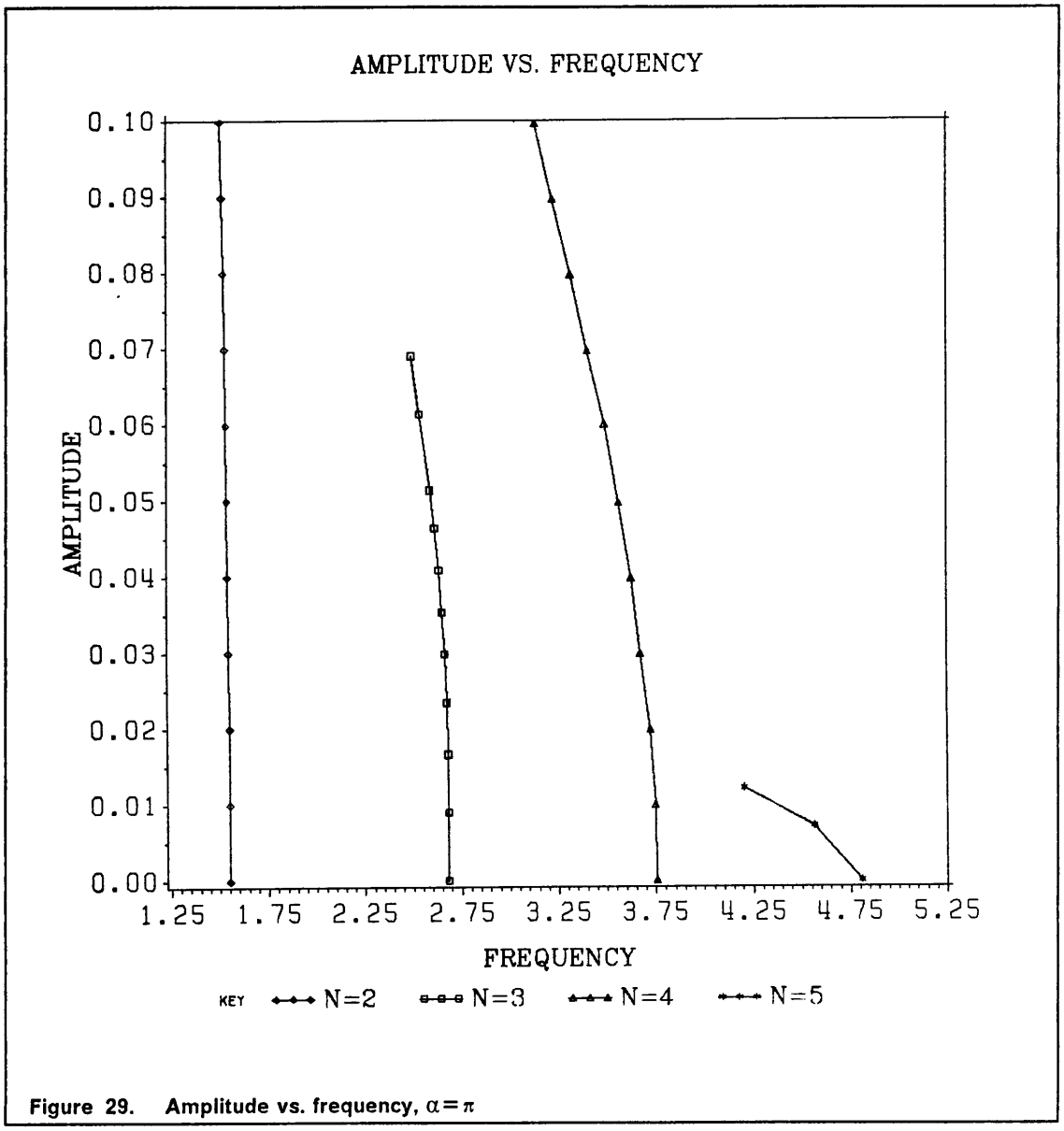

Figure 29. Amplitude vs. frequency, $\alpha = \pi$

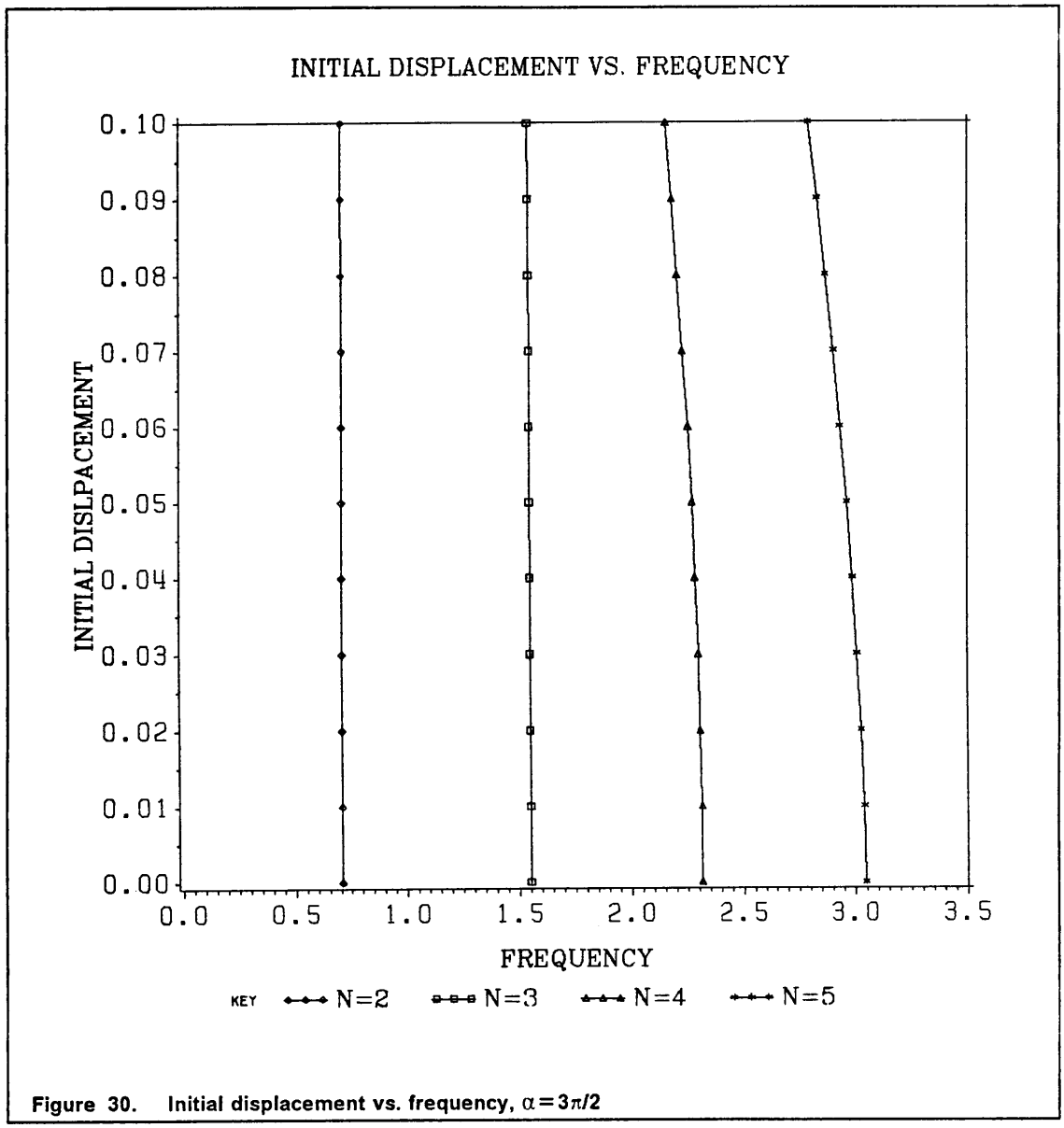

Figure 30. Initial displacement vs. frequency, $\alpha = 3\pi/2$

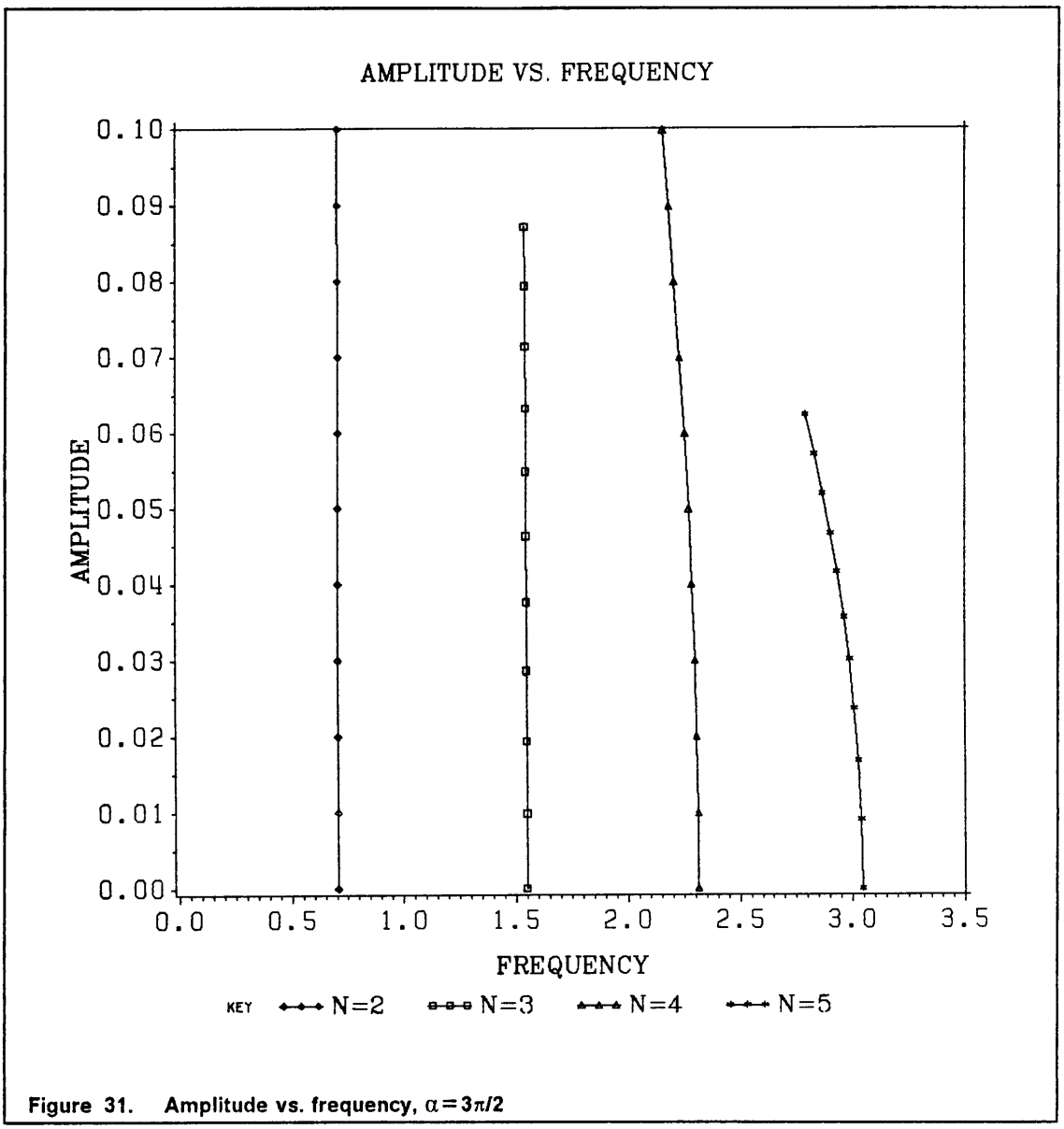

Figure 31. Amplitude vs. frequency, $\alpha = 3\pi/2$

Results of the Two-Term Solution

Figure 32 through Figure 41 show plots of u_i versus time for $\alpha = \pi/2$, where u_i is the non-dimensional displacement term u_1 or u_2 shown in equation 3.28.

Figure 42 through Figure 52 show plots of u_i versus time for $\alpha = \pi$.

Figure 53 through Figure 63 show plots of u_i versus time for $\alpha = 3\pi/2$.

Table 3 and Table 4 show frequencies for the first term of the two-term approximation. Frequencies are shown for initial displacements of 0.00001 to 0.010. The term u_o indicates the initial displacement which is equal to both u_1 and u_2. The frequencies for the second term are not shown in a table; however, they are the same as those for the first term and can be found in the tables by simply switching the values of n_1 and n_2 and locating the corresponding frequency for the first term of the approximation.

For the two-term solutions the calculated amplitudes were all very close to the initial displacements. For example, in the case where the initial displacement was 0.01, the calculated amplitudes for all the mode combinations were between 0.009 and 0.011. For this reason, tables of amplitudes for all the mode combinations are not presented as was done for the one-term solution. The shift phenomenon seen in the plots of the one-term solution is not as prominent in the two-term results. However, it can be seen slightly in the plots of amplitude versus frequency. Figure 64 to Figure 67 show plots of initial displacement versus frequency and amplitude versus frequency for $\alpha = \pi$ and $3\pi/2$ for the first term of the following mode combinations: $n_1 = 2, n_2 = 3$; $n_1 = 3, n_2 = 4$; $n_1 = 4, n_2 = 3$; $n_1 = 5, n_2 = 3$. These combinations are chosen as each of the modes n=2 through n=5 are represented. The trend of the frequency to decrease as the initial displacement is increased is also seen in the two-term results as evidenced in the plots of displacement versus frequency. However, it is not as ob-

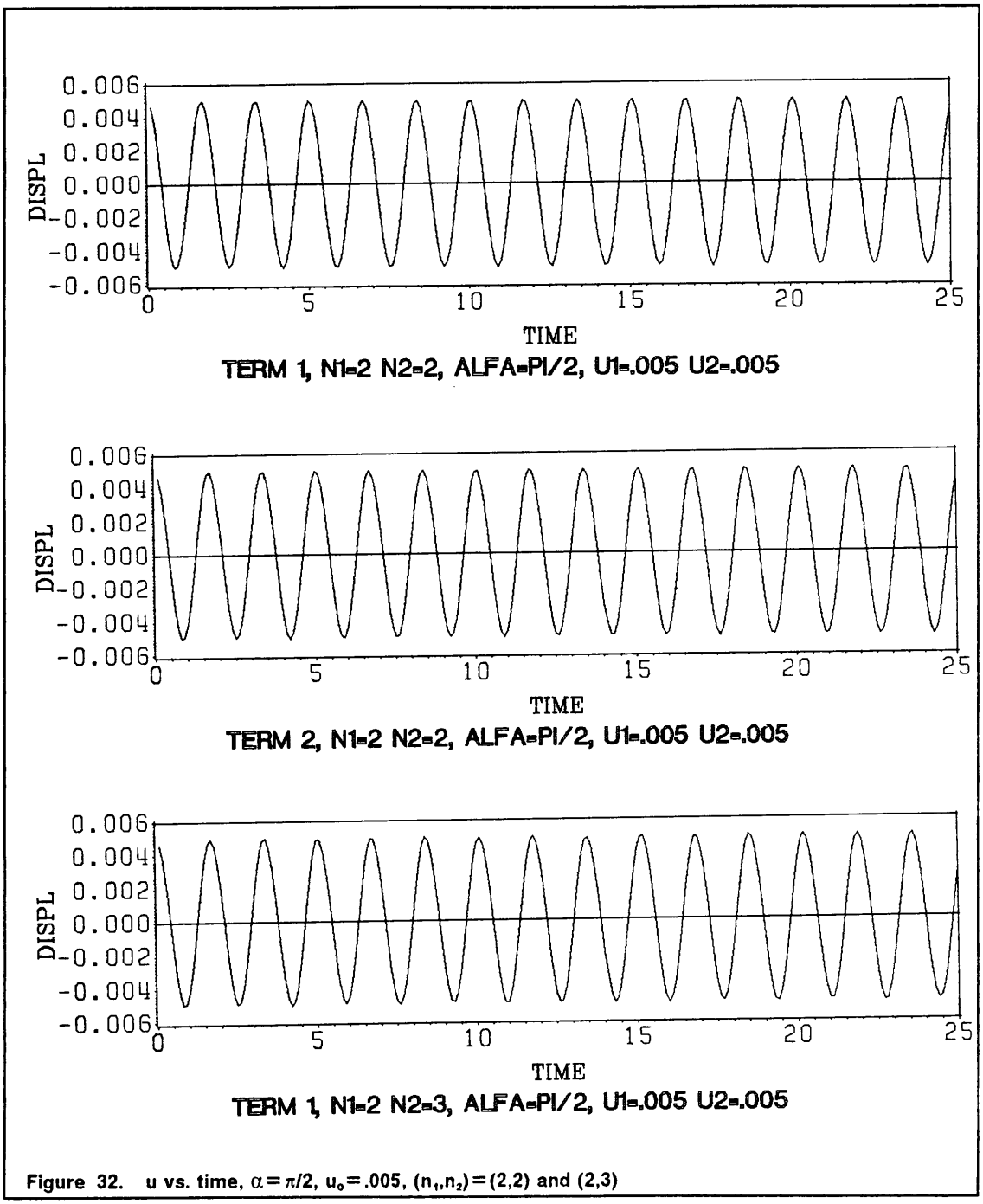

Figure 32. u vs. time, $\alpha = \pi/2$, $u_o = .005$, $(n_1,n_2) = (2,2)$ and (2,3)

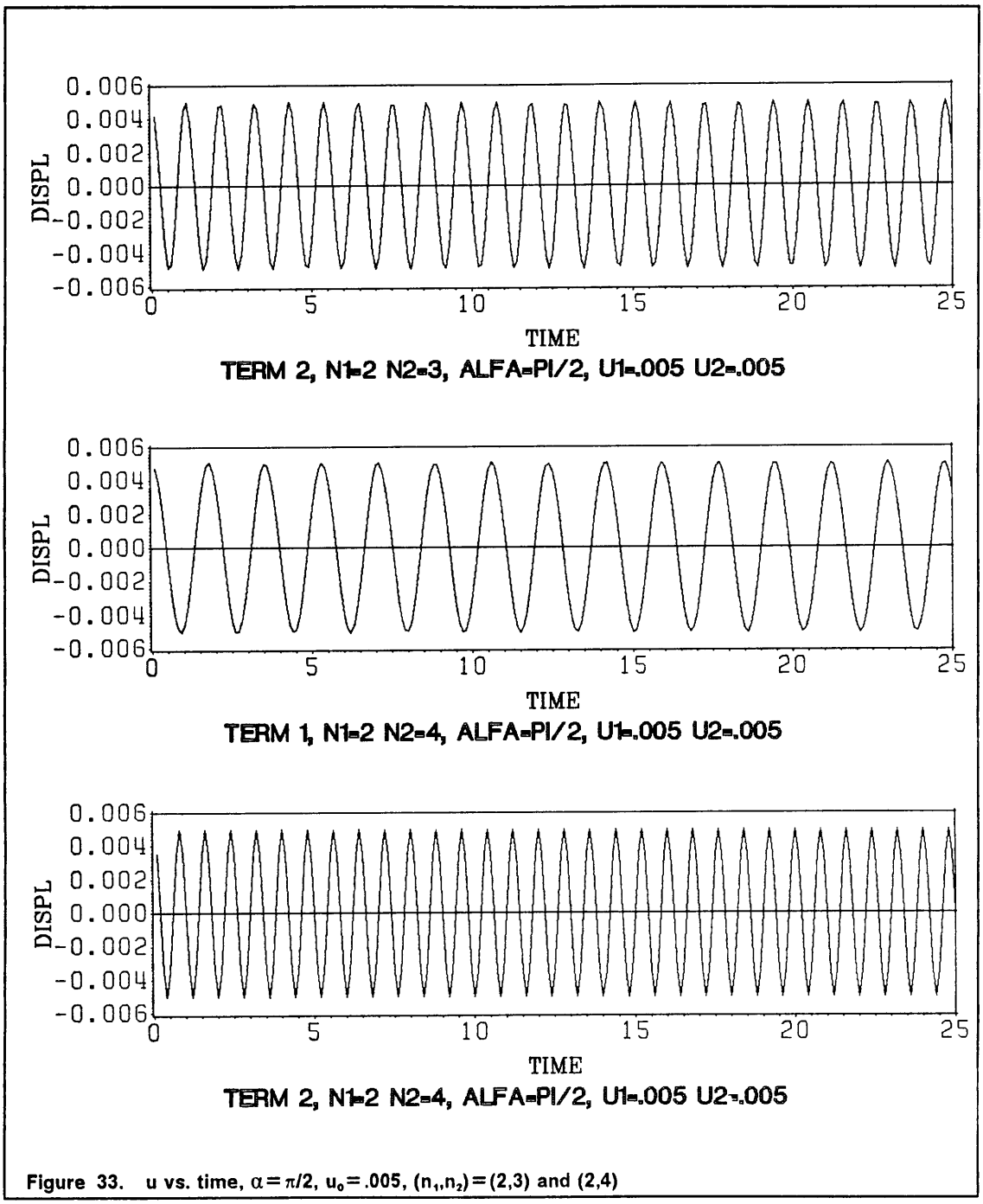

Figure 33. u vs. time, $\alpha = \pi/2$, $u_o = .005$, $(n_1,n_2) = (2,3)$ and $(2,4)$

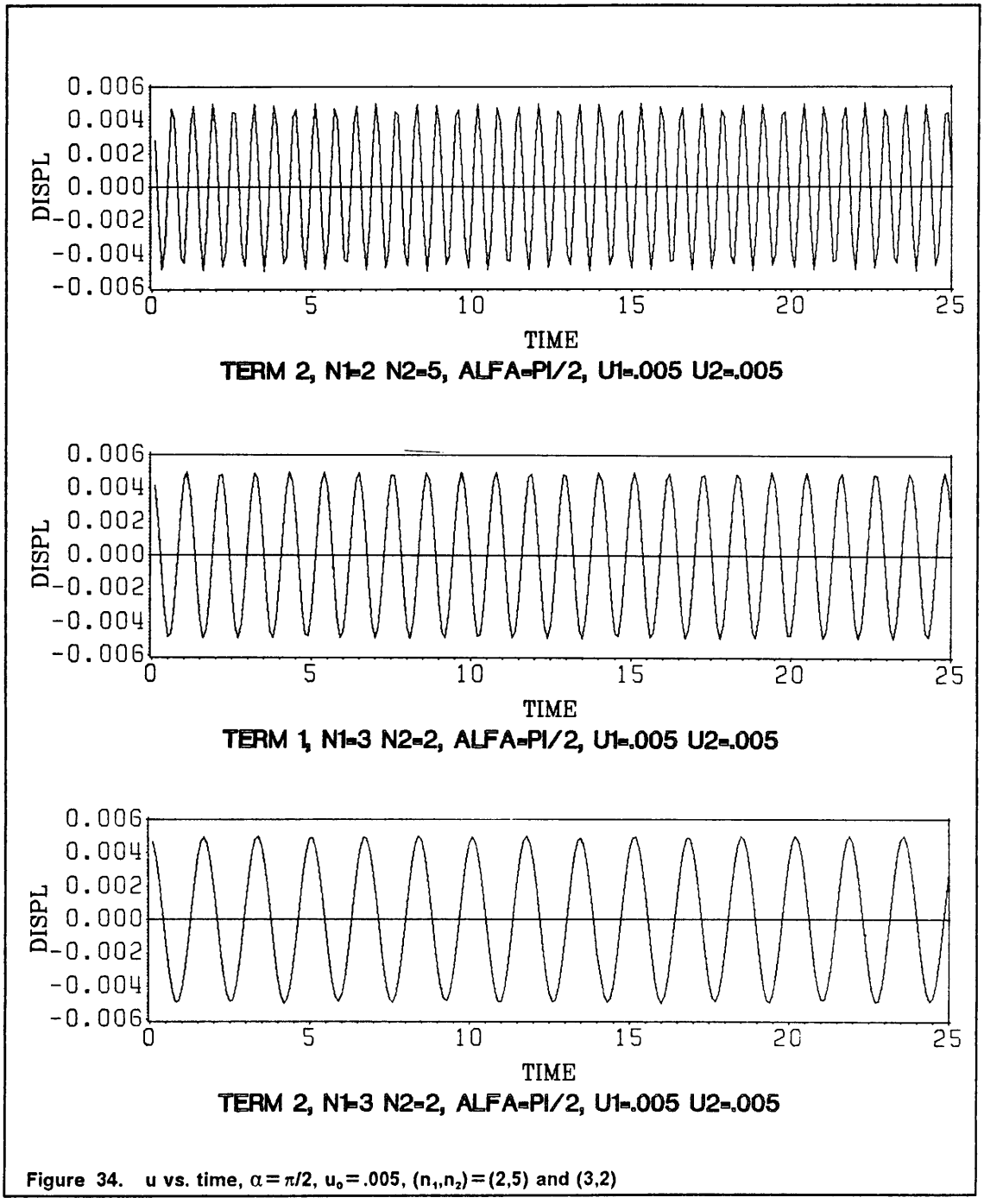

Figure 34. u vs. time, $\alpha = \pi/2$, $u_o = .005$, $(n_1,n_2) = (2,5)$ and $(3,2)$

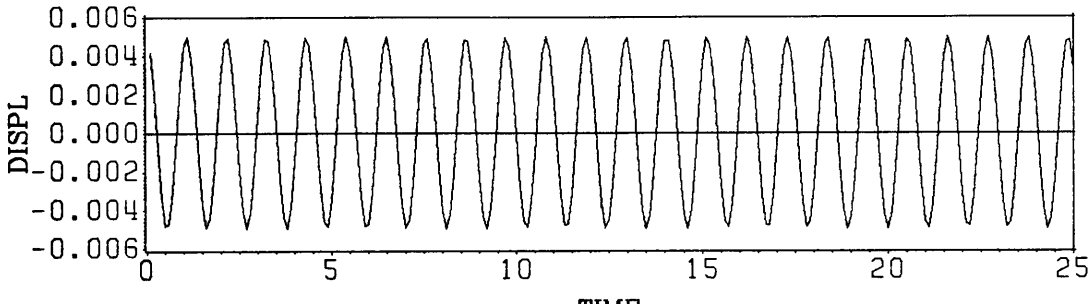

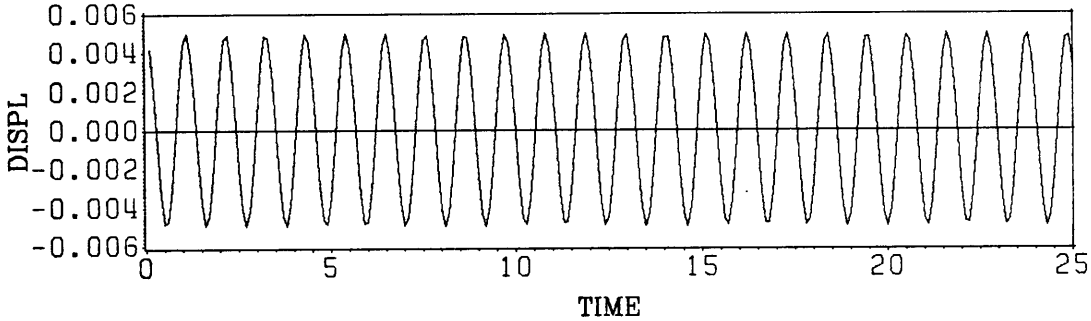

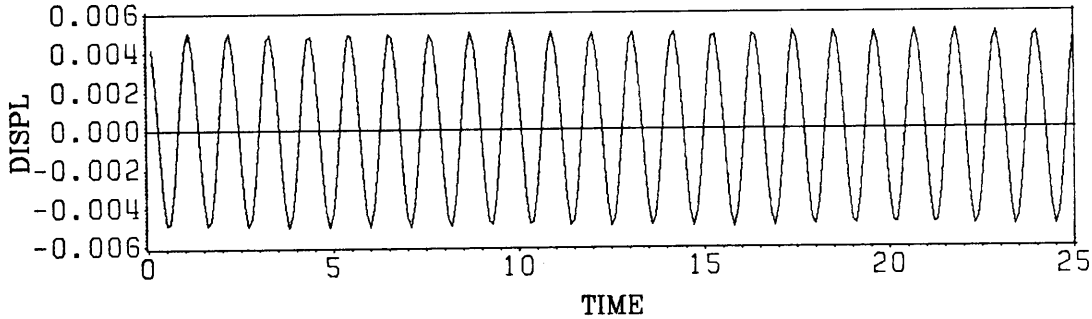

Figure 35. u vs. time, $\alpha = \pi/2$, $u_o = .005$, $(n_1,n_2) = (3,3)$ and (3,4)

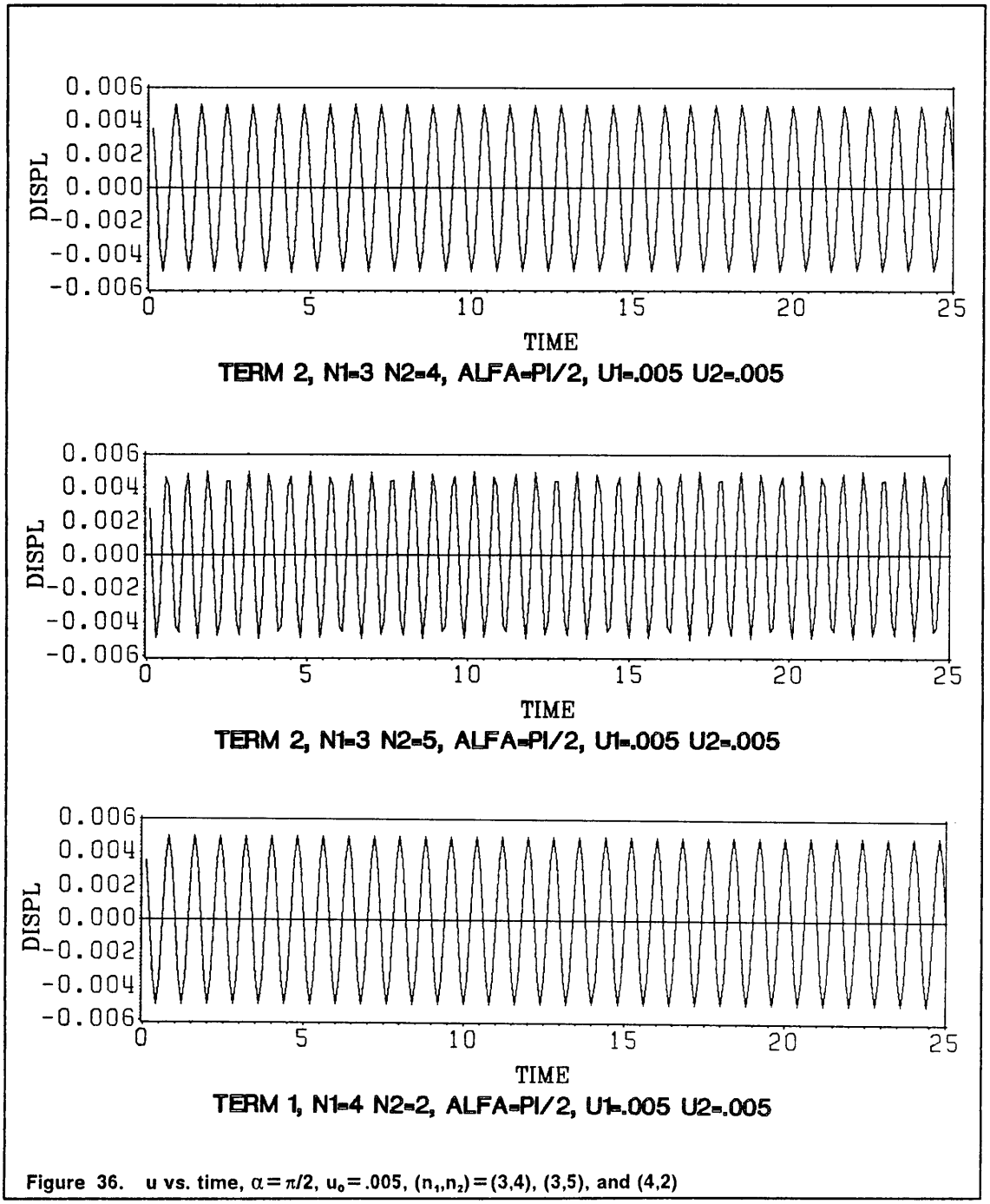

Figure 36. u vs. time, $\alpha = \pi/2$, $u_o = .005$, $(n_1,n_2) = (3,4)$, (3,5), and (4,2)

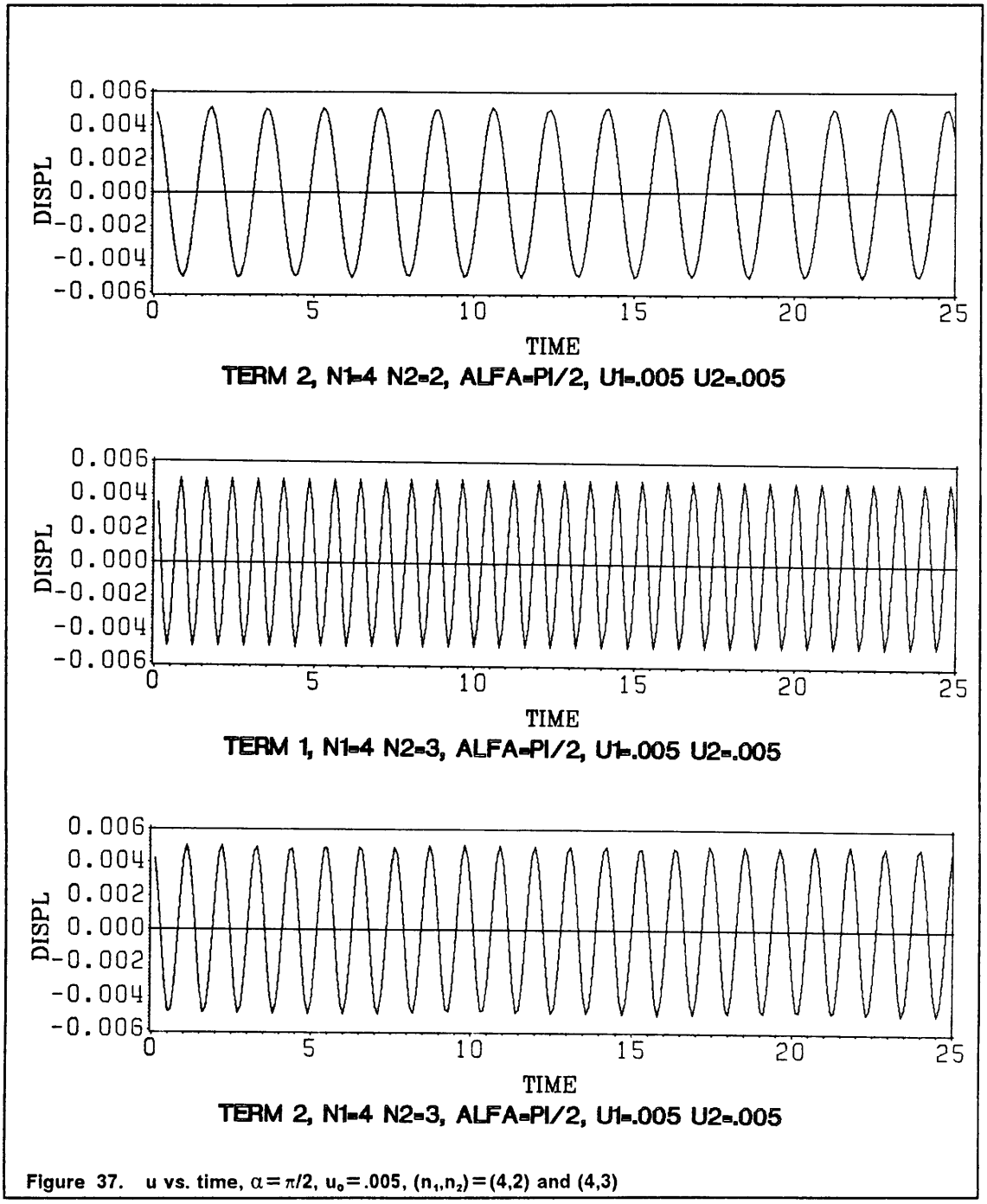

Figure 37. u vs. time, $\alpha = \pi/2$, $u_o = .005$, $(n_1,n_2) = (4,2)$ and $(4,3)$

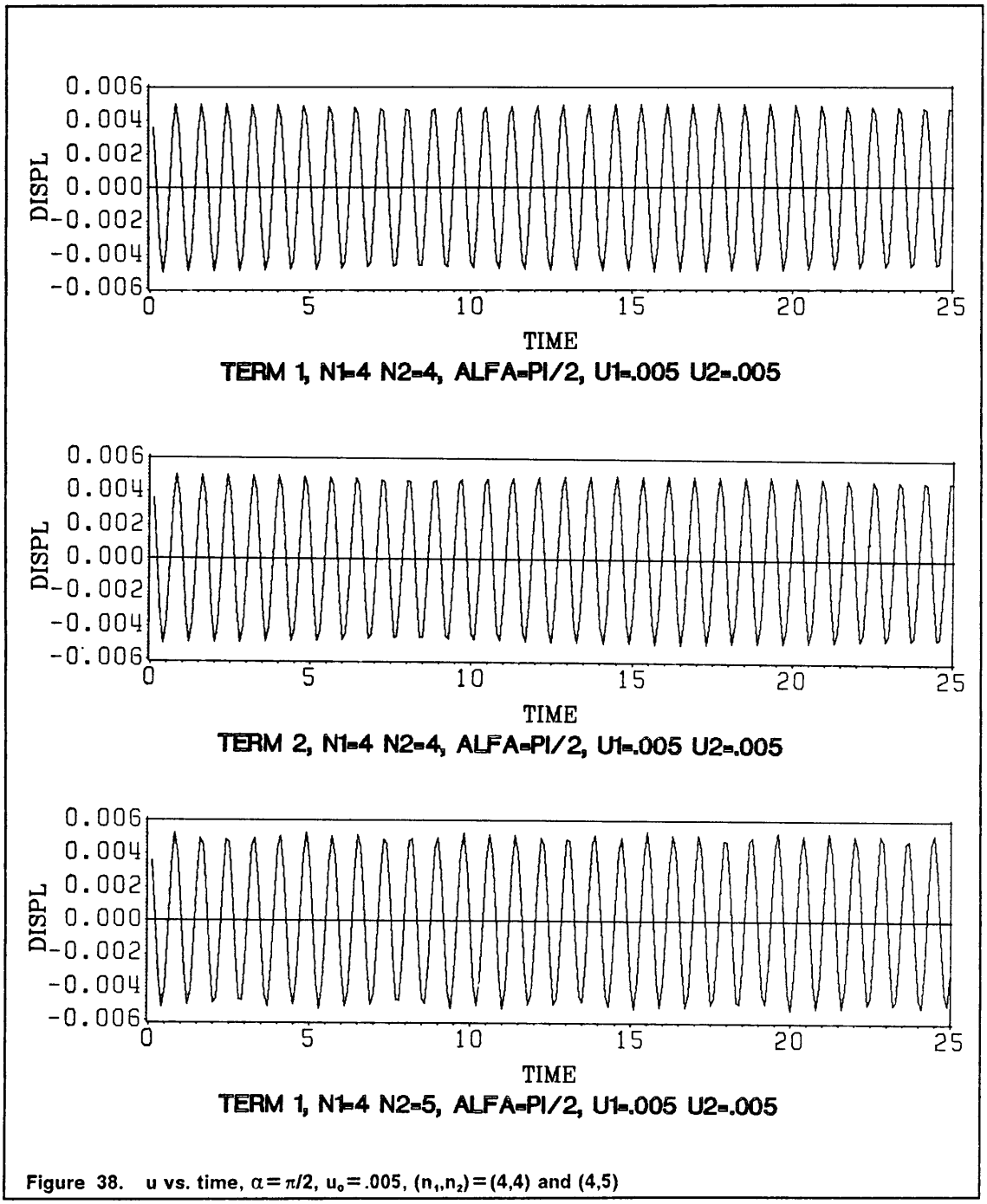

Figure 38. u vs. time, $\alpha = \pi/2$, $u_o = .005$, $(n_1, n_2) = (4,4)$ and (4,5)

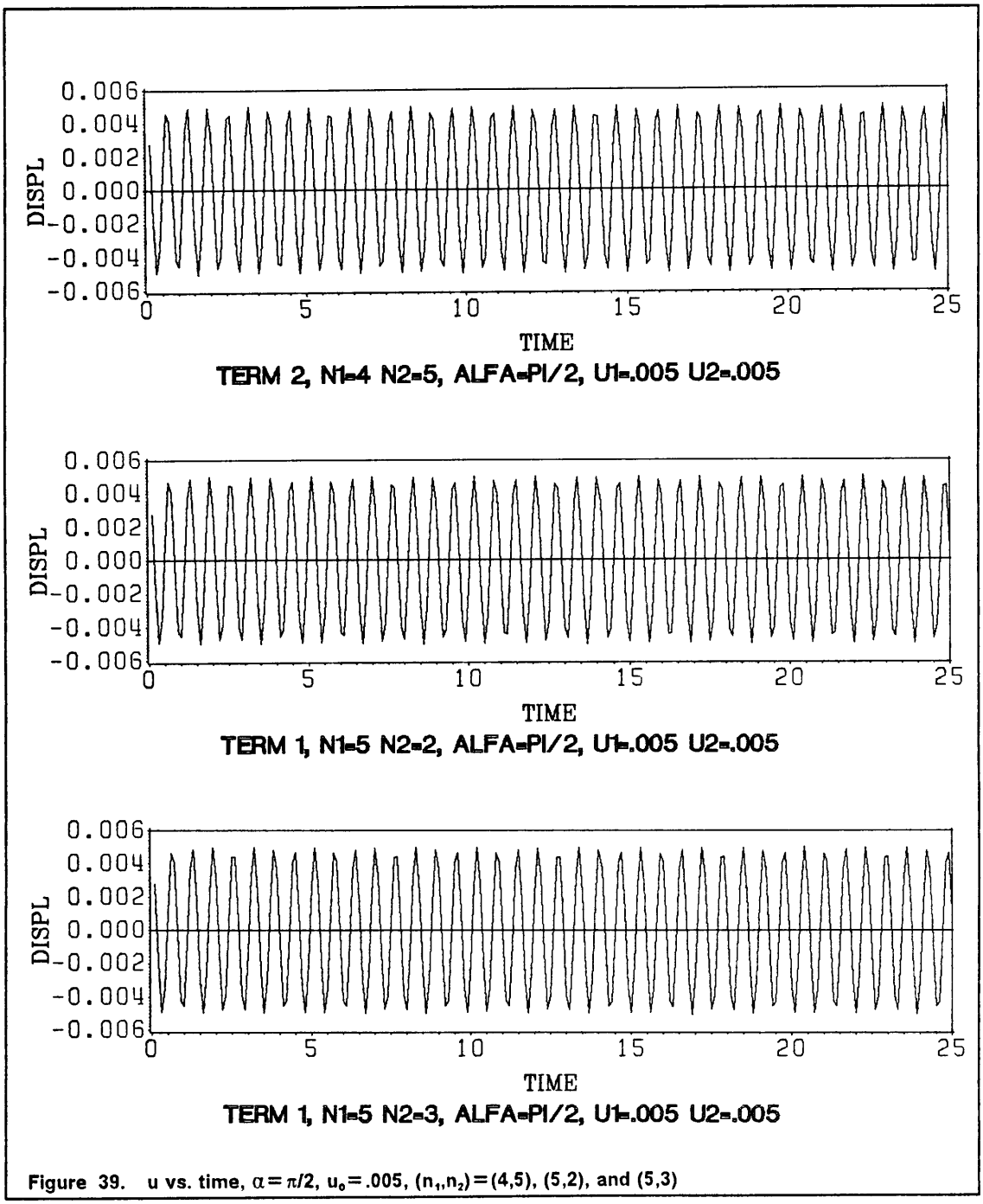

Figure 39. u vs. time, $\alpha = \pi/2$, $u_o = .005$, $(n_1,n_2) = (4,5)$, (5,2), and (5,3)

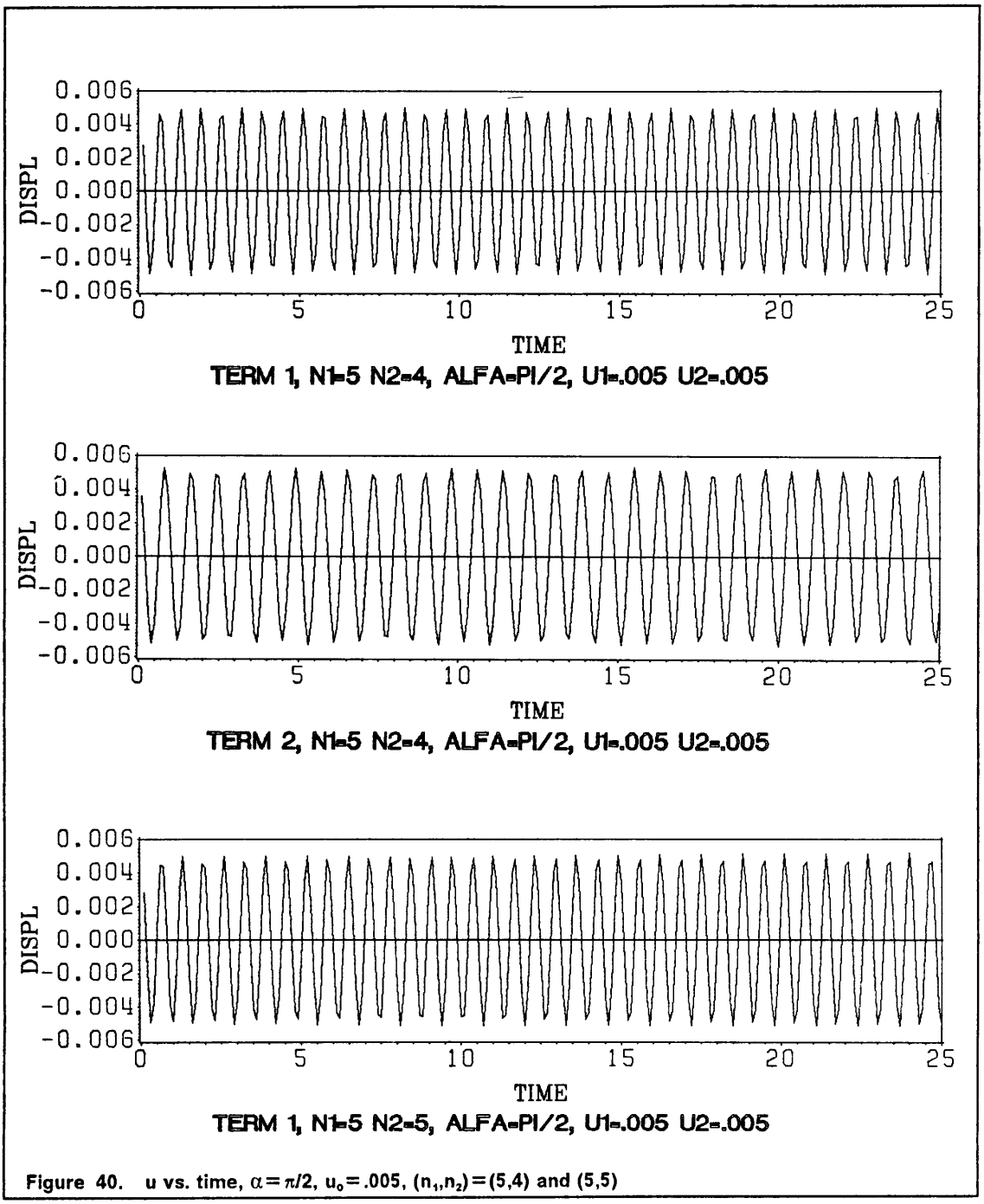

Figure 40. u vs. time, $\alpha = \pi/2$, $u_o = .005$, $(n_1,n_2) = (5,4)$ and $(5,5)$

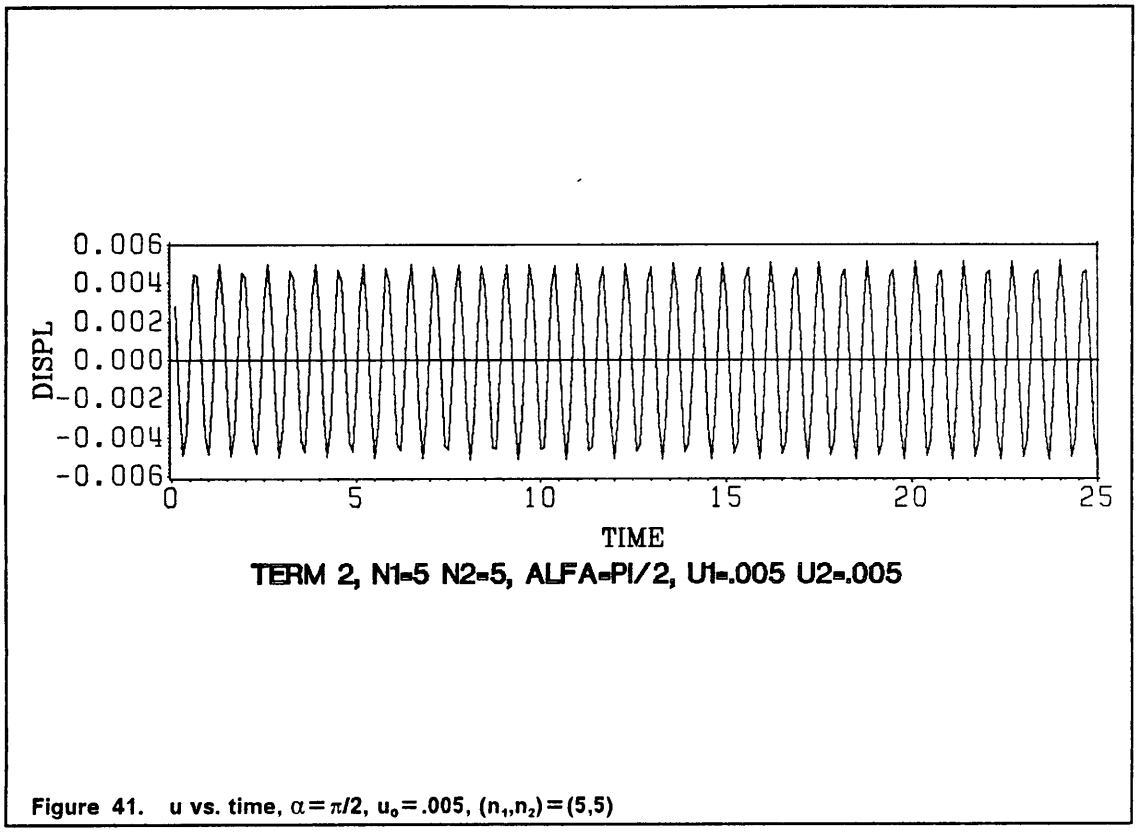

Figure 41. u vs. time, $\alpha = \pi/2$, $u_o = .005$, $(n_1,n_2) = (5,5)$

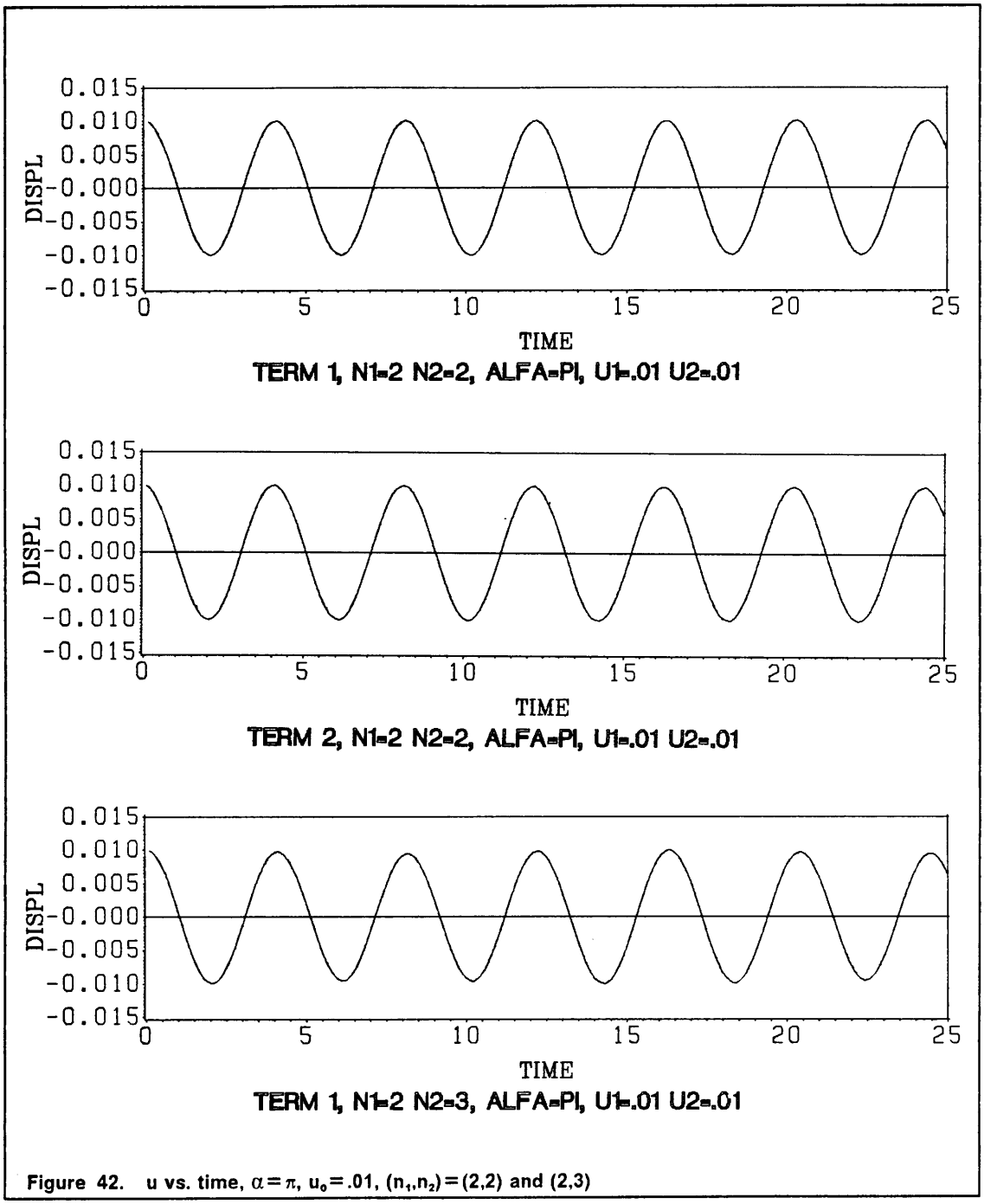

Figure 42. u vs. time, $\alpha = \pi$, $u_0 = .01$, $(n_1, n_2) = (2,2)$ and (2,3)

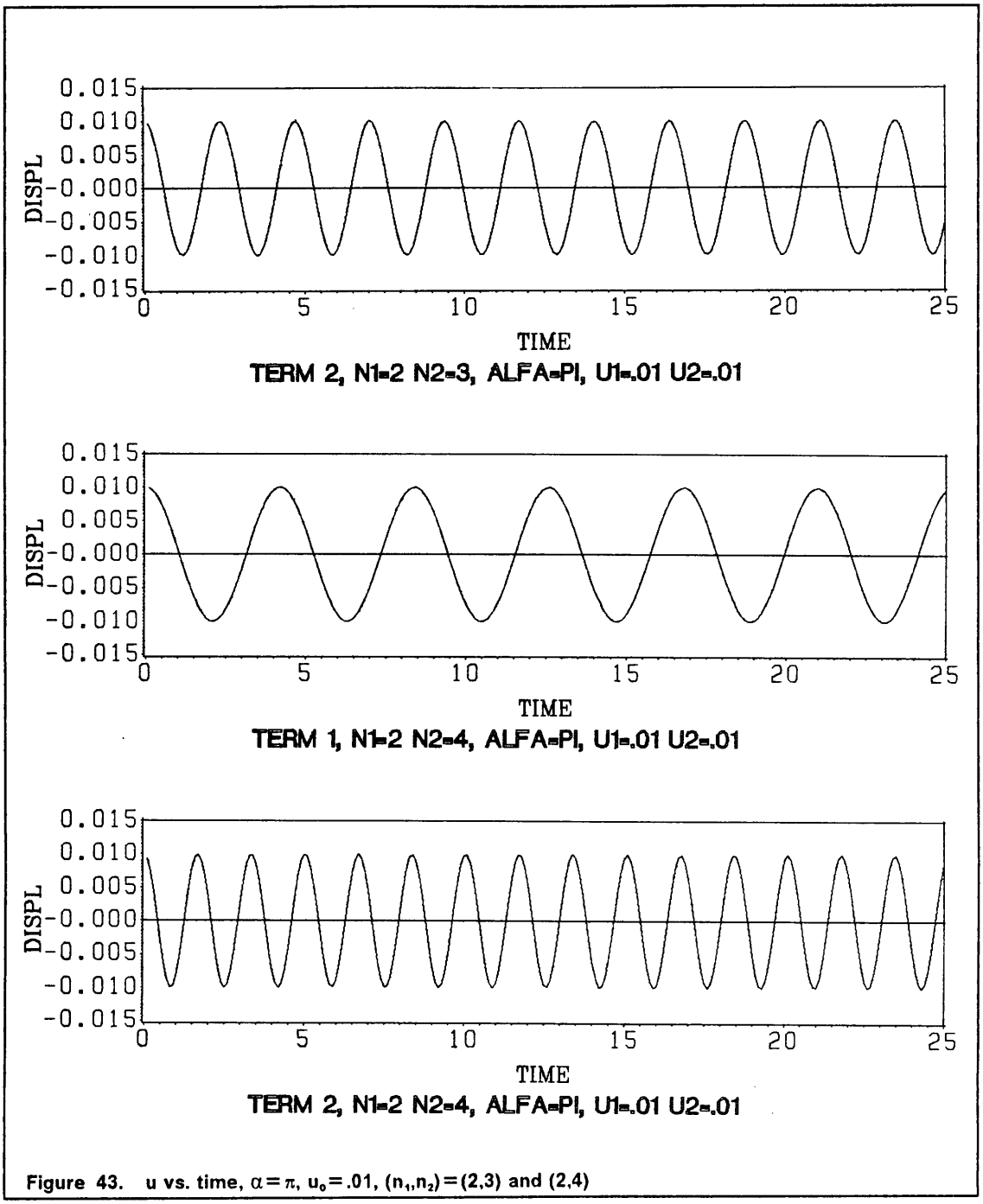

Figure 43. u vs. time, $\alpha = \pi$, $u_0 = .01$, $(n_1,n_2) = (2,3)$ and $(2,4)$

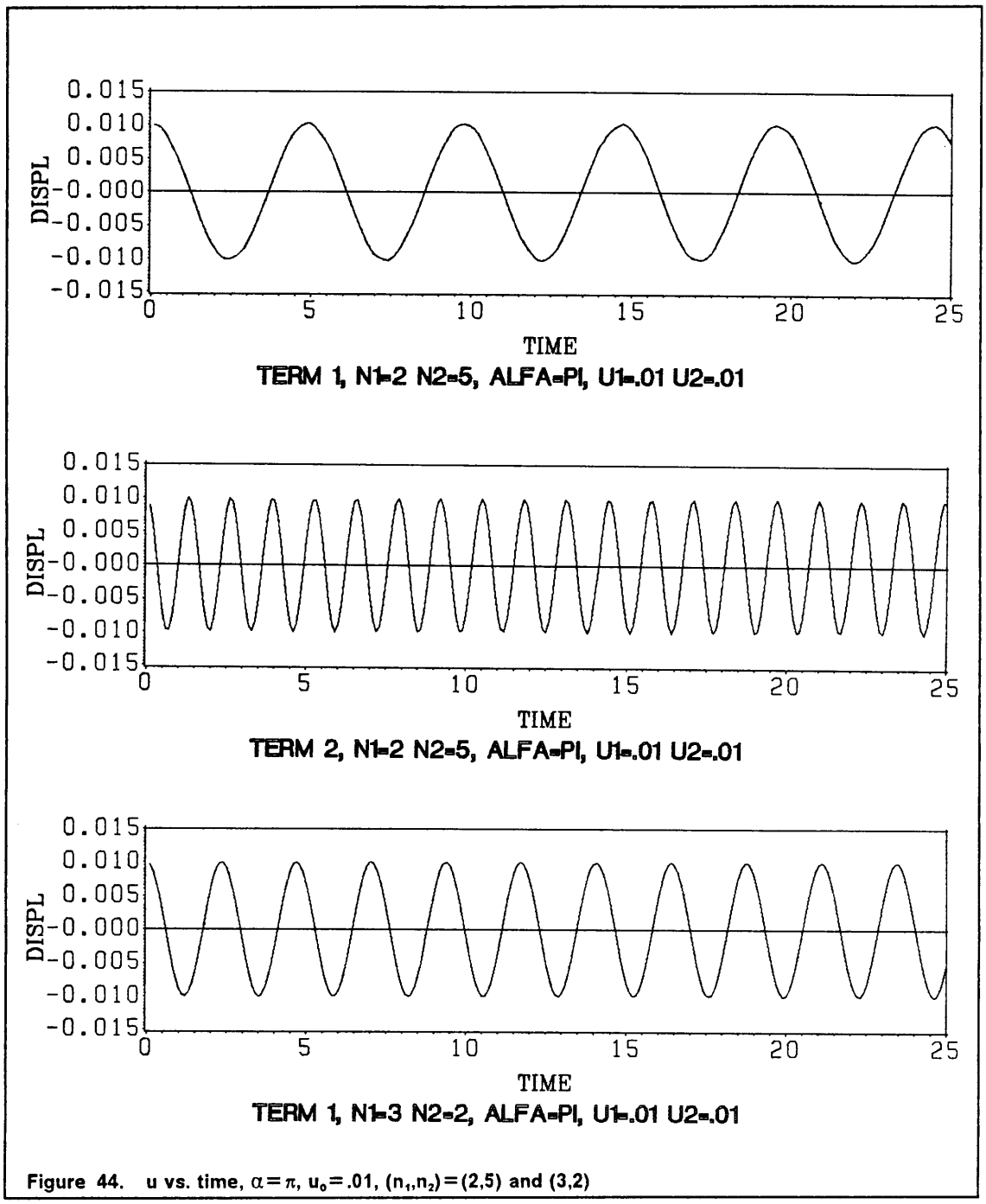

Figure 44. u vs. time, $\alpha = \pi$, $u_o = .01$, $(n_1, n_2) = (2,5)$ and $(3,2)$

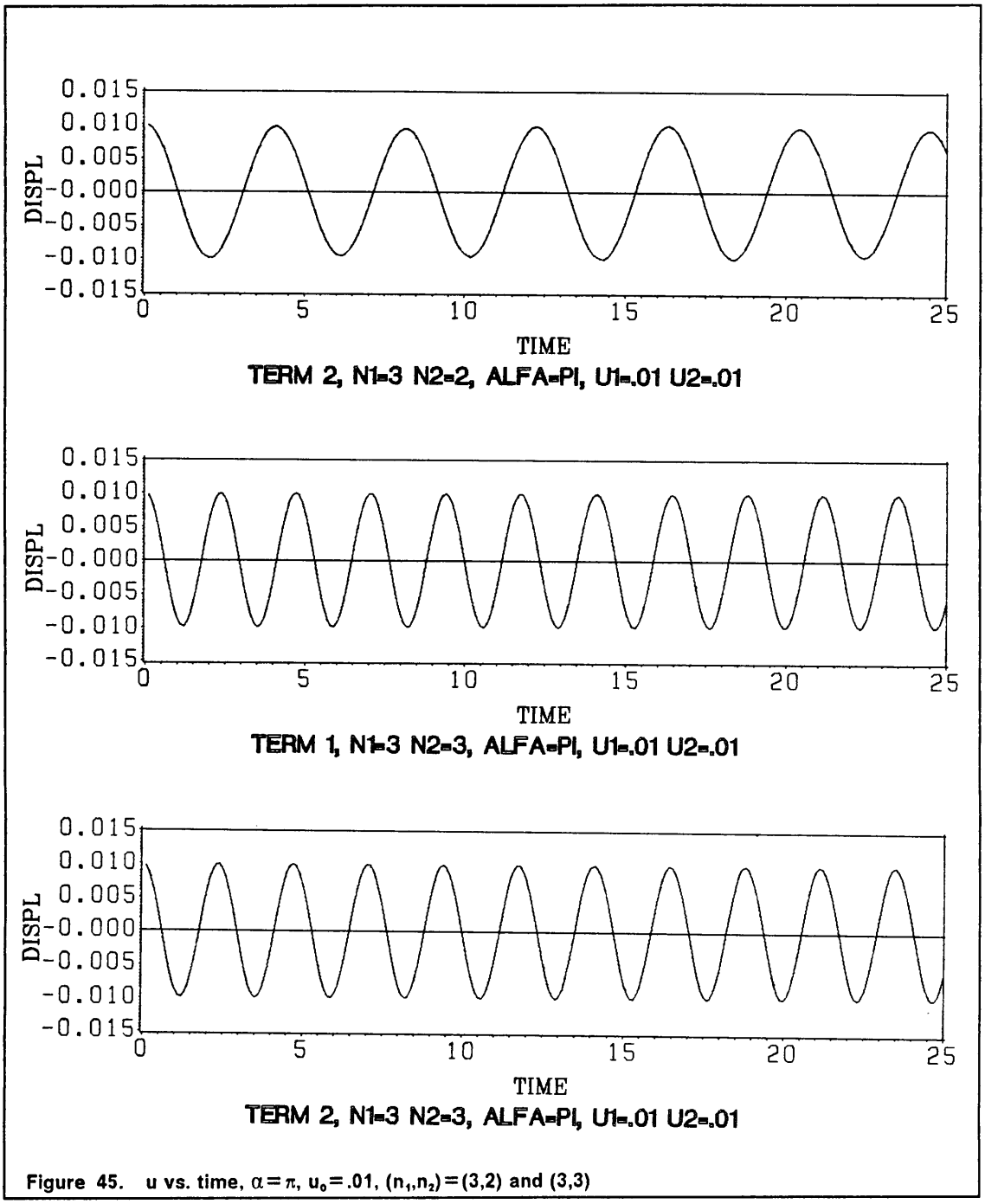

Figure 45. u vs. time, $\alpha = \pi$, $u_o = .01$, $(n_1, n_2) = (3,2)$ and $(3,3)$

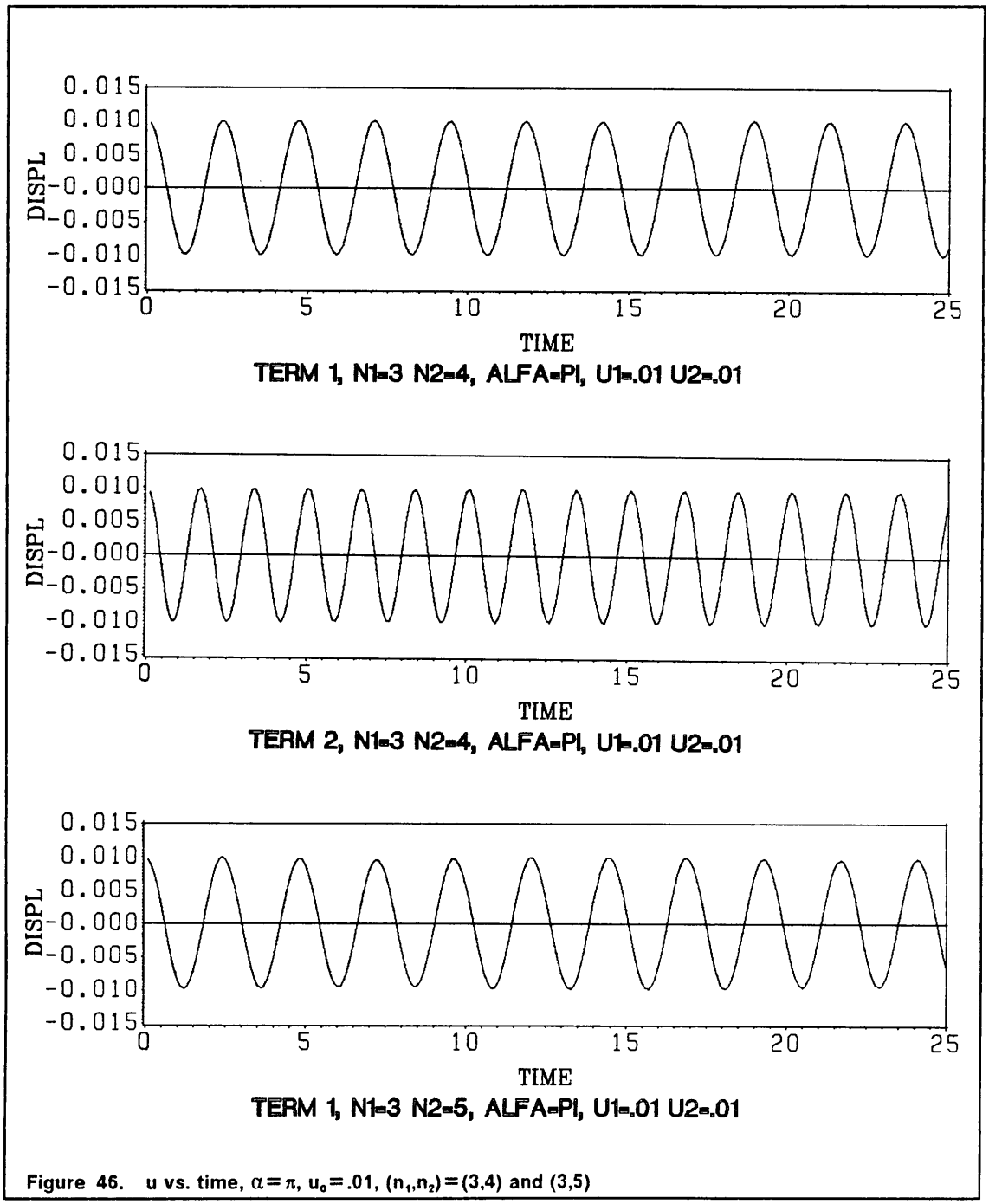

Figure 46. u vs. time, $\alpha = \pi$, $u_o = .01$, $(n_1, n_2) = (3,4)$ and $(3,5)$

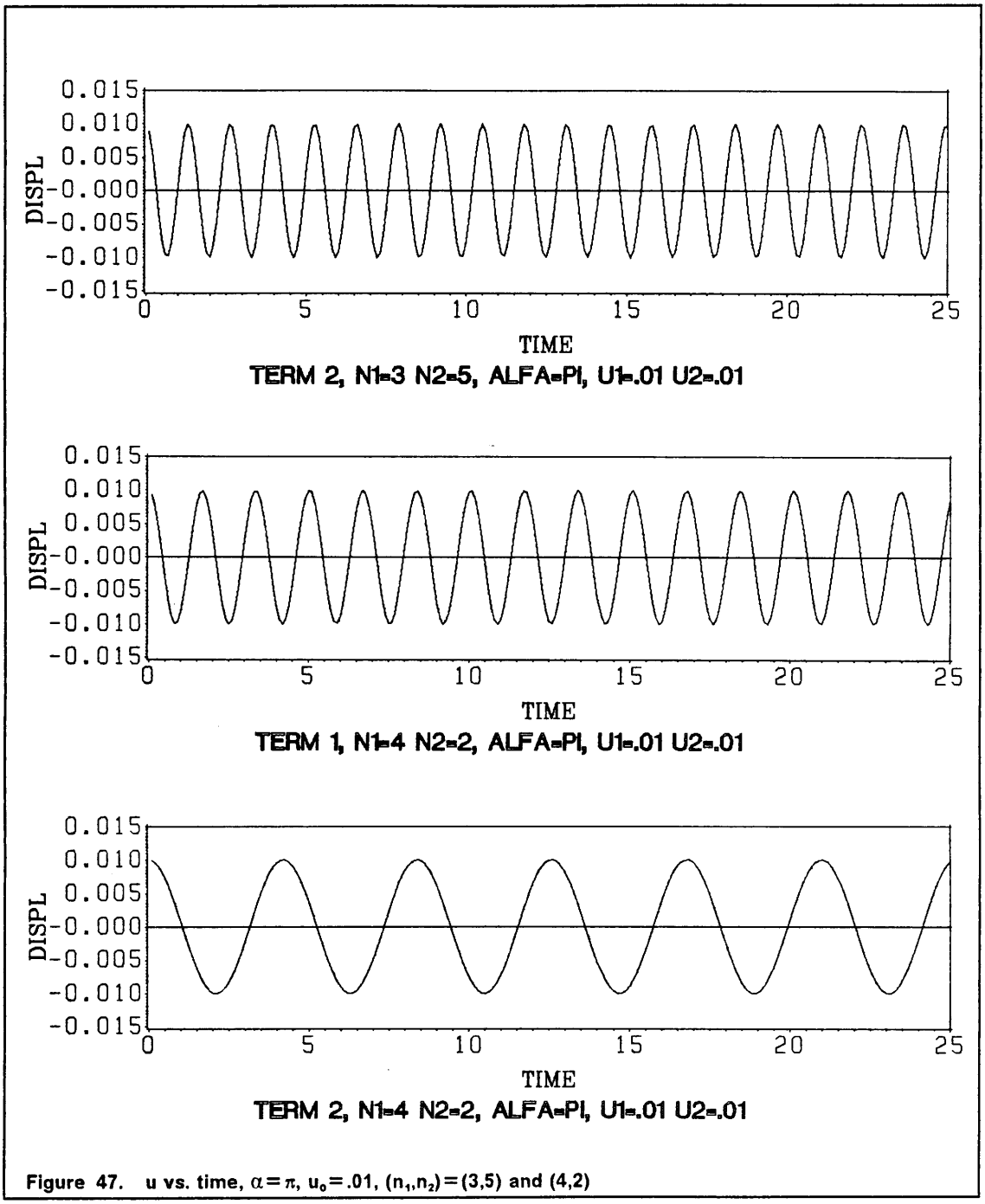

Figure 47. u vs. time, $\alpha = \pi$, $u_o = .01$, $(n_1, n_2) = (3,5)$ and $(4,2)$

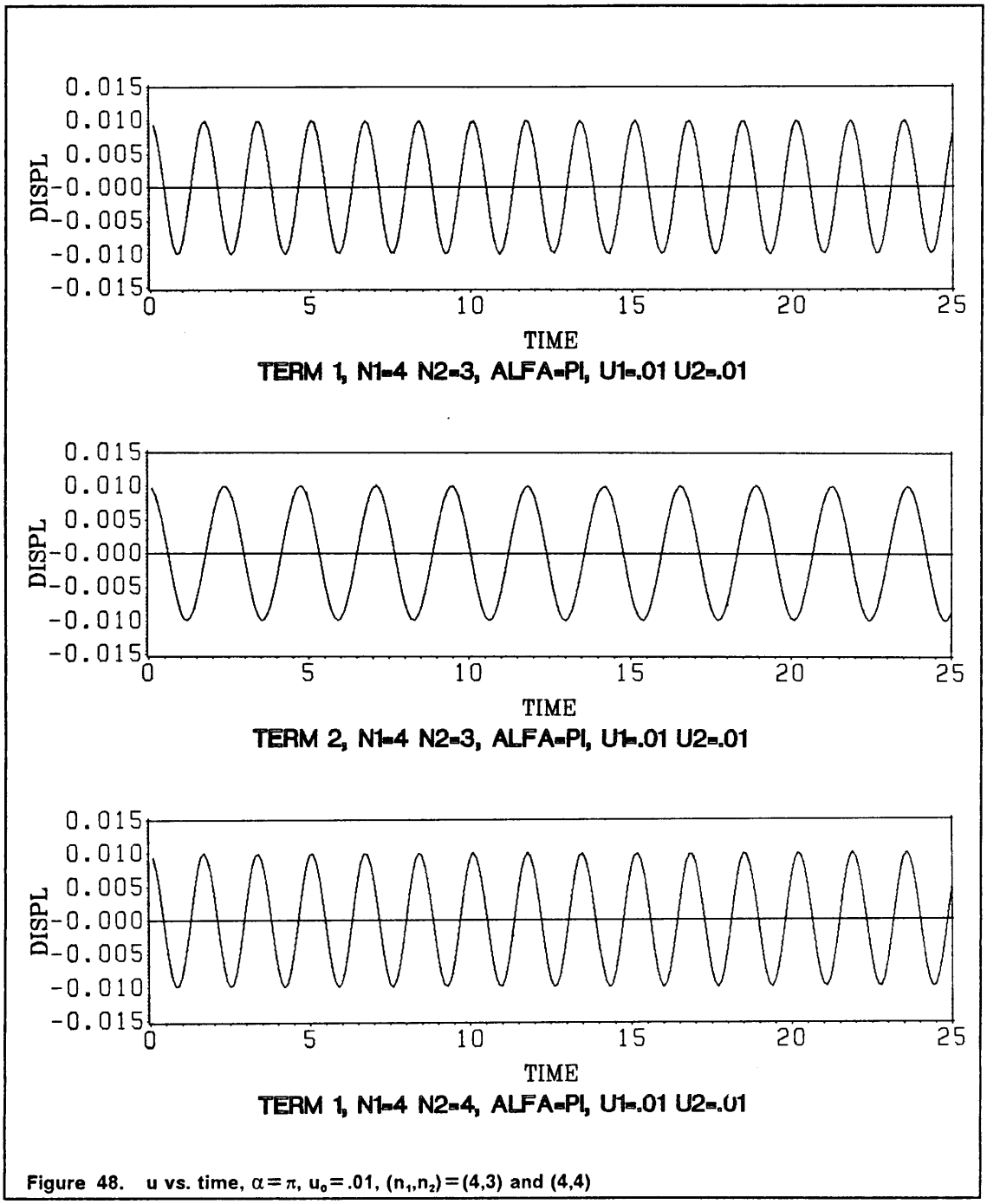

Figure 48. u vs. time, $\alpha = \pi$, $u_o = .01$, $(n_1, n_2) = (4,3)$ and $(4,4)$

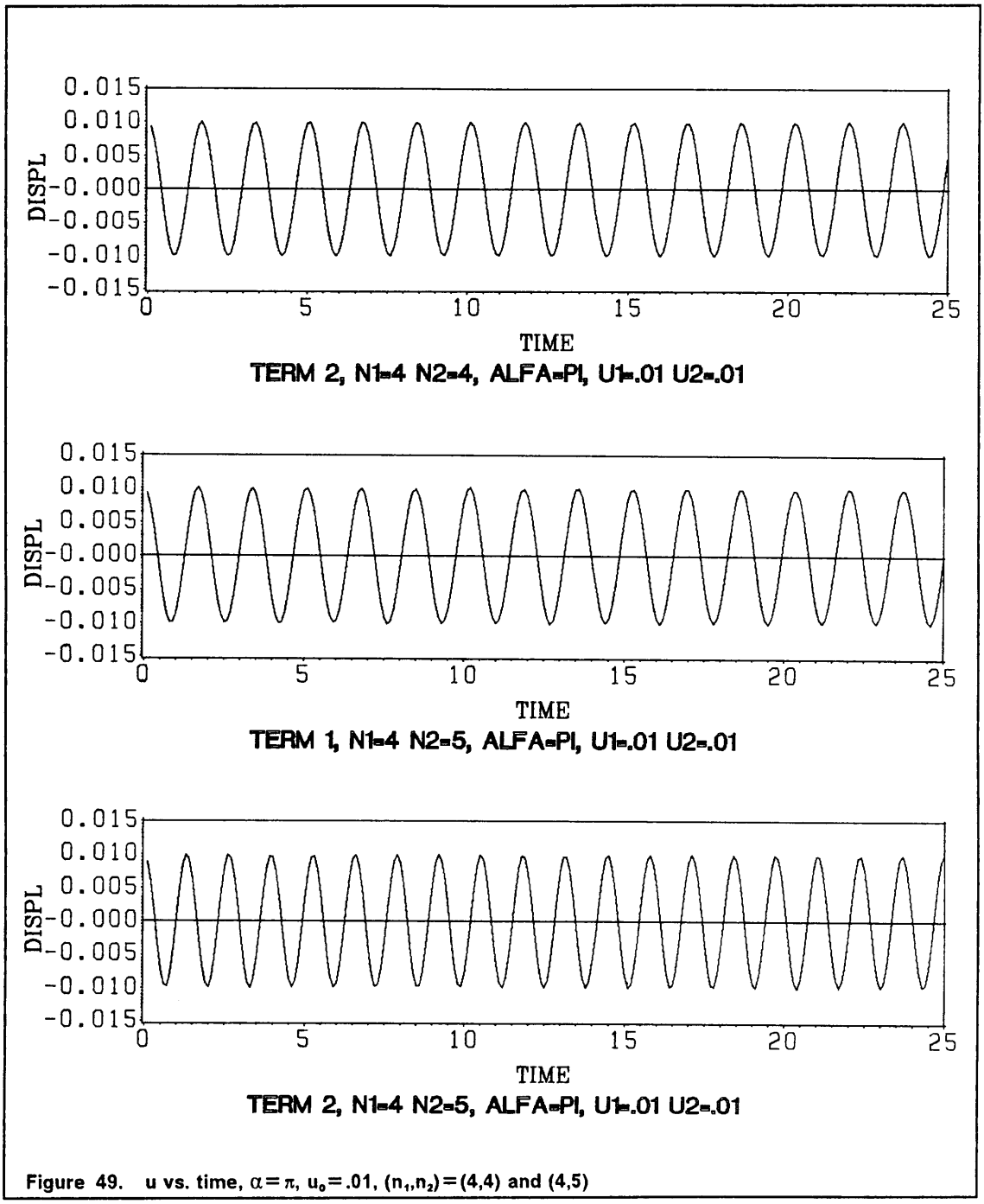

Figure 49. u vs. time, $\alpha = \pi$, $u_o = .01$, $(n_1, n_2) = (4,4)$ and $(4,5)$

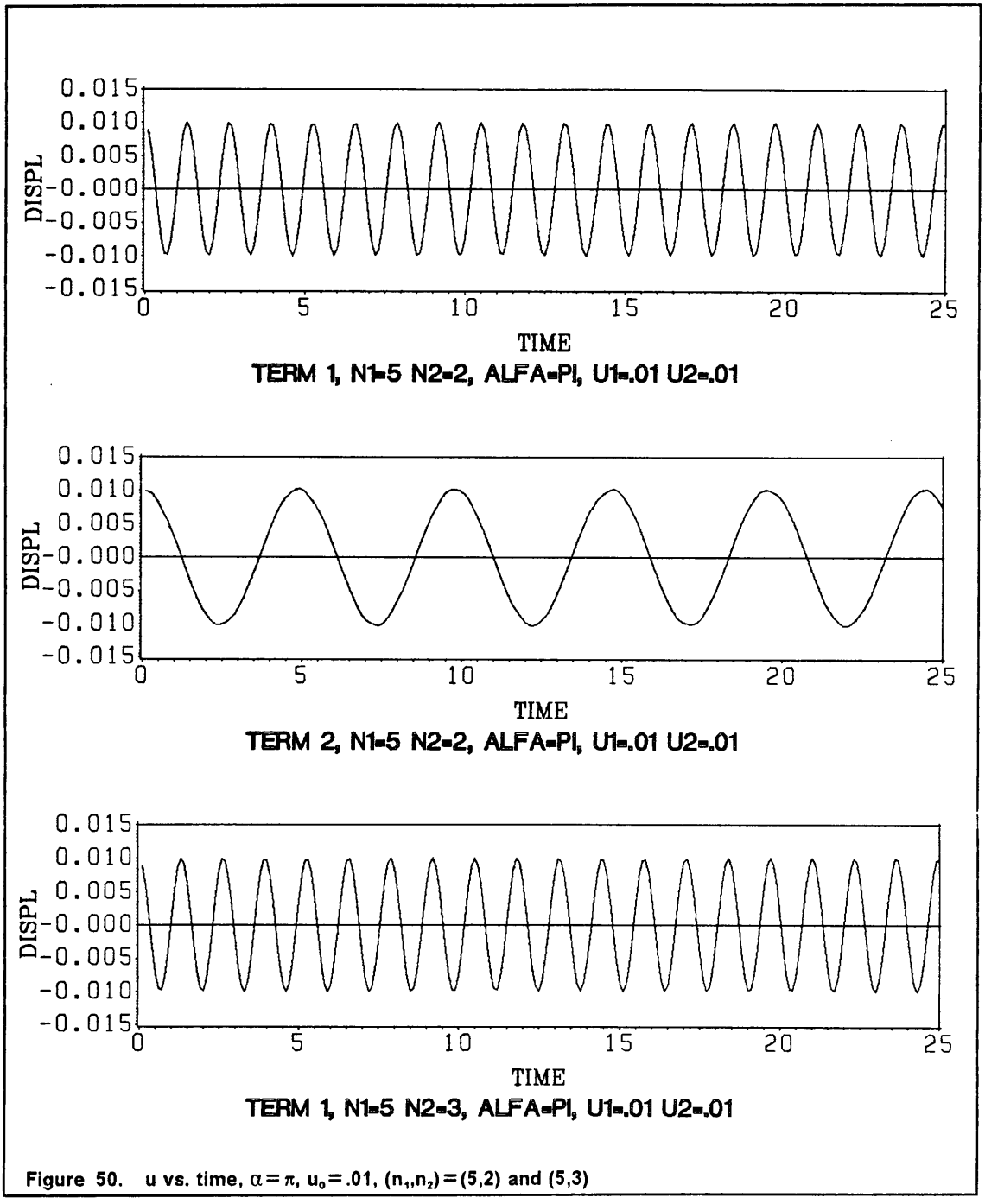

Figure 50. u vs. time, $\alpha = \pi$, $u_o = .01$, $(n_1,n_2) = (5,2)$ and $(5,3)$

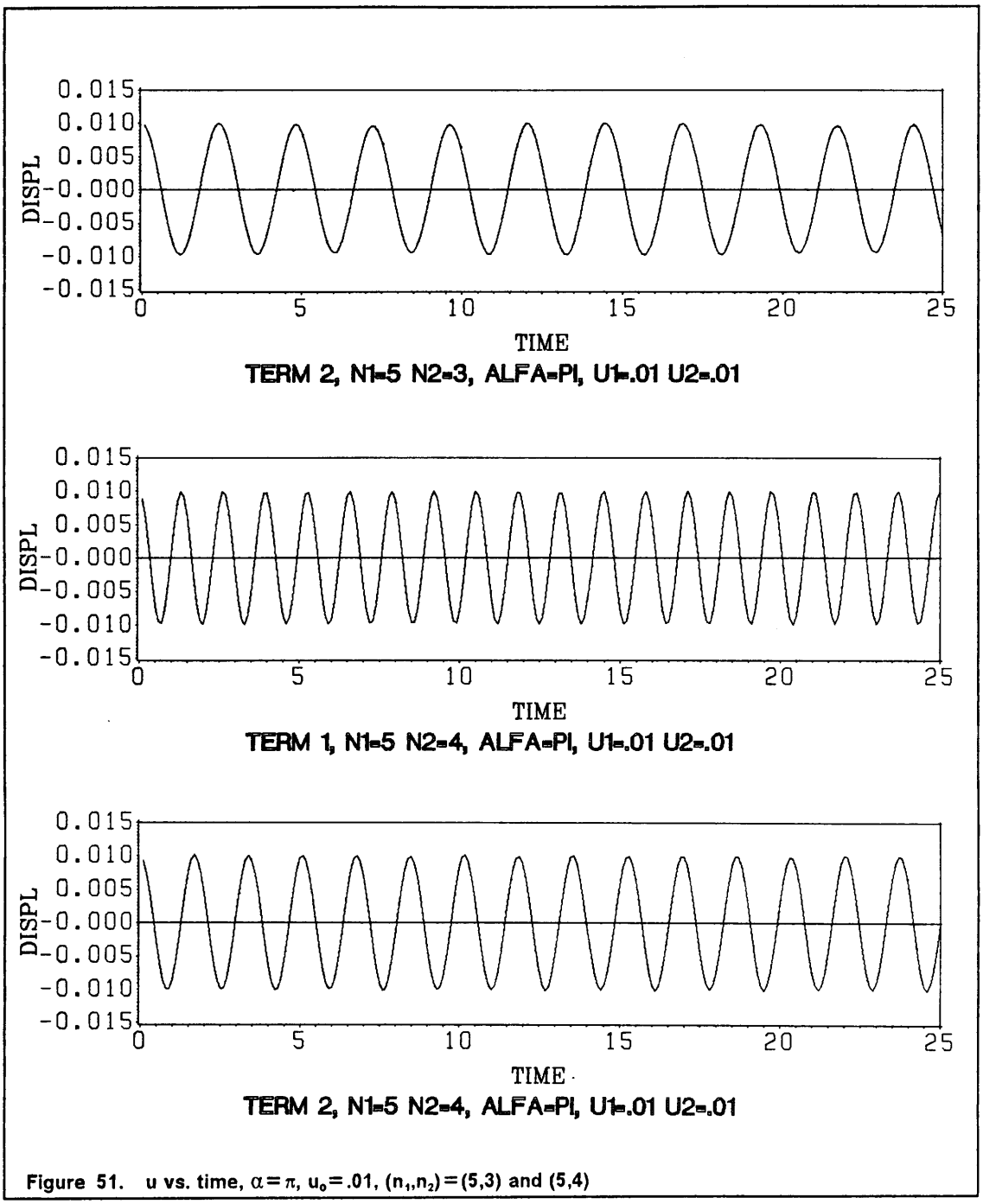

Figure 51. u vs. time, $\alpha = \pi$, $u_o = .01$, $(n_1, n_2) = (5,3)$ and $(5,4)$

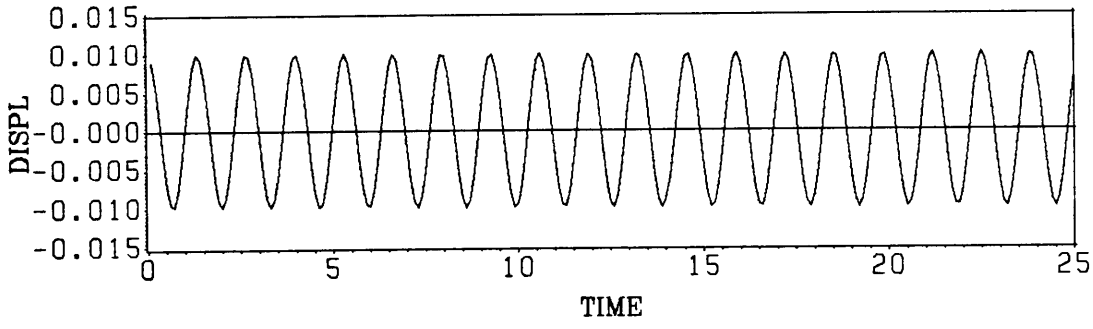

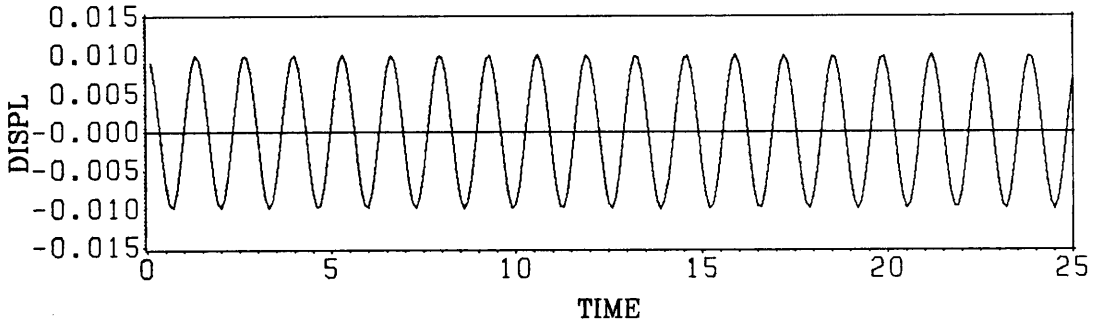

Figure 52. u vs. time, $\alpha = \pi$, $u_o = .01$, $(n_1, n_2) = (5,5)$

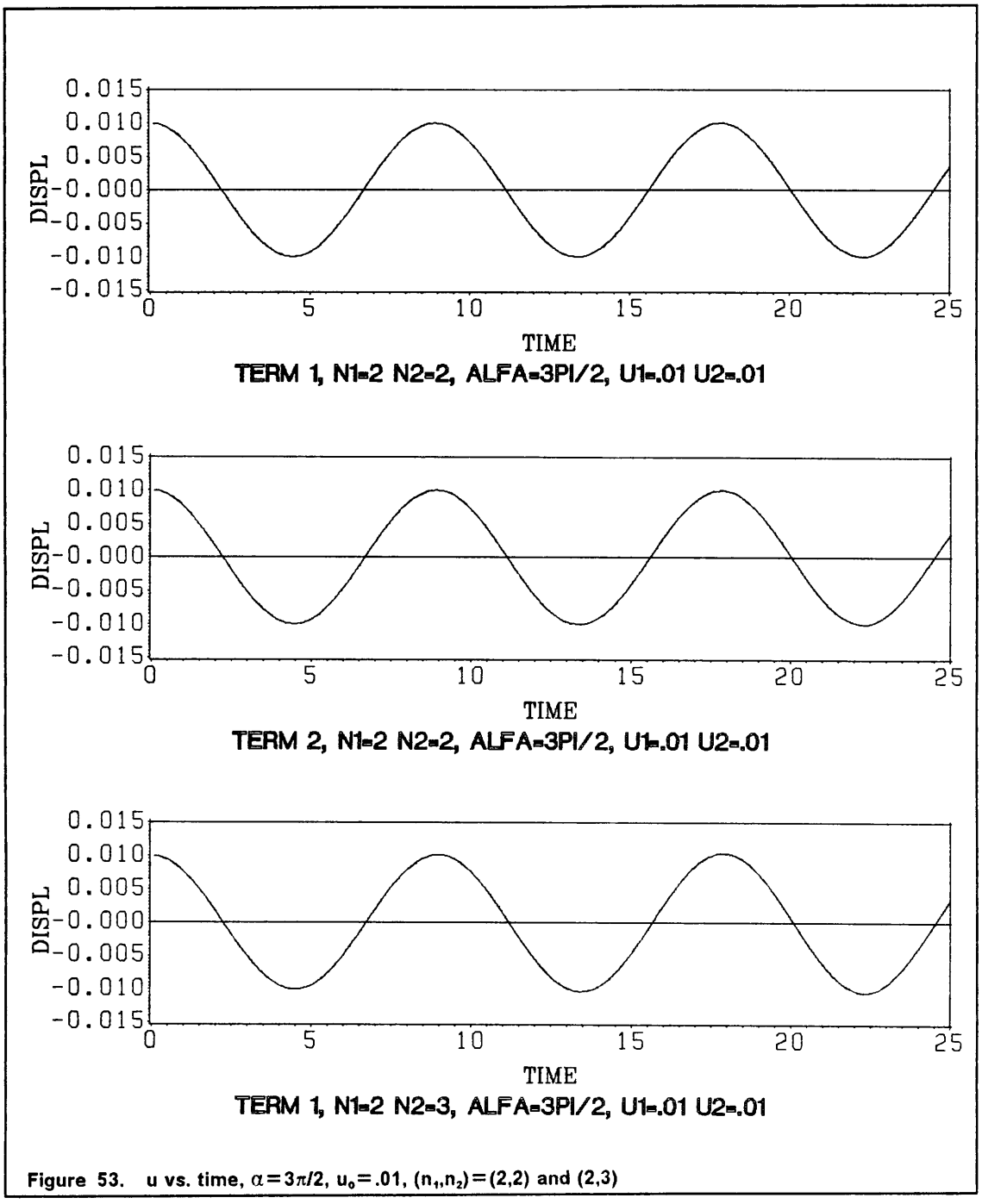

Figure 53. u vs. time, $\alpha = 3\pi/2$, $u_o = .01$, $(n_1, n_2) = (2,2)$ and $(2,3)$

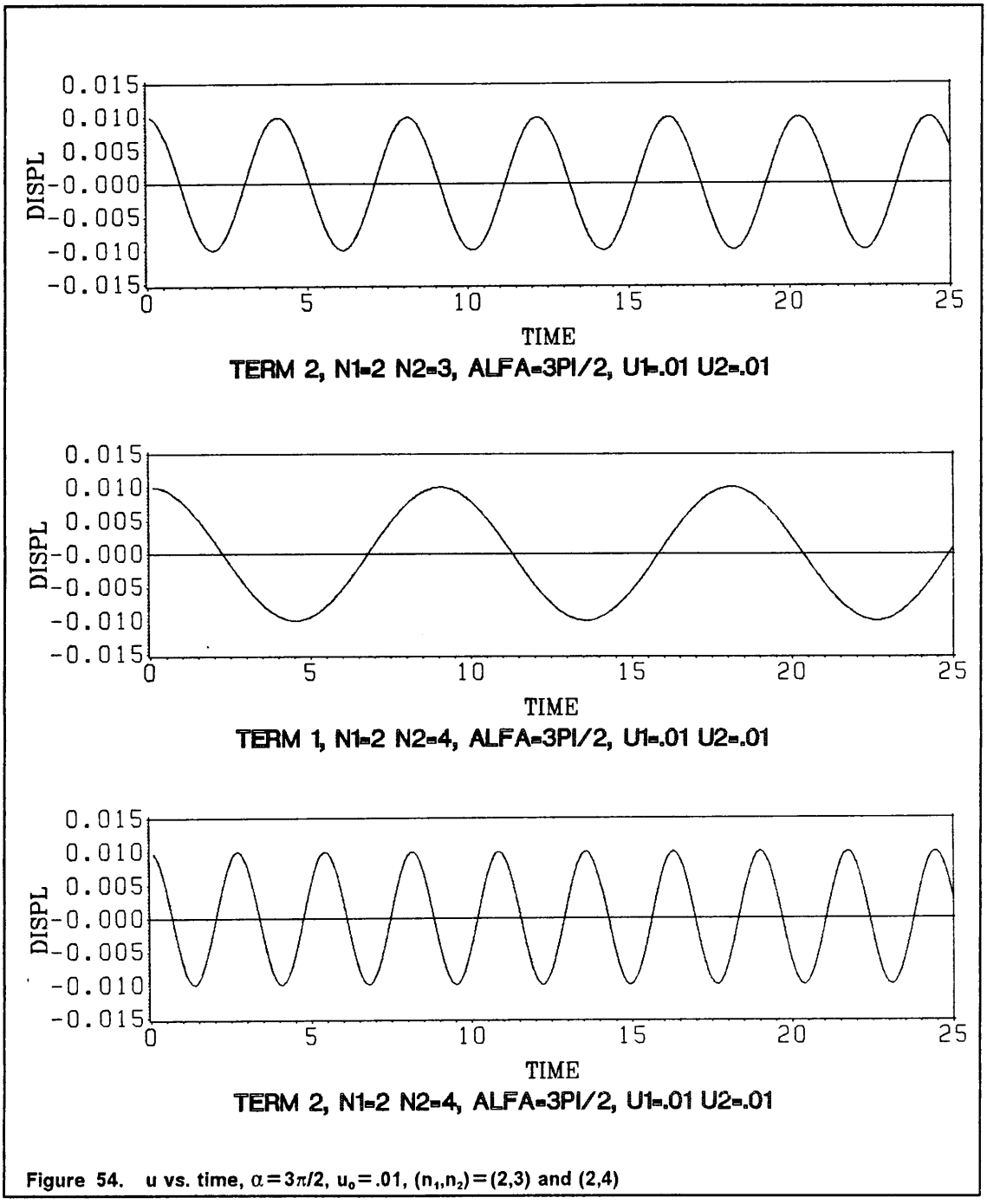

Figure 54. u vs. time, $\alpha = 3\pi/2$, $u_o = .01$, $(n_1,n_2) = (2,3)$ and $(2,4)$

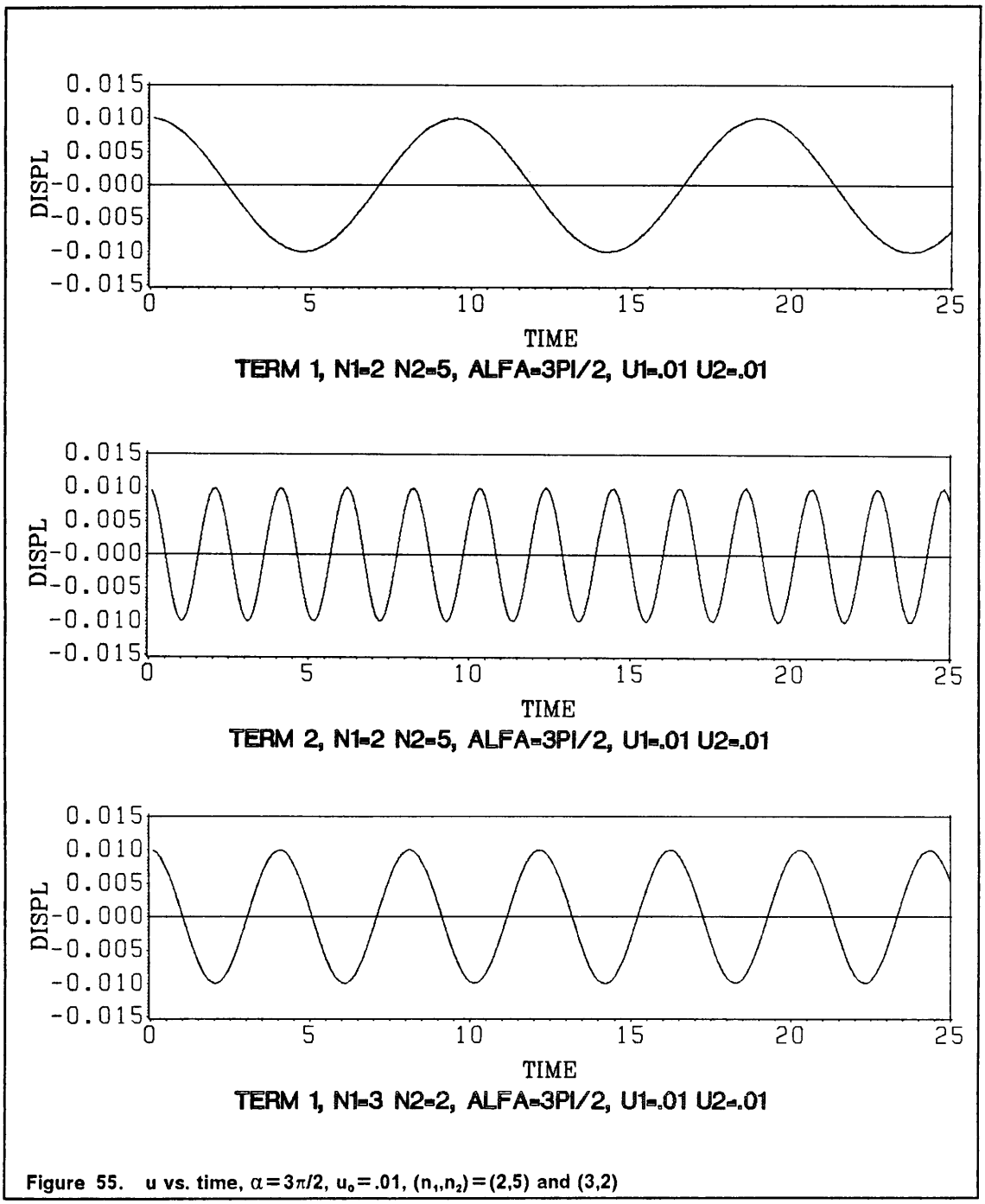

Figure 55. u vs. time, $\alpha = 3\pi/2$, $u_o = .01$, $(n_1, n_2) = (2,5)$ and $(3,2)$

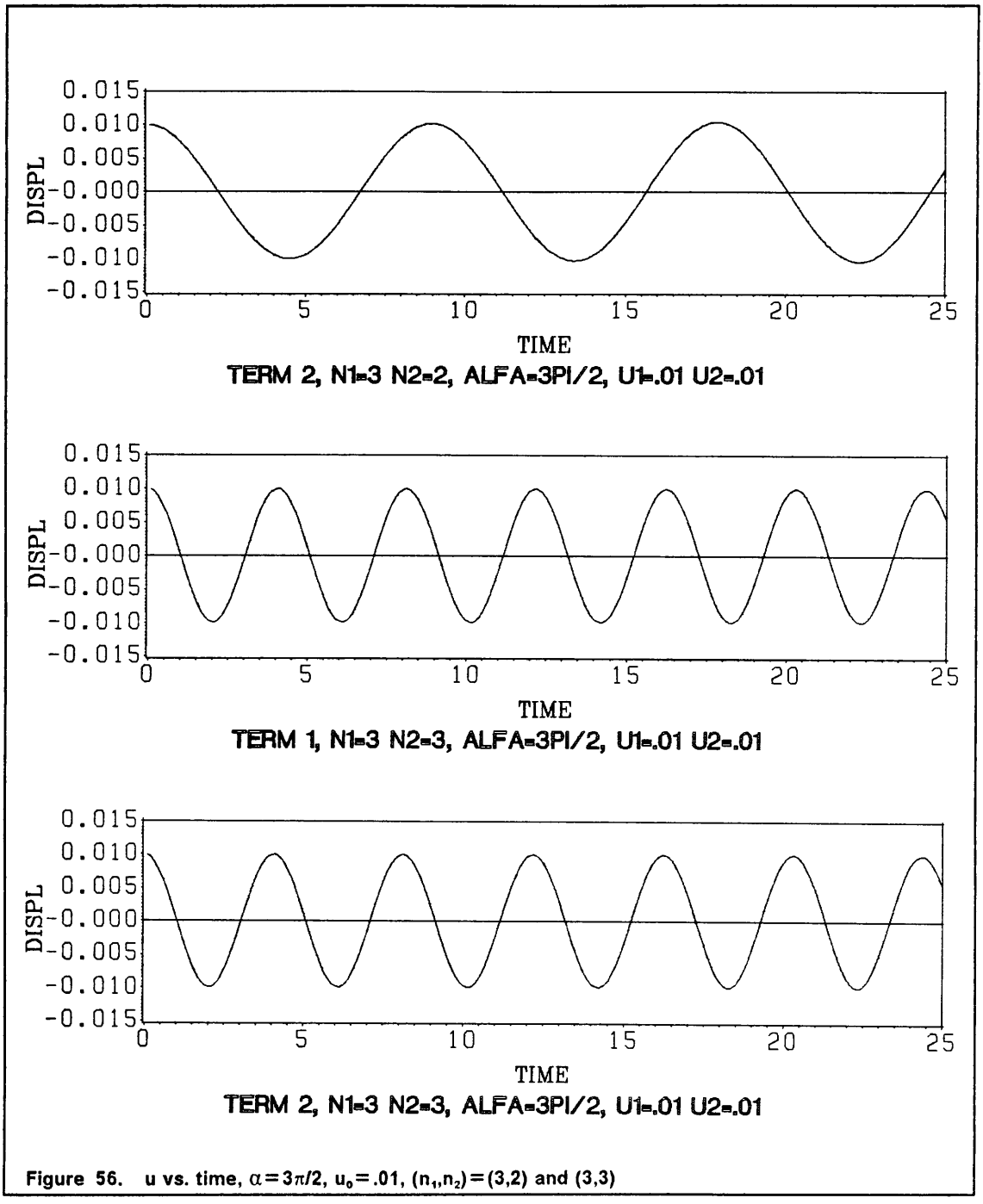

Figure 56. u vs. time, $\alpha = 3\pi/2$, $u_0 = .01$, $(n_1,n_2) = (3,2)$ and $(3,3)$

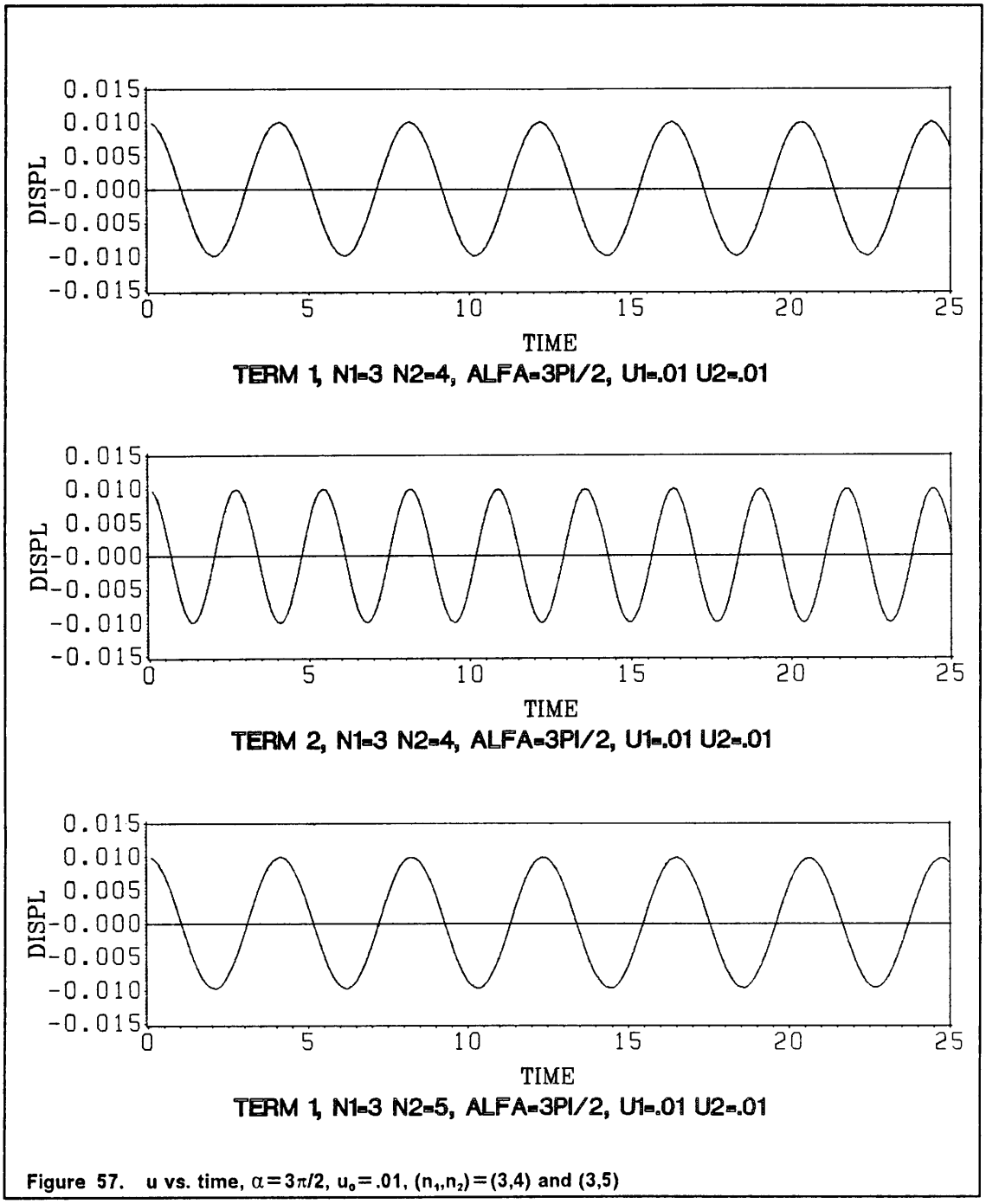

Figure 57. u vs. time, $\alpha = 3\pi/2$, $u_0 = .01$, $(n_1, n_2) = (3,4)$ and $(3,5)$

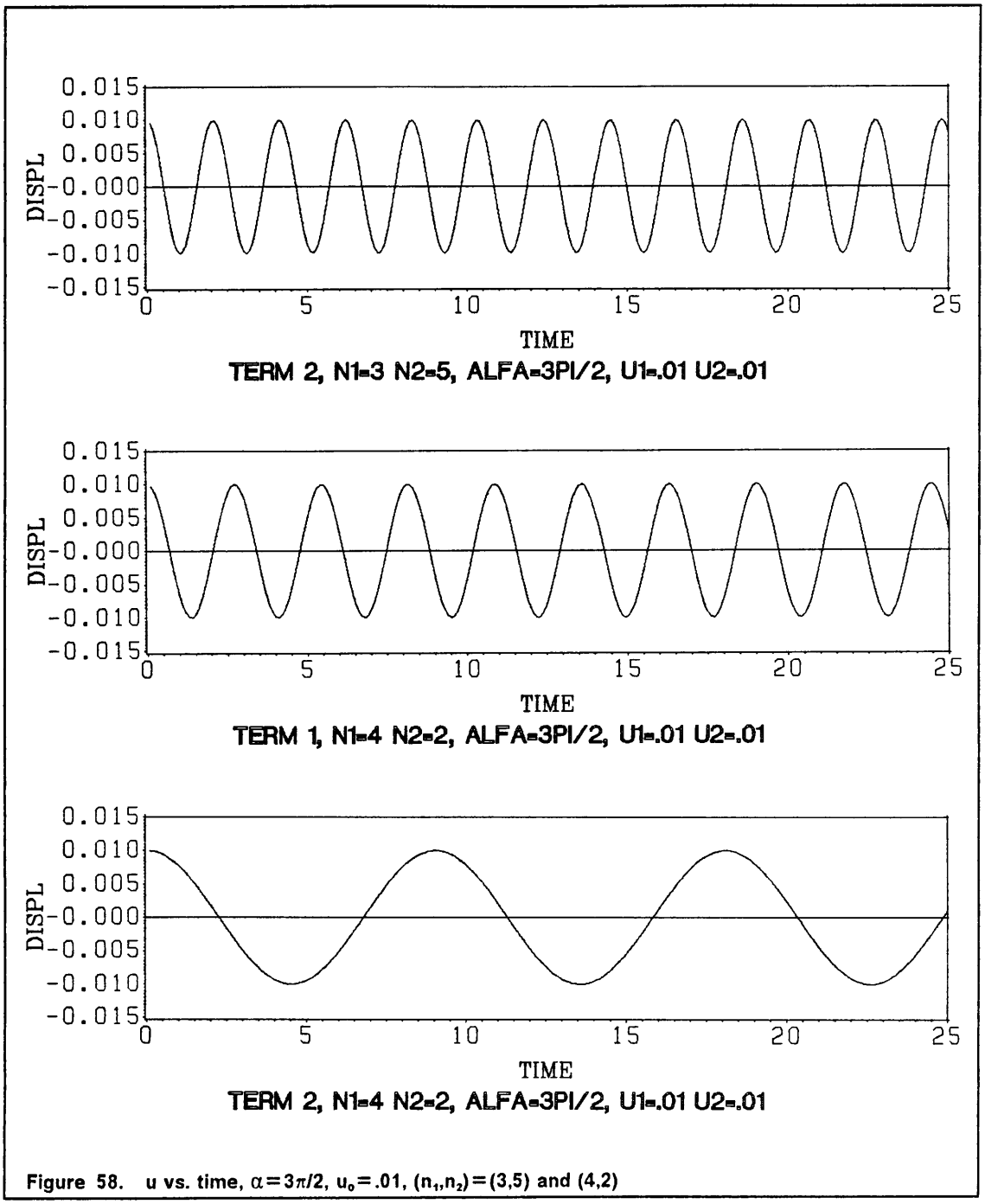

Figure 58. u vs. time, $\alpha = 3\pi/2$, $u_o = .01$, $(n_1,n_2) = (3,5)$ and $(4,2)$

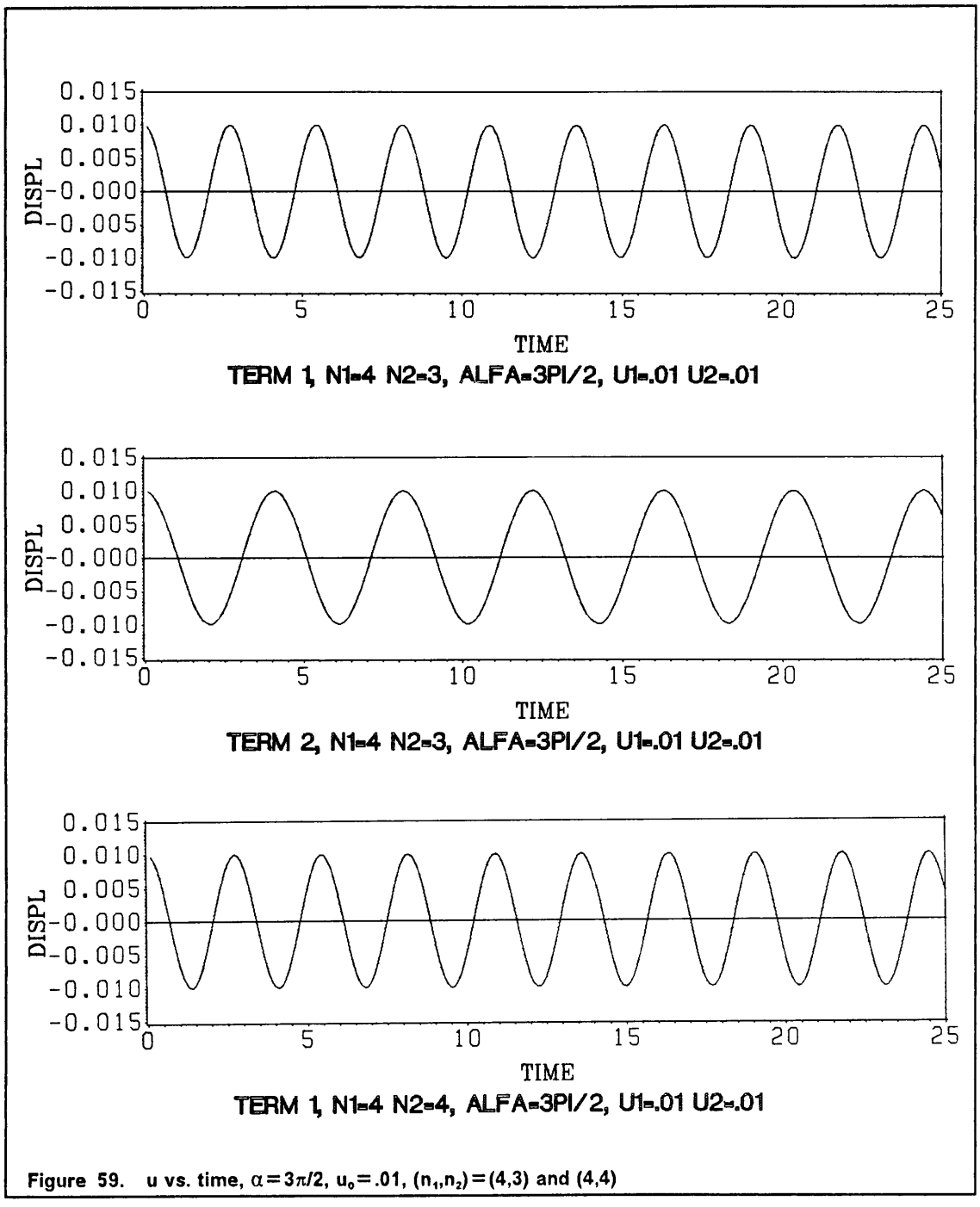

Figure 59. u vs. time, $\alpha = 3\pi/2$, $u_o = .01$, $(n_1, n_2) = (4,3)$ and $(4,4)$

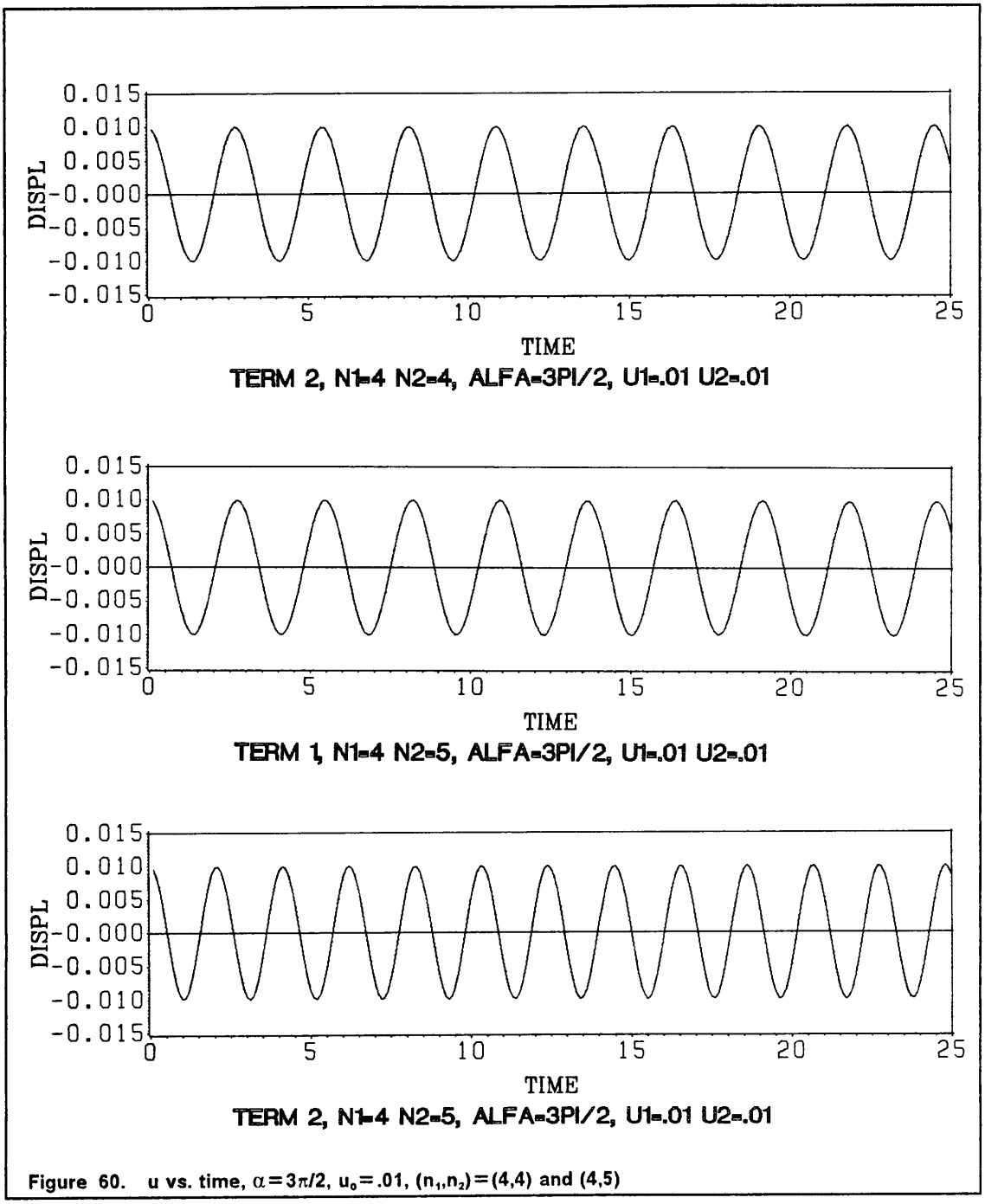

Figure 60. u vs. time, $\alpha = 3\pi/2$, $u_0 = .01$, $(n_1,n_2) = (4,4)$ and $(4,5)$

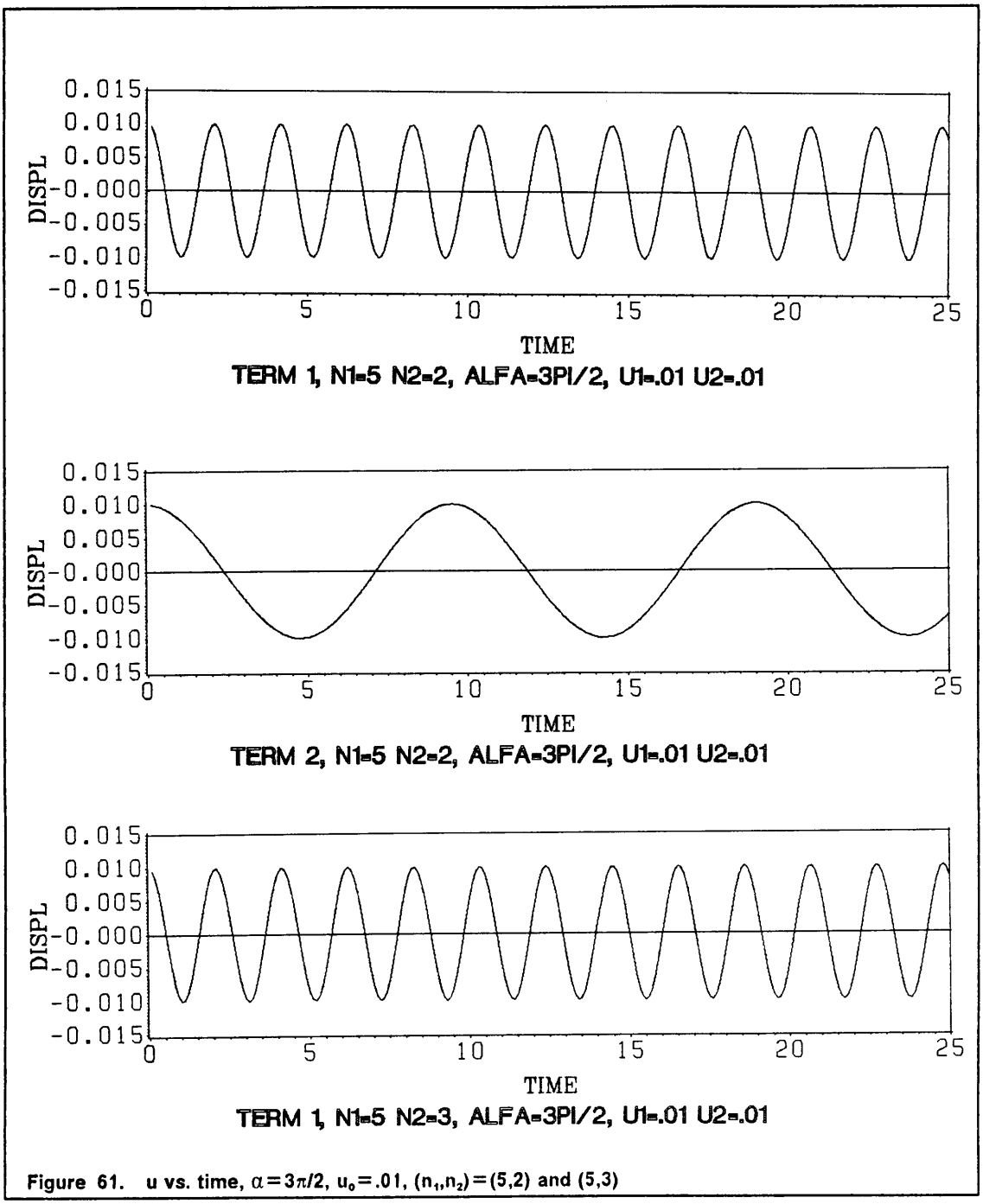

Figure 61. u vs. time, $\alpha = 3\pi/2$, $u_0 = .01$, $(n_1, n_2) = (5,2)$ and $(5,3)$

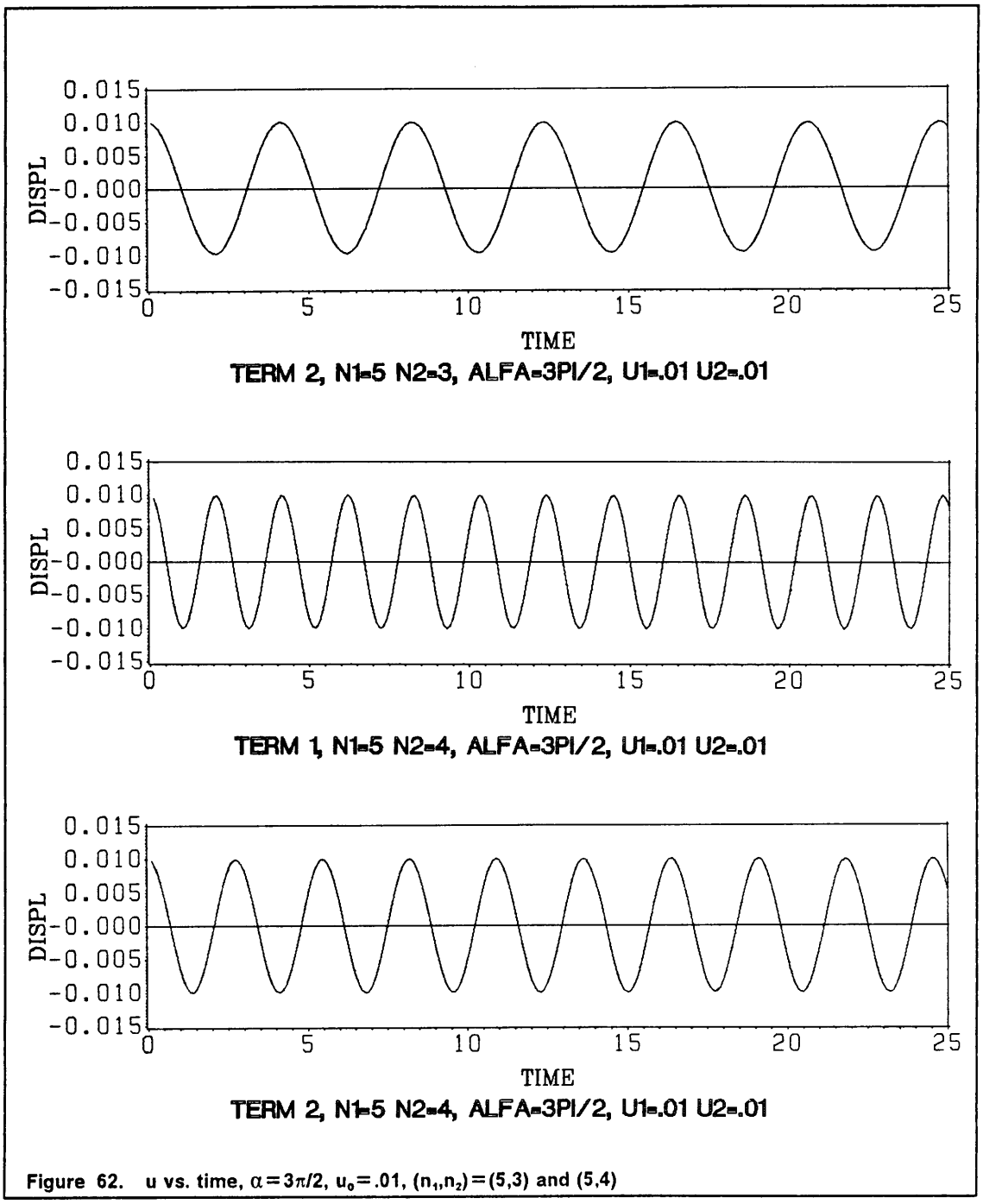

Figure 62. u vs. time, $\alpha = 3\pi/2$, $u_0 = .01$, $(n_1,n_2) = (5,3)$ and $(5,4)$

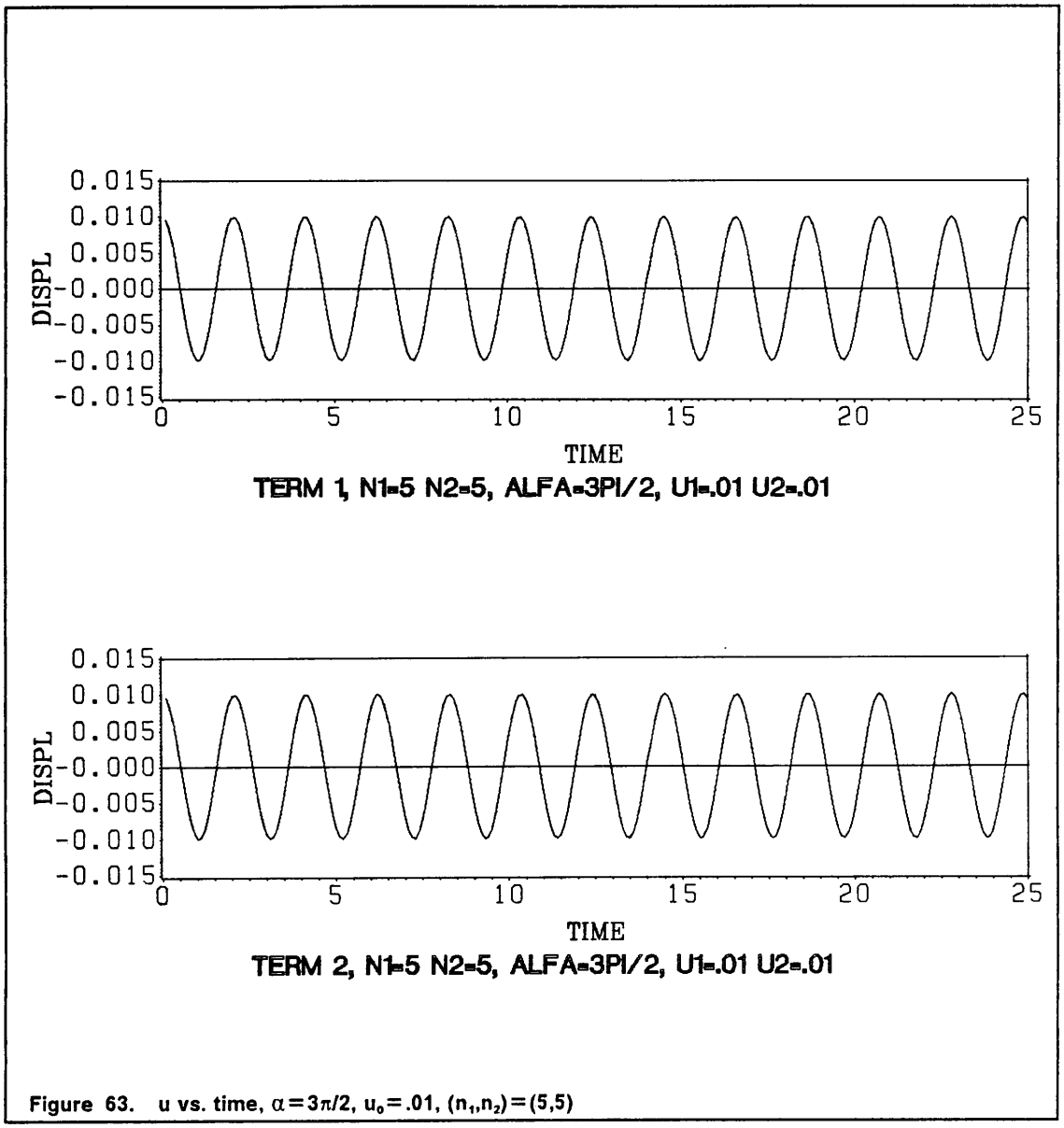

Figure 63. u vs. time, $\alpha = 3\pi/2$, $u_o = .01$, $(n_1,n_2) = (5,5)$

Table 3. Table of frequencies for the two-term Galerkin solution, for $u_o = u_1 = u_2 = 0.00, 0.005$

u_o	n_1	α	$n_2 = 2$	$n_2 = 3$	$n_2 = 4$	$n_2 = 5$
0.000	2	π/2	3.7552	3.7552	3.7552	3.7552
		π	1.5497	1.5497	1.5497	1.5497
		3π/2	0.7060	0.7060	0.7060	0.7060
	3	π/2	5.8358	5.8358	5.8358	5.8358
		π	2.6823	2.6823	2.6823	2.6823
		3π/2	1.5497	1.5497	1.5497	1.5497
	4	π/2	7.8701	7.8701	7.8701	7.8701
		π	3.7552	3.7552	3.7552	3.7552
		3π/2	2.3145	2.3145	2.3145	2.3145
	5	π/2	9.8938	9.8938	9.8938	9.8938
		π	4.8082	4.8082	4.8082	4.8082
		3π/2	3.0456	3.0456	3.0456	3.0456
0.005	2	π/2	3.7422	3.7313	3.5565	---
		π	1.5479	1.5479	1.5359	1.5032
		3π/2	0.7060	0.7060	0.7030	0.6943
	3	π/2	5.8238	5.8118	5.7656	5.8178
		π	2.6823	2.6823	2.6765	2.6680
		3π/2	1.5497	1.5497	1.5479	1.5427
	4	π/2	7.8540	7.8540	7.8060	7.6937
		π	3.7552	3.7552	3.7472	3.7432
		3π/2	2.3145	2.3145	2.3145	2.3120
	5	π/2	9.8535	9.8535	9.8534	9.6565
		π	4.8033	4.7983	4.7983	4.7934
		3π/2	3.0456	3.0456	3.0456	3.0424

Table 4. Table of frequencies for the two-term Galerkin solution, for $u_o = u_1 = u_2 = 0.010$

u_o	n_1	α	$n_2 = 2$	$n_2 = 3$	$n_2 = 4$	$n_2 = 5$
0.100	2	π/2	3.7273	---	---	---
		π	1.5497	1.5410	1.4960	1.2852
		3π/2	0.7060	0.7060	0.6943	0.6605
	3	π/2	---	---	---	---
		π	2.6794	2.6765	2.6624	2.6066
		3π/2	1.5479	1.5479	1.5445	1.5240
	4	π/2	---	---	---	---
		π	3.7472	3.7472	3.7273	3.7077
		3π/2	2.3145	2.3120	2.3095	2.3045
	5	π/2	---	---	---	---
		π	4.7884	4.7835	4.7771	4.7470
		3π/2	3.0424	3.0392	3.0392	3.0238

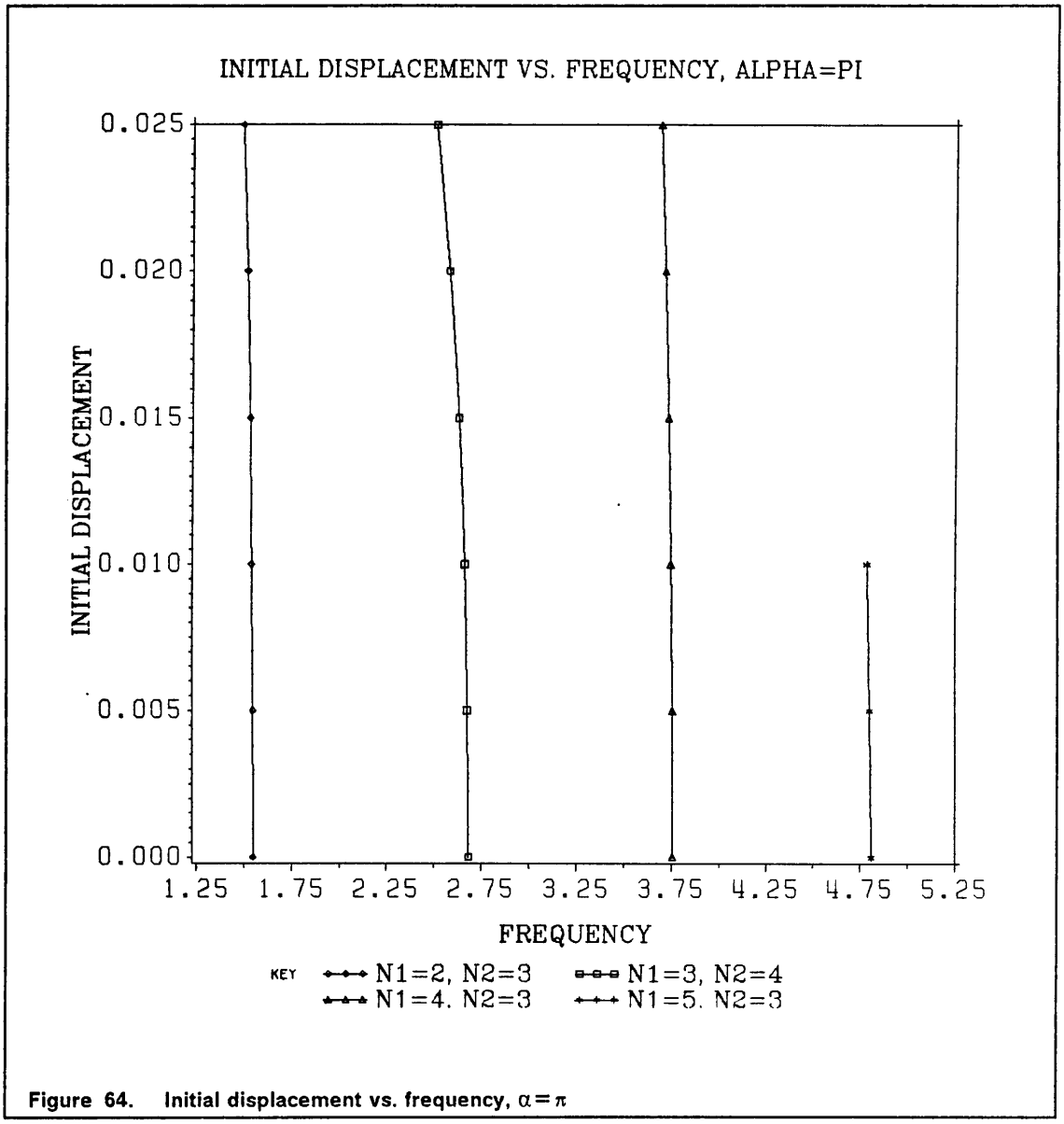

Figure 64. Initial displacement vs. frequency, $\alpha = \pi$

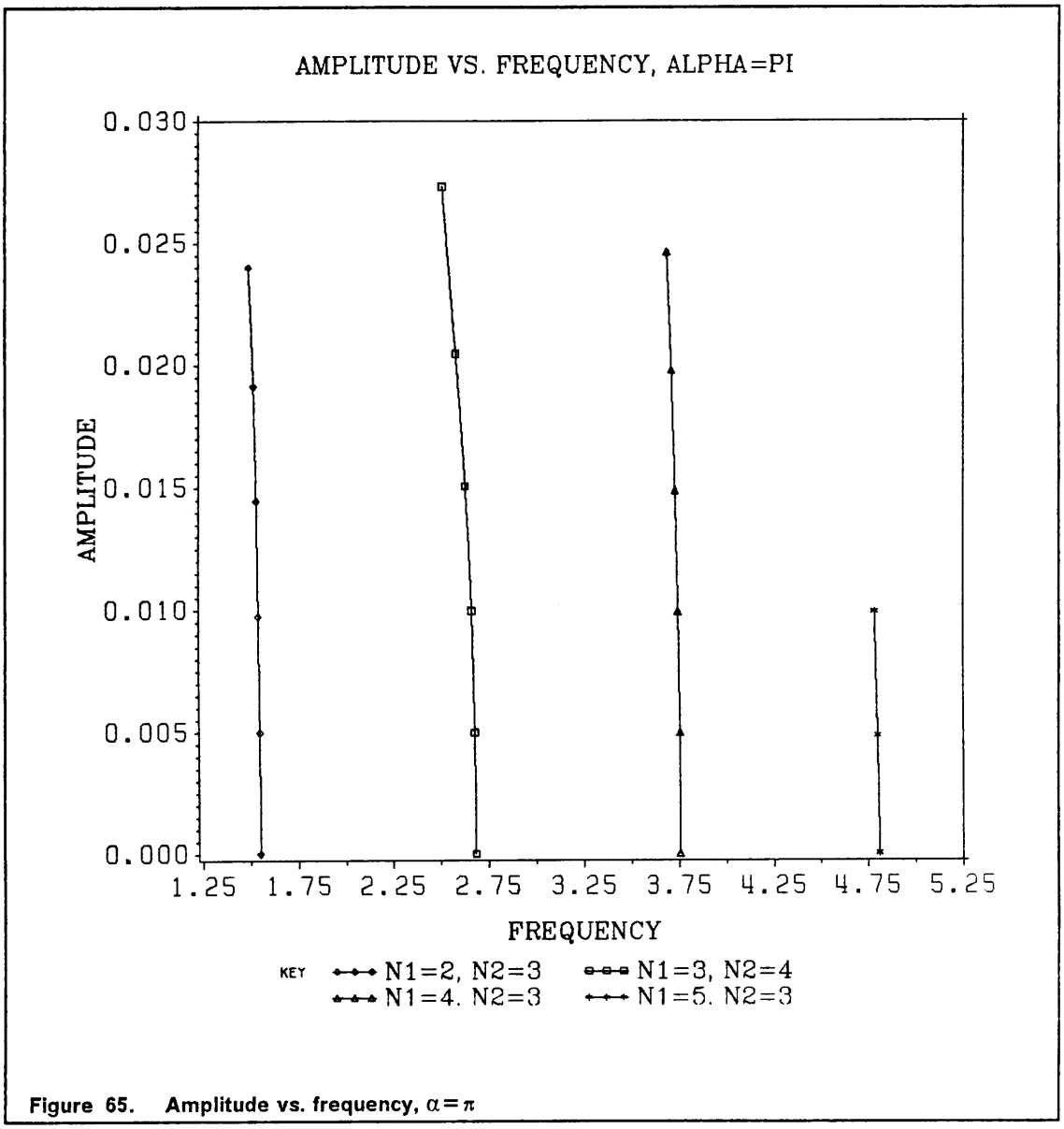

Figure 65. Amplitude vs. frequency, $\alpha = \pi$

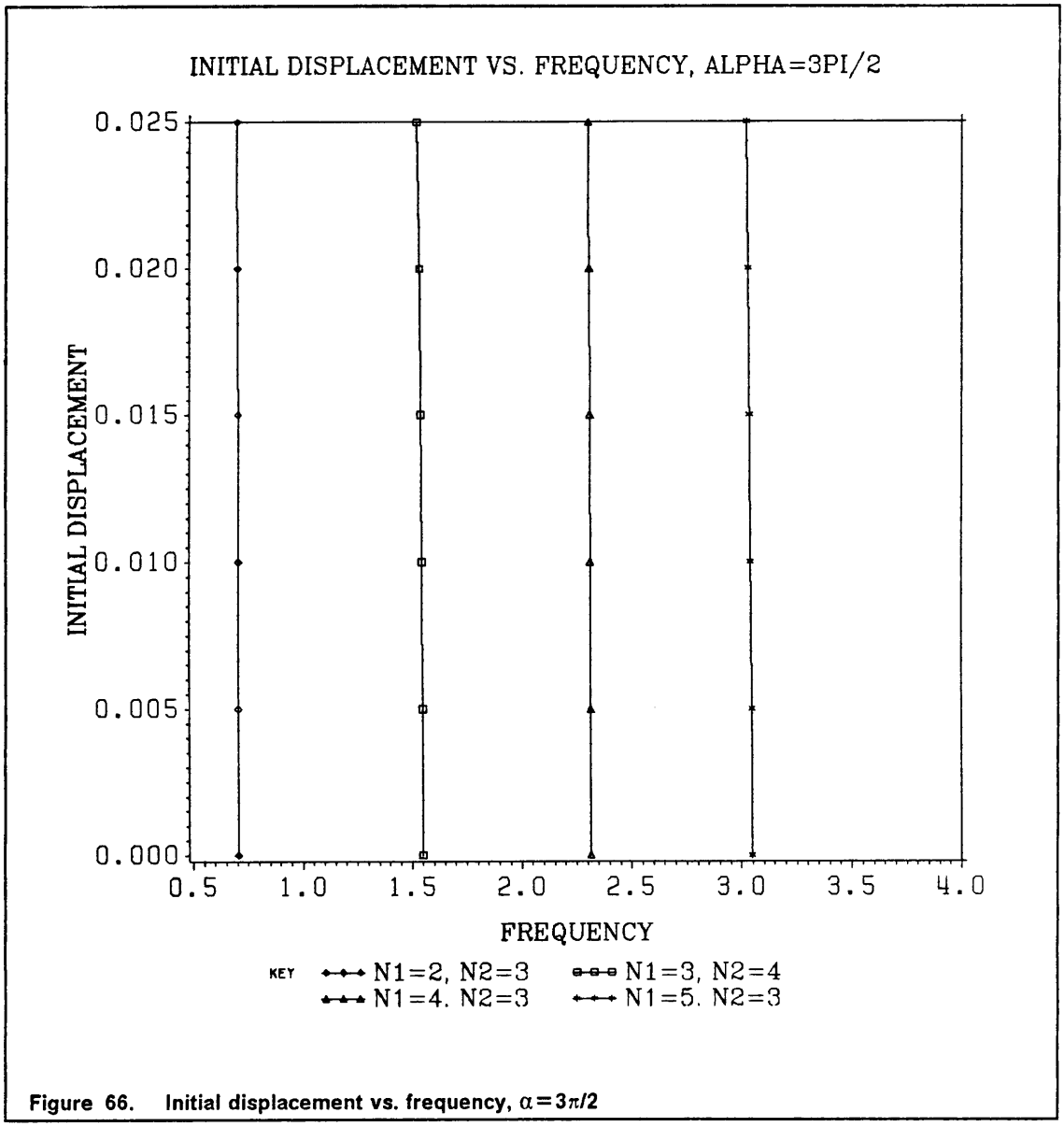

Figure 66. Initial displacement vs. frequency, $\alpha = 3\pi/2$

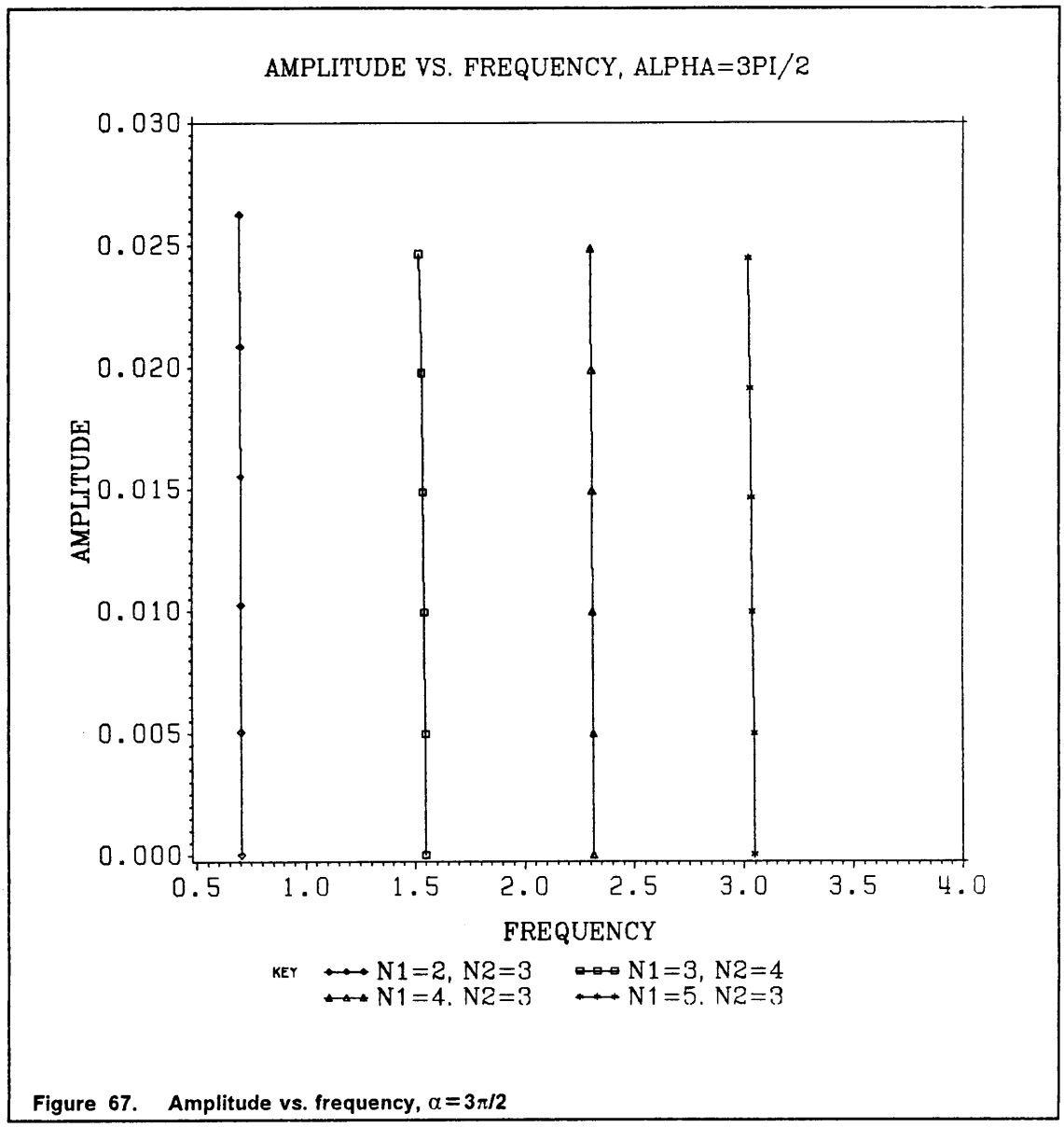

Figure 67. Amplitude vs. frequency, $\alpha = 3\pi/2$

vious in the plots as they only go up to an initial displacement of 0.025. This is because in the cases where $n=3$, 4, or 5, the computer program fails to yield appropriate results beyond an initial displacement of 0.025.

Comparison of Results

The frequencies calculated using the one- and two-term approximations compare favorably with those calculated by Hsieh [8] and Firt [5]. Hsieh presents his results in the form of eigenvalues, as shown in equation 2.35, while Firt presents both eigenvalues and frequencies, as shown in equations 2.29 and 2.34. The frequencies calculated in this thesis tend to be slightly higher than those of Hsieh and Firt, yet are sufficiently accurate for dynamic analysis. Table 5 shows a comparison of the frequencies.

The frequencies calculated with the one-term approximation agree closely with those calculated with the two-term approximation.

Table 5. Comparison of natural frequencies

α	mode	Galerkin	Hsieh [8]	Firt [5]
$\pi/2$	1	3.7552	3.5522	
	2	5.8358	5.4947	
	3	7.8701	7.7717	
	4	9.8938	9.7018	
π	1	1.5497	1.3054	1.3076
	2	2.6823	2.4418	2.4434
	3	3.7552	3.6128	3.6152
	4	4.8082	4.8114	4.6744
$3\pi/2$	1	0.7060	0.5359	
	2	1.5497	1.3430	
	3	2.3145	2.1648	
	4	3.0456	2.9159	

Conclusions and Recommendations

Conclusions

As a result of a review of the literature and the analysis performed in this thesis, several conclusions are drawn. These conclusions are presented in the paragraphs below.

The solution of the equation of motion for an air-inflated dam using a one- and two-term Galerkin approximation yields frequencies as reported in Table 1 on page 59, Table 3 on page 101 and Table 4 on page 102. Comparison with the calculated frequencies of Hsieh [8] and Firt [5] shows that the results shown in the tables agree with a sufficient degree of accuracy. Comparison of the results of the one-term Galerkin approximation to the results of the two-term Galerkin approximation shows that the frequencies of the individual terms agree well. It can be concluded that the one- and two-term Galerkin approximations using the sine functions as shown in equations 3.23 and 3.29 provide a sufficient degree of accuracy to perform a dynamic analysis of an inflatable dam.

The one-term approximation indicates that for the cases where $n=3$ and 5, the inflatable dam will not oscillate about the equilibrium state, but about some positive displacement.

The effects of the the nonlinear terms can be seen in the plots of initial displacement and amplitude versus frequency shown in the previous chapter. The general trend of the frequency to decrease as the initial displacement or amplitude is increased is a result of the nonlinear terms in the equation of motion. It can be concluded that the nonlinear terms have an effect on the frequency of the dam, but that the effect is not major.

In the course of the analysis it was found that for certain cases the computer program was unable to provide an appropriate solution. It was found during the analysis that results were unobtainable for $\alpha = \pi/2$ where $n=5$ and $u>.005$, and $n=3$ and $u>.02$, for both the one- and the two-term approximations. It can be concluded that in order to obtain results for these cases, an alternative solution routine must be used, or DVERK must be tuned in some way to provide an appropriate solution.

Recommendations for Further Study

Research in any field typically creates as many questions as it does answers. This thesis leaves open several areas where further study is warranted. Several of these areas are discussed below.

In the course of this study, problems were encountered when trying to obtain results for certain cases, where $n=3$ or 5 and the initial displacement was greater than 0.02. Further work is needed with an alternative solution algorithm to obtain results for these cases.

This thesis considers values of n from 2 to 5. Additional studies could be made considering higher modes. Also, equations for a three- or four-term approximation could be derived, and frequencies and amplitudes compared to those of the one- and two-term results.

In the future there is a need for the water-inflated dam to be considered. A method for modeling the hydrodynamic effects of the internal water, as well as the external loads of the impounded water, would need to be developed. The effects of both upstream and downstream water pressure as well as crest overflow could be considered in the study.

In Binnie's [3] second paper, he discusses the three-dimensional vibrations that the inflatable weir undergoes prior to the failure. This demonstrates a need for further research considering three-dimensional effects. Binnie and colleagues advise that extra strength be incorporated into design to account for unforeseen modes of vibration, thus demonstrating the need for further research to better understand the dynamic nature of the inflatable dam.

Bibliography

1. Anwar, H. O., "Inflatable Dams," Journal of the Hydraulics Division, ASCE, Vol. 93, May 1967, pp. 99-119.

2. Binnie, G. M., "The Theory of Flexible Dams Inflated by Water Pressure," Journal of Hydraulic Research, Vol. 11, 1973, pp. 61-68.

3. Binnie, G. M., Thomas, A. R., and Gwyther, J. R., "Inflatable Weir Used During Construction of The Mangla Dam," Proceedings of The Institution of Civil Engineers, Part 1: Design and Construction, Vol. 54, 1973, pp. 625-639.

4. Fagan, T. D., "Effects of Membrane Weight on Vibration of Air-Inflated Dams," M. S. Thesis, Virginia Polytechnic Institute and State University, Blacksburg, Virginia, 1987.

5. Firt, V., *Statics, Formfinding, and Dynamics of Air-Supported Membrane Structures,* Martinus Nijhof Publishers, The Hague, 1983.

6. Harrison, H. B., "The Analysis and Behavior of Inflatable Membrane Dams Under Static Loading," Proceedings of The Institution of Civil Engineers, Vol. 45, 1970, pp. 661-676.

7. Henrych, J., *The Dynamics of Arches and Frames,* Elsevier Scientific Publishing Company, Amsterdam, 1981, pp.21-27.

8. Hsieh, J. C., Ph.D. dissertation in progress, Virginia Polytechnic Institute and State University, Blacksburg, Virginia, 1987.

9. International Mathematical and Statistical Libraries, Inc., *DVERK Differential Equation Solver Routine,* Houston, Texas, 1982.

10. Irvine, H. M., *Cable Structures,* The MIT Press, Cambridge, Massachusetts, 1981, pp. 31-38.

11. Marshall, E. R., "Some Technical and Economic Evaluations of an Inflatable Dam as an Emergency Flood Control System," M. S. Thesis, Virginia Polytechnic Institute and State University, Blacksburg, Virginia, 1984.

12. Parbery, R., D., "A Continuous Method of Analysis of the Inflatable Dam," Proceedings of The Institution of Civil Engineers, Part 2, Vol. 65, Vol. 61, 1976, pp. 725-736.

13. Parbery, R. D., "Factors Affecting the Membrane Dam Inflated by Air Pressure," Proceedings of The Institution of Civil Engineers, Part 2, Vol. 65, 1978, pp. 645-654.

14. "Presenting The Imbertson Fabridam," Firestone Coated Fabrics Company, Akron, Ohio, 1968.

15. "Report of an Investigation into the Failure of an Inflatable Dam," University of Sydney, Civil Engineering Laboratories, Investigation Report No. S89, May, 1969.

16. Watson, R., "A Note on the Shapes of Flexible Dams," Journal of Hydraulic Research, Vol. 23, 1985, pp. 179-194.

Appendix A. Program SOLVE1

The FORTRAN program for the solution of the differential equation 3.25 resulting from the one-term Galerkin approximation is shown on the following pages. The variables describing the differential equation are Q1 through Q5, which are the constants c_1 through c_5 shown in equation 3.26, and YPRIME(1) and YPRIME(2), which are the expressions shown in equation 3.27.

```
C        PROGRAM :  SOLVE1 FORTRAN A
C     ********************************************
C     NON-LINEAR OSCILLATIONS OF THE INFLATABLE DAMS
C          SOLUTION OF ONE-PARAMETER GALERKIN
C       APPROXIMATION USING IMSL SUBROUTINE DVERK
C     ********************************************
C
C     BY: JIM LEEUWRIK        DATE: JANUARY 15, 1987
C
C     PURPOSE:
C     THIS PROGRAM SOLVES THE EQUATION OF MOTION FOR THE ONE-TERM
C     GALERKIN APPROXIMATION METHOD.  THE IMSL SUBROUTINE DVERK IS
C     USED FOR THE SOLUTION OF THE DIFFERENTIAL EQUATION, WHICH IS
C     ENTERED INTO THE PROGRAM IN SUBROUTINE EQNS.  THE PROGRAM
C     CALCULATES THE SOLUTION FOR GIVEN ALPHA AND INITIAL DISPLACEMENT
C     AND N=2, 3, 4, AND 5.
C
C     ------------------ INITIALIZE ------------------------
C
      IMPLICIT REAL*8(A-H,O-Z)
      EXTERNAL EQNS, SYSCAL
      INTEGER ICOUNT
      CHARACTER DEFOUT*50, OUTPUT*6
      COMMON ALFA,PI,V,Q1,Q2,Q3,Q4,Q5,MODE
      DIMENSION Y(2),C(24),W(2,9)
C
C     ------------------ BEGIN MAIN LOOP ---------------------
C
      DO 5000 ICOUNT = 1,4
C
      NW=2
      N=2
      XEND=0.D0
      Y(1)=0.09D0
      Y(2)=0.D0
      TOL = 1.0D-4
      IND=1
C
C     ------------------ CHANGE PARAMETERS ---------------------
C
      READ(5,*) MODE,OUTPUT
      DEFOUT = 'FILEDEF 12 DISK ' // OUTPUT // ' OUT A (RECFM V)'
      CALL SYSCAL(DEFOUT,50,IRTCDE)
      REWIND (UNIT=12)
      PI = 3.141592653589793D0
      ALFA = PI*(1.0D0)
C
C     ----------------- BEGIN EXECUTION LOOP --------------------
C
      DO 10 K = 1,500
           X = XEND
           XEND = FLOAT(K)*.1D0
           CALL DVERK(N,EQNS,X,Y,XEND,TOL,IND,C,NW,W,IER)
           IF(IND.LT.0.OR.IER.GT.0)GOTO 20
           WRITE(12,110) X,Y(1)
 110       FORMAT(1X,F4.1,2X,F12.10)
```

```
  10 CONTINUE
     CLOSE(UNIT=12)
     CALL SYSCAL('CLEAR',5,IRTCDE)
C
 5000 CONTINUE
     STOP
C
C    ---------- ERROR HANDLING ----------
C
  20 CONTINUE
     WRITE(6,*) IND,IER,TOL,XEND
     STOP
     END
C
C    ---------- SUBROUTINE EQNS LISTING ----------
C
     SUBROUTINE EQNS(N,X,Y,YPRIME)
     IMPLICIT REAL*8(A-H,O-Z)
     COMMON ALFA,PI,V,Q1,Q2,Q3,Q4,Q5,MODE
     DIMENSION YPRIME(N),Y(N)
     V = FLOAT(MODE)*PI/ALFA
     Q1 = ALFA*(1.D0+V**2.D0)/2.D0
     Q2 = 4.D0*(1.D0-(-1.D0)**MODE)*((V**2+1.D0)*(V**2-1.D0)
    +/3.D0*V)
     Q3 = (9.D0*ALFA)/4.D0*(V**2-1.D0)**2
     Q4 = (ALFA*V**2)/2.D0*(V**2-1.D0)
     Q5 = (4.D0*V)/3.D0*(1.D0-(-1)**MODE)*(V**2-1.D0)**2
     YPRIME(1) = Y(2)
     YPRIME(2) = (-Q4*Y(1)-Q5*(Y(1)**2))/(Q1+Q2*Y(1)+Q3*(Y(1))
    +**2)
     RETURN
     END
```

Appendix B. Program SOLVE2

The FORTRAN program for the solution of the differential equation resulting from the two-term Galerkin approximation is shown on the following pages. The variables describing the equation are: Q1 through Q34, which are the constants c_1 through c_{34}, shown in equation 3.31, XINT1 through XINT20, which are the integrals shown in equation 3.32, ATERM, BTERM, CTERM, DTERM, ETERM, AND FTERM, which are the expressions for a, b c, d, e, and f, shown in equation 3.34, and YPRIME(1), YPRIME(2), YPRIME(3), and YPRIME(4), which are the expressions in equation 3.35.

```
C            PROGRAM :  SOLVE2 FORTRAN A
C     ************************************************
C       NON-LINEAR OSCILLATIONS OF INFLATABLE DAMS
C     SOLUTION OF TWO PARAMETER GALERKIN APPROXIMATION
C           USING IMSL SUBROUTINE DVERK.
C     ************************************************
C
C       BY:  JIM LEEUWRIK      DATE:  JAN. 15, 1987
C
C     PURPOSE:
C     THIS PROGRAM SOLVES THE EQUATION OF MOTION FOR THE TWO-TERM
C     GALERKIN APPROXIMATION METHOD.  THE IMSL SUBROUTINE DVERK
C     IS USED FOR THE SOLUTION OF THE DIFFERENTIAL EQUATION, WHICH
C     IS ENTERED INTO THE PROGRAM IN SUBROUTINE EQNS.  THE PROGRAM
C     CALCULATES THE SOLUTION FOR GIVEN ALPHA, INITIAL DISPLACEMENTS,
C     AND COMBINATIONS OF N1 AND N2 = 2, 3, 4, 5.
C
C
C     ************INITIALIZE*************
C
      IMPLICIT REAL*8(A-H,O-Z)
      EXTERNAL EQNS
      EXTERNAL SYSCAL
      INTEGER N,IND,NW,IER,K,MODE1,MODE2,IO,IRTCDE,INCR
      CHARACTER*8 OUTPUT, DEFOUT*50
      COMMON ALFA,PI,MODE1,MODE2
      COMMON Q1,Q2,Q3,Q4,Q5,Q6,Q7,Q8,Q9,Q10,Q11,Q12,Q13,Q14
      COMMON Q15,Q16,Q17,Q18,Q19,Q20,Q21,Q22,Q23,Q24,Q25,Q26
      COMMON Q27,Q28,Q29,Q30,Q31,Q32,Q33,Q34
      COMMON XINT1,XINT2,XINT3,XINT4,XINT5,XINT6,XINT7
      COMMON XINT8,XINT9,XINT10,XINT11,XINT12,XINT13,XINT14
      COMMON XINT15,XINT16,XINT17,XINT18,XINT19,XINT20
      DIMENSION Y(4),C(24),W(4,9)
C
C     ************** BEGIN SYSTEM LOOP ***************
C
      DO 1000 INCR = 1,32
C
C
      NW = 4
      N =  4
      XEND = 0.D0
      Y(1) = 0.010D0
      Y(2) = 0.D0
      Y(3) = 0.010D0
      Y(4) = 0.D0
      TOL = 1.0D-4
      IND = 1
C
C     ************CHANGE PARAMETERS*****************
C
      READ(5,*) MODE1,MODE2,IO,OUTPUT
      DEFOUT = 'FILEDEF 12 DISK ' // OUTPUT // ' OUT T (RECFM V)'
      CALL SYSCAL(DEFOUT,50,IRTCDE)
      REWIND(UNIT=12)
      PI = 3.141592653589793D0
```

```
      ALFA = PI*(1.0D0)
      V1 = FLOAT(MODE1)*PI/ALFA
      V2 = FLOAT(MODE2)*PI/ALFA
C
C     ---------- CONSTANTS ----------
C
      Q1 = (V1**4)-(V1**2)
      Q2 = 1.D0+(V1**2)
      Q3 = (V2**4)-(V2**2)
      Q4 = 1.D0+(V2**2)
      Q5 = (V1**2)-2.D0*(V1**4)+(V1**6)
      Q6 = -4.D0+3.D0*(V1**2)+(V1**4)
      Q7 = -2.D0*(V1**2)*(V2**2)+(V2**2)+(V1**2)-(V1**4)
     +-(V2**4)+(V1**2)*(V2**4)+(V1**4)*(V2**2)
      Q8 = 5.D0*(V1**2)-4.D0-(V1**4)+2.D0*(V1**2)*(V2**2)-2.D0*(V2**2)
      Q9 = 5.D0*(V2**2)-4.D0-(V2**4)+2.D0*(V1**2)*(V2**2)-2.D0*(V1**2)
      Q10 = -2.D0*(V2**4)+(V2**2)+(V2**6)
      Q11 = -4.D0+3.D0*(V2**2)+(V2**4)
      Q12 = 2.D0*(V1**6)-4.D0*(V1**4)+2.D0*(V1**2)
      Q13 = 2.D0*(V1**4)-2.D0*(V1**2)
      Q14 = 4.D0*(V1**3)*(V2**3)-4.D0*V1*(V2**3)-4.D0*(V1**3)*V2
     + +4.D0*V1*V2
      Q15 = 2.D0*(V1**3)*V2-2.D0*V1*V2
      Q16 = 2.D0*V1*(V2**3)-2.D0*V1*V2
      Q17 = 2.D0*(V2**6)-4.D0*(V2**4)+2.D0*(V2**2)
      Q18 = 2.D0*(V2**4)-2.D0*(V2**2)
      Q19 = 6.D0-12.D0*(V1**2)+6.D0*(V1**4)
      Q20 = 6.D0-13.D0*(V1**2)-(V1**6)+(V1**4)*(V2**2)+(V2**2)
     +-2.D0*(V1**2)*(V2**2)+8.D0*(V1**4)
      Q21 = 12.D0-13.D0*(V2**2)+(V2**4)-(V1**2)*(V2**4)
     + +12.D0*(V1**2)*(V2**2)-(V1**4)+(V1**4)*(V2**2)-11.D0*(V1**2)
      Q22 = 6.D0-13.D0*(V2**2)-(V2**6)+(V1**2)
     +-2.D0*(V1**2)*(V2**2)+8.D0*(V2**4)+(V1**2)*(V2**4)
      Q23 = 12.D0-13.D0*(V1**2)+(V1**4)-(V1**4)*(V2**2)
     + +12.D0*(V1**2)*(V2**2)-(V2**4)+(V1**2)*(V2**4)-11.D0*(V2**2)
      Q24 = 6.D0-12.D0*(V2**2)+6.D0*(V2**4)
      Q25 = 0.D0
      Q26 = -2.D0*(V1**6)+4.D0*(V1**4)-2.D0*(V1**2)
      Q27 = 2.D0*(V1**4)*(V2**2)-2.D0*(V1**2)*(V2**2)+2.D0*(V1**4)
     + +2.D0*(V1**2)
      Q28 = 2.D0*(V1**5)*V2+2.D0*V1*V2
      Q29 = -2.D0*(V1**3)*(V2**3)+6.D0*V1*(V2**3)+2.D0*(V1**3)*V2
     +-2.D0*V1*V2
      Q30 = 2.D0*V1*(V2**5)+2.D0*V1*V2
      Q31 = -2.D0*(V1**3)*(V2**3)+6.D0*(V1**3)*V2+2.D0*V1*(V2**3)
     +-2.D0*V1*V2
      Q32 = -2.D0*(V2**6)+4.D0*(V2**4)-2.D0*(V2**2)
      Q33 = 2.D0*(V1**2)*(V2**4)-2.D0*(V1**2)*(V2**2)+2.D0*(V2**4)
     + +2.D0*(V2**2)
      Q34 = 0.D0
C
C     ---------- INTEGRALS ----------
C
      XINT1 = ALFA/2.D0
      XINT2 = 2.D0/(3.D0*V1)*(1-(-1)**MODE1)
      XINT3 = 2.D0/(3.D0*V2)*(1-(-1)**MODE2)
```

```
      XINT4 = 3.D0*ALFA/8.D0
      XINT5 = ALFA/8.D0
      IF(V2.EQ.(2.D0*V1))THEN
      XINT6 = 0.D0
      ELSE
      XINT6 = -2.D0*(V1**2)*(1-(-1)**MODE2)/(V2*((V2**2)-4.D0*(V1**2)))
      ENDIF
      IF(V1.EQ.(2.D0*V2))THEN
      XINT7 = 0.D0
      ELSE
      XINT7 = -2.D0*(V2**2)*(1-(-1)**MODE1)/(V1*((V1**2)-4.D0*(V2**2)))
      ENDIF
      XINT8 = 1.D0/(3.D0*V1)*(1.D0-(-1.D0)**MODE1)
      XINT9 = 0.D0
      XINT10 = 0.D0
      XINT11 = 0.D0
      XINT12 = ALFA/4.D0
      XINT13 = ALFA/4.D0
      IF((3.D0*V1).EQ.V2) THEN
      XINT14 = ALFA/8.D0
      ELSE
      XINT14 = 0.D0
      ENDIF
      IF((3.D0*V2).EQ.V1) THEN
      XINT15 = ALFA/8.D0
      ELSE
      XINT15 = 0.D0
      ENDIF
      IF(V2.EQ.(2.D0*V1))THEN
      XINT16 = 0.D0
      ELSE
      XINT16 = ((V2**2)-2.D0*(V1**2))*(1.D0-(-1.D0)**MODE2)/
     +(V2*((V2**2)-4.D0*(V1**2)))
      ENDIF
      IF(V2.EQ.(2.D0*V1))THEN
      XINT17 = 0.D0
      ELSE
      XINT17 = V1*(1.D0-(-1.D0)**MODE2)/(4.D0*(V1**2)-(V2**2))
      ENDIF
      IF(V1.EQ.(2.D0*V2))THEN
      XINT18 = 0.D0
      ELSE
      XINT18 = V2*(1.D0-(-1.D0)**MODE1)/(4.D0*(V2**2)-(V1**2))
      ENDIF
      IF(V1.EQ.(2.D0*V2))THEN
      XINT19 = 0.D0
      ELSE
      XINT19 = ((V1**2)-2.D0*(V2**2))*(1.D0-(-1.D0)**MODE1)/
     +(V1*((V1**2)-4.D0*(V2**2)))
      ENDIF
      XINT20 = 1.D0/(3.D0*V2)*(1.D0-(-1.D0)**MODE2)
C
C     ************BEGIN EXECUTION LOOP**************
C
      DO 10 K = 1,500
         X = XEND
```

```
      XEND = FLOAT(K)*.1D0
      CALL DVERK(N,EQNS,X,Y,XEND,TOL,IND,C,NW,W,IER)
      IF(IND.LT.0.OR.IER.GT.0.)GOTO 20
      WRITE(12,110) X,Y(IO)
110     FORMAT(1X,F4.1,2X,F12.10)
 10 CONTINUE
    CLOSE(UNIT=12)
    CALL SYSCAL('CLEAR',5,IRTCDE)
1000 CONTINUE
    STOP
C
C    ************ERROR HANDLING**************
C
 20 CONTINUE
    WRITE(6,*) IND,IER,TOL,XEND
    STOP
    END
C
C    ************SUBROUTINE LISTING*************
C
    SUBROUTINE EQNS(N,X,Y,YPRIME)
    IMPLICIT REAL*8(A-H,O-Z)
    INTEGER N,MODE1,MODE2
    COMMON ALFA,PI,MODE1,MODE2
    COMMON Q1,Q2,Q3,Q4,Q5,Q6,Q7,Q8,Q9,Q10,Q11,Q12,Q13,Q14
    COMMON Q15,Q16,Q17,Q18,Q19,Q20,Q21,Q22,Q23,Q24,Q25,Q26
    COMMON Q27,Q28,Q29,Q30,Q31,Q32,Q33,Q34
    COMMON XINT1,XINT2,XINT3,XINT4,XINT5,XINT6,XINT7
    COMMON XINT8,XINT9,XINT10,XINT11,XINT12,XINT13,XINT14
    COMMON XINT15,XINT16,XINT17,XINT18,XINT19,XINT20
    DIMENSION YPRIME(N),Y(N)
C
C    ---------- EQUATIONS AND TERMS ----------
C
    ATERM = Q2*XINT1+Q6*Y(1)*XINT2+Q9*Y(3)*XINT6+Q13*Y(1)*XINT8
   + +Q16*Y(3)*XINT17+Q19*Y(1)**2*XINT4+Q22*Y(3)**2*XINT12
   + +Q25*Y(1)**2*XINT5+Q27*Y(1)*Y(3)*XINT14-Q29*Y(1)*Y(3)*XINT14
   + +Q32*Y(3)**2*XINT13
C
    BTERM = Q8*Y(1)*XINT6+Q11*Y(3)*XINT7+Q15*Y(1)*XINT17
   + +Q18*Y(3)*XINT19+Q23*Y(1)*Y(3)*XINT12+Q26*Y(1)**2*XINT14
   +-Q28*Y(1)**2*XINT14+Q33*Y(1)*Y(3)*XINT13+Q34*Y(3)**2*XINT15
C
    CTERM = -Q1*Y(1)*XINT1-Q5*Y(1)**2*XINT2-Q7*Y(1)*Y(3)*XINT6
   +-Q12*Y(1)**2*XINT8-Q14*Y(1)*Y(3)*XINT17-Q17*Y(3)**2*XINT19
   +-Q10*Y(3)**2*XINT7
C
    DTERM = Q6*Y(1)*XINT6+Q9*Y(3)*XINT7+Q13*Y(1)*XINT16
   + +Q21*Y(1)*Y(3)*XINT12+Q25*Y(1)**2*XINT14+Q27*Y(1)*Y(3)*XINT13
   +-Q30*Y(3)**2*XINT15+Q22*Y(3)**2*XINT15+Q16*Y(3)*XINT18
C
    ETERM = Q4*XINT1+Q8*Y(1)*XINT7+Q11*Y(3)*XINT3+Q15*Y(1)*XINT18
   + +Q18*Y(3)*XINT20+Q20*Y(1)**2*XINT12+Q24*Y(3)**2*XINT4
   + +Q26*Y(1)**2*XINT13-Q31*Y(1)*Y(3)*XINT15+Q33*Y(1)*Y(3)*XINT15
   + +Q34*Y(3)**2*XINT5
C
```

```
      FTERM = -Q3*Y(3)*XINT1-Q5*Y(1)**2*XINT6-Q7*Y(1)*Y(3)*XINT7
     +-Q10*Y(3)**2*XINT3-Q12*Y(1)**2*XINT16-Q14*Y(1)*Y(3)*XINT18
     +-Q17*Y(3)**2*XINT20
C
      YPRIME(1) = Y(2)
      YPRIME(2) = (CTERM*ETERM-BTERM*FTERM)/(ATERM*ETERM-BTERM*DTERM)
      YPRIME(3) = Y(4)
      YPRIME(4) = (ATERM*FTERM-CTERM*DTERM)/(ATERM*ETERM-BTERM*DTERM)
C
      RETURN
      END
```

Appendix C. Programs FRQAMP1 and FRQAMP2

The FORTRAN programs for calculating the period, frequency, and amplitude of the response are shown on the following pages.

```
C                PROGRAM :  FRQAMP1 FORTRAN A
C     ****************************************************************
C          NON-LINEAR OSCILLATIONS OF INFLATABLE DAMS
C        CALCULATION OF FREQUENCY AND AMPLITUDE VALUES FOR OUTPUT
C                PROGRAM SOLVE1 AND SOLVE2
C     ****************************************************************
C
C
C           BY: JIM LEEUWRIK          DATE: FEB. 9, 1987
C
C     ---------------------- INITIALIZE -----------------------------
C
      IMPLICIT REAL*8(A-H,O-Z)
      EXTERNAL SYSCAL
      INTEGER I1,I,N,N1,K,K1,ICOUNT,IFILE
      CHARACTER*50 DEFIN , OUTPUT*4
      DIMENSION Y(0:1500),X(0:1500),XMAX(0:500),XMIN(0:500),YMAX(0:500)
      DIMENSION SLOPE(0:1500),YMIN(0:500)
C
      DO 10 IFILE  = 1,4
C
C
C     ---------------------- READ INPUT DATA ------------------------
C
      N = 0.D0
      N1 = 0.D0
      SUMP = 0.D0
      SUMN = 0.D0
      SUM1 = 0.D0
      SUM2 = 0.D0
      M = 0
      M1 = 0
      Y(0) = 0.D0
      X(0) = 0.D0
C
      DO 2 IZ = 0,500
        YMAX(IZ) = 0.D0
        XMAX(IZ) = 0.D0
        YMIN(IZ) = 0.D0
        XMIN(IZ) = 0.D0
        SLOPE(IZ) = 0.D0
    2 CONTINUE
C
      ICOUNT = 500
C
      READ(5,*) MODE,OUTPUT
      DEFIN = 'FILEDEF 12 DISK ' // OUTPUT // ' OUT A'
      CALL SYSCAL(DEFIN,50,IRTCDE)
C
      DO 11 I = 1,ICOUNT
      READ(12,9) X(I),Y(I)
    9 FORMAT(F5.1,F14.10)
   11 CONTINUE
      REWIND(UNIT=12)
C
C     ------------------ LOCATE POSITIVE PEAKS ----------------------
C
```

```
      I = 0
      TEMP = 0.D0
  210 I = I + 1
  220 IF(I.GT.ICOUNT)GOTO 440
          SLOPE(I) = (Y(I)-Y(I-1))/(X(I)-X(I-1))
          IF (SLOPE(I).LT.0.D0) GOTO 340
          IF(Y(I).LE.TEMP) GOTO 210
          TEMP = Y(I)
          M = I
      GOTO 210
C
C     ---------- SAVE POSITIVE PEAKS ----------
C
  340 N = N + 1
      XMAX(N) = X(M)
      YMAX(N) = Y(M)
      TEMP = 0.D0
  380 IF (SLOPE(I).GT.0.D0) GOTO 220
      I = I + 1
      SLOPE(I) = (Y(I)-Y(I-1))/(X(I)-X(I-1))
      IF(I.GT.ICOUNT) GOTO 440
      GOTO 380
  440 CONTINUE
C
C     ---------- LOCATE NEGATIVE PEAKS ----------
C
      I1 = 0
      TEMP1 = 1.0D4
  500 I1 = I1 + 1
  510 IF(I1.GT.ICOUNT)GOTO 730
          SLOPE(I1) = (Y(I1)-Y(I1-1))/(X(I1)-X(I1-1))
          IF(SLOPE(I1).GT.0.D0) GOTO 630
          IF(Y(I1).GE.TEMP1) GOTO 500
          TEMP1 = Y(I1)
          M1 = I1
      GOTO 500
C
C     ---------- SAVE NEGATIVE PEAKS ----------
C
  630 N1 = N1 + 1
      XMIN(N1) = X(M1)
      YMIN(N1) = Y(M1)
      TEMP1 = 1.0D4
  670 IF(SLOPE(I1).LT.0.D0) GOTO 510
      I1 = I1 + 1
      SLOPE(I1) = (Y(I1)-Y(I1-1))/(X(I1)-X(I1-1))
      IF(I1.GT.ICOUNT) GOTO 730
      GOTO 670
  730 CONTINUE
C
C     ---------- CALCULATE FREQUENCY AND AMPLITUDE ----------
C
      DO 980 K = N,3,-1
          SUMP = SUMP + (XMAX(K) - XMAX(K-1))
          SUMN = SUMN + (XMIN(K) - XMIN(K-1))
```

```
 980 CONTINUE
C
      TPER = (SUMN/DBLE(N-2) + SUMP/DBLE(N-2))/2.D0
      FREQ = 2.D0*3.141592654D0/TPER
C
      DO 1060 K1 = N,2,-1
        SUM1 = SUM1 + YMAX(K1)
        SUM2 = SUM2 + YMIN(K1)
 1060 CONTINUE
C
      AMPLP = SUM1/DBLE(N-1)
      AMPLN = SUM2/DBLE(N-1)
      AMPL = (DABS(AMPLP) + DABS(AMPLN))/2.D0
C
C     ---------- WRITE OUTPUT TO FILE ----------
C
      WRITE(6,1200) MODE,FREQ,AMPL
 1200 FORMAT(1X,I1,3X,F8.4,3X,F14.8)
C
C
C     ---------- LOOP TERMINATION ----------
C
C
      CLOSE(UNIT=12)
   10 CONTINUE
      STOP
      END
```

```
C                PROGRAM :  FRQAMP2 FORTRAN A
C     ****************************************************************
C          NON-LINEAR OSCILLATIONS OF INFLATABLE DAMS
C        CALCULATION OF FREQUENCY AND AMPLITUDE VALUES FOR OUTPUT
C                PROGRAM SOLVE1 AND SOLVE2
C     ****************************************************************
C
C           BY: JIM LEEUWRIK          DATE: FEB. 9, 1987
C
C     ---------------------- INITIALIZE -----------------------------
C
      IMPLICIT REAL*8(A-H,O-Z)
      EXTERNAL SYSCAL
      INTEGER I1,I,N,N1,K,K1,ICOUNT,IFILE
      CHARACTER*50 DEFIN , OUTPUT*8
      DIMENSION Y(0:1500),X(0:1500),XMAX(0:500),XMIN(0:500),YMAX(0:500)
      DIMENSION SLOPE(0:1500),YMIN(0:500)
C
      DO 10 IFILE  = 1,32
C
C
C     ---------------------- READ INPUT DATA ------------------------
C
      N = 0.D0
      N1 = 0.D0
      SUMP = 0.D0
      SUMN = 0.D0
      SUM1 = 0.D0
      SUM2 = 0.D0
      M = 0
      M1 = 0
      Y(0) = 0.D0
      X(0) = 0.D0
C
      DO 2 IZ = 0,500
        YMAX(IZ) = 0.D0
        XMAX(IZ) = 0.D0
        YMIN(IZ) = 0.D0
        XMIN(IZ) = 0.D0
        SLOPE(IZ) = 0.D0
    2 CONTINUE
C
      ICOUNT = 500
C
      READ(5,*) MODE1,MODE2,IO,OUTPUT
      DEFIN = 'FILEDEF 12 DISK ' // OUTPUT // ' OUT A'
      CALL SYSCAL(DEFIN,50,IRTCDE)
C
      DO 11 I = 1,ICOUNT
      READ(12,9) X(I),Y(I)
    9 FORMAT(F5.1,F14.10)
   11 CONTINUE
      REWIND(UNIT=12)
C
C     ------------------- LOCATE POSITIVE PEAKS ----------------------
C
```

```
      I = 0
      TEMP = 0.D0
  210 I = I + 1
  220 IF(I.GT.ICOUNT)GOTO 440
          SLOPE(I) = (Y(I)-Y(I-1))/(X(I)-X(I-1))
          IF (SLOPE(I).LT.0.D0) GOTO 340
          IF(Y(I).LE.TEMP) GOTO 210
          TEMP = Y(I)
          M = I
      GOTO 210
C
C     ---------- SAVE POSITIVE PEAKS ----------
C
  340 N = N + 1
      XMAX(N) = X(M)
      YMAX(N) = Y(M)
      TEMP = 0.D0
  380 IF (SLOPE(I).GT.0.D0) GOTO 220
      I = I + 1
      SLOPE(I) = (Y(I)-Y(I-1))/(X(I)-X(I-1))
      IF(I.GT.ICOUNT) GOTO 440
      GOTO 380
  440 CONTINUE
C
C     ---------- LOCATE NEGATIVE PEAKS ----------
C
      I1 = 0
      TEMP1 = 1.0D4
  500 I1 = I1 + 1
  510 IF(I1.GT.ICOUNT)GOTO 730
          SLOPE(I1) = (Y(I1)-Y(I1-1))/(X(I1)-X(I1-1))
          IF(SLOPE(I1).GT.0.D0) GOTO 630
          IF(Y(I1).GE.TEMP1) GOTO 500
          TEMP1 = Y(I1)
          M1 = I1
      GOTO 500
C
C     ---------- SAVE NEGATIVE PEAKS ----------
C
  630 N1 = N1 + 1
      XMIN(N1) = X(M1)
      YMIN(N1) = Y(M1)
      TEMP1 = 1.0D4
  670 IF(SLOPE(I1).LT.0.D0) GOTO 510
      I1 = I1 + 1
      SLOPE(I1) = (Y(I1)-Y(I1-1))/(X(I1)-X(I1-1))
      IF(I1.GT.ICOUNT) GOTO 730
      GOTO 670
  730 CONTINUE
C
C     ---------- CALCULATE FREQUENCY AND AMPLITUDE ----------
C
      DO 980 K = N,3,-1
          SUMP = SUMP + (XMAX(K) - XMAX(K-1))
          SUMN = SUMN + (XMIN(K) - XMIN(K-1))
```

```
 980 CONTINUE
C
     TPER = (SUMN/DBLE(N-2) + SUMP/DBLE(N-2))/2.D0
     FREQ = 2.D0*3.141592654D0/TPER
C
     DO 1060 K1 = N,2,-1
       SUM1 = SUM1 + YMAX(K1)
       SUM2 = SUM2 + YMIN(K1)
1060 CONTINUE
C
     AMPLP = SUM1/DBLE(N-1)
     AMPLN = SUM2/DBLE(N-1)
     AMPL = (DABS(AMPLP) + DABS(AMPLN))/2.D0
C
C    ---------- WRITE OUTPUT TO FILE ----------
C
     WRITE(6,1200) IO,MODE1,MODE2,FREQ,AMPL
1200 FORMAT(1X,3(3X,I1),3X,F8.4,3X,F14.8)
C
C
C    ---------- LOOP TERMINATION ----------
C
C
     CLOSE(UNIT=12)
  10 CONTINUE
     STOP
     END
```

The vita has been removed from the scanned document